Sedimentology of the Aspelintoppen Formation (Eocene-Oligocene), Brogniartfjella, Svalbard

Olav Aleksander Naurstad

Thesis for Master degree

In Sedimentology/ Petroleum Geology

09.12.2014

Department of Earth Science

University of Bergen[1]

The University Centre in Svalbard

Department of Arctic Geology

The University Centre in Svalbard[2]

Abstract:

The following study investigate the vertical changes in fluvial channel and interchannel geometry and facies architecture of the Aspelintoppen Formation in the Cenozoic Central Basin on Svalbard. Sedimentary structures was predominantly developed by unidirectional traction currents. The channelized sandstone bodies are ribbon shaped and is characterized by low sinuosity. This architecture was promoted by cohesive banks that limiting lateral accretion and resulted in channel fill dominated by vertical aggradation of dunes and bars. The studied section shows a clear dominance of interchannel sheet sandstone and laminated mudstone deposits, which volumetrically comprises five times as much deposits as fluvial channels. Abundance of leaf imprints, roots traces and ichnotaxa assemblages of the *Scoyenia* and *Mermia* ichnofacies, indicates lateral extensive and highly vegetated swamps, and ephemeral lakes, which are suggested to be flooded for longer periods of time.

Evolution of the sedimentary infill is best explained by high floodplain aggradation and shifting of main channel segments triggered by base-level changes, resulting in channel avulsion. Aggradational rates are reflected by the high degree of channel avulsion and large thickness of vertically connected crevasse splay complexes. Syn-tectonic deposition during uplift of the West Spitsbergen fold-and-thrust belt and foreland basin subsidence promoted a relatively high gradient of the fluvial system, resulting in great volumes of sediments being transported to the floodplain and bypassed to the basin.

Base-level changes favourable for avulsion of major channel segments (trunk and major distributary channels) is subsequently promoted by high floodplain aggradation and possibly by sea-level rise, influencing distal parts of the fluvial system and/or by high stream flow breaching channel banks, redirecting the channel to a more preferred location.

Characteristics of the studied succession points to a sedimentary basin with high sedimentation rates and subsidence which would promote the high aggradational rates suggested for the fluvial system of the Aspelintoppen Formation.

Acknowledgements:

This thesis is part of a master's degree in petroleum geology at the Department of Earth Science at the University of Bergen.

I would like to thank my supervisor William Helland-Hansen and co-supervisors Sten-Andreas Grundvåg and Maria Jensen for help during fieldwork and help with the writing process and outline of the thesis. Special thanks to Lars Haug Holen for assistance during long rainy days in the field during the 2013 field season and Dirk Knaust (Statoil ASA) for help recognizing and later interpreting trace fossils during the 2014 field season.

I would also like to thank the logistics department at UNIS for training and practicalities making it possible to carry out the field work in a safe and comfortable way. The writing of this thesis in full color was made possible by the generous support by Statoil ASA.

Olav A. Naurstad

....

Olav Aleksander Naurstad

Bergen, 9 December 2014

Index

1 INTRODUCTION

1.1 Purpose of study

Little work has been done on the Aspelintoppen Formation (Plink-Bjørklund, 2005) compared to its deltaic counterpart in the underlying and partly interfingering Battfjellet Formation . Most work on the Aspelintoppen Formation has been confined to the western part of the basin, especially along the northern shores of Van Keulenfjorden, where outcrops are many and of good quality.

The purpose of this study is to do a detailed sedimentological investigation of the Aspelintoppen Formation through facies stacking pattern and sandstone body geometry analyses. The results will be combined in order to generate a model for the fluvial system and its development in the western parts of the Central Basin. The evolution of the fluvial system of the Aspelintoppen Formation and its relations to the delta front and sandy slope wedges of the Battfjellet Formation will be discussed. The boundary between the shallow marine Battfjellet Formation and the mainly continental Aspelintoppen Formation will also be discussed in light of the findings presented in this study.

1.2 Previous work

Previous studies of the Aspelintoppen Formation are limited to very general stratigraphic studies (Atkinson, 1963; Kellogg, 1975; Major and Nagy, 1972). A noble extension is the work done by Plink-Bjørklund (2005). In contrast the underlying Battfjellet Formation has been studied in much greater detail. The lack of thorough studies of the Aspelintoppen Formation relate to the remote location of outcrops and, the general pour quality of outcrops.

Manum and Throndsen (1978) conducted a virtrinte-reflectance study of the abundant coal horizons located in the formation to estimate its age and maximum thickness. The studied tertiary succession at Nordenskiöldfjellet was estimated to have been 2700 meters (m) thick, implying that approximately 1700 m of sediments have been eroded. Age estimations indicate that the Aspelintoppen Formation was deposited from Eocene to Oligocene times. Steel et al. (1981) presented an interpretation of the Aspelintoppen Formation in the Nordenskiöld Land, central Spitsbergen. This study concluded that the formation was dominantly of a delta plain origin, with mainly floodplain and lacustrine deposits. One of the most recent, and extensive study of the Aspelintoppen Formation was carried out by Plink-Bjørklund (2005) at Brogniartfjella as well as Storvola. Plink-Bjørklund (2005) divided the sedimentary deposits of the formation into seven facies associations; 1) fluvial deposits, 2) tidally influenced fluvial deposits, 3) high-sinuosity tidal channels, 4) low-sinuosity tidal channels, 5) upper-flow-regime tidal flats, 6) tidal sand bars, 7) and mixed to muddy tidal flat deposits. To explain the high degree of tidal influence in the strata Plink-Bjørklund (2005) applied a incised valley model indicating low-stand fluvial deposits, transgressive estuarine deposits and highstand estuarine deposits. Fluvial deposits here represent the basal parts of the incised valley infill, which is covered by tide-dominated estuarine deposits. Coastal plain aggradation was suggested to take place during estuarine infilling of the incised valley.

The latest study of the Aspelintoppen Formation was conducted by Clifton (2012). This study includes a detailed environmental and paleogeoraphical interpretation, mainly on the basis of the abundant leaf prints located in the formation. Clifton (2012) concluded that the Aspelintoppen Formation was similar to today's Canadian high arctic climate, with broad lowland floodplain environments that was subjected to frequent flooding episodes.

Most areas of this study have not yet been investigated, and therefore provide important arguments for the interpretation of the fluvial systems' development.

1.3 Study area

The Central Basin covers most parts of the central and southern parts of Spitsbergen. Spitsbergen is the largest island of the Svalbard archipelago, which is located in the north-western corner of the Barents Sea (fig. 1.1). The study area is located in the south-western area of the Central Basin, on the northern side of Van Keulenfjorden. The main log was obtained from the western portion of Brogniartfjella, extending for the entire vertical length of the formation, which is approximately 500 m long (fig. 1.1). The log was located at an altitude between 340 and 840 m above sea-level (m.a.sl.) (fig. 1.1). Outcrops were reached by hiking up from the camp location in Davisdalen (fig. 1.1). The Aspelintoppen Formation can be traced over the entire length of the mountain, which stretches approximately five kilometres (km). The field work was carried out over two summers; three weeks in 2013 and one week in 2014. The entire logged section is presented in the thesis appendix.

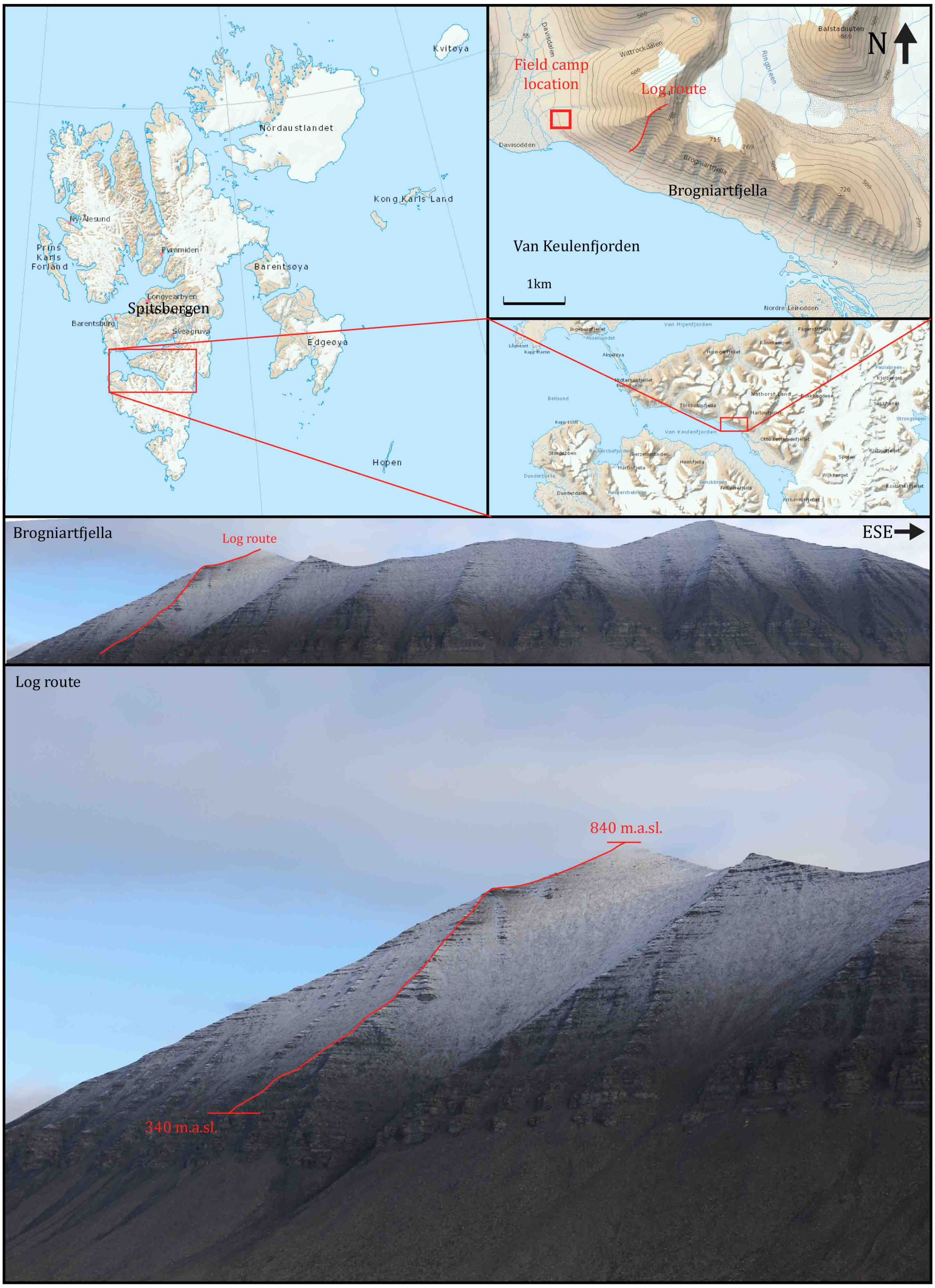

Figure 1.1: Overview map of study location and picture of the logged section. (map: Norsk Polarinstitutt, pictures taken by Sten-Andreas Grundvåg).

2 METHODS

2.1 Field work

The main data for this thesis was obtained from conventional sedimentological investigation, mainly consisting of measuring vertical sections. Logging is based on documentation of features such as thickness, boundaries, geometry, sedimentary structures, texture, and mineralogy of sedimentary strata. In addition, trace fossils was carefully described and recorded in order to aid the environmental interpretation of the various facies associations. For consistency in the interpretation of the sediments, a grain-size identification sheet, hand lens, measuring stick and geological hammer were used. For documentation purposes graph paper, necessary writing equipment and camera was used. Frequent precipitation and the high altitude resulted in bad conditions for photography, creating a foggy appearance in many of the photos. Identification of larger sandstone bodies and vertical trends were observed from a distance and later from photo mosaics. Other measurements methods conducted include paleocurrent measurements by the use of a geological compass as well as altitude measurements by the use of GPS. Since the GPS altitude measurements are based on satellites, uncertainties in readings are assumed to occur from locations and from day-to-day weather changes.

The location of the logged section was selected on the basis of its vertical extent, consequently assumed to reflect the most complete representation of environmental changes within the formation (fig. 1.1). Every sandstone bed in the logged section was carefully measured, whereas thickness of debris covered sections were estimated using the measuring stick. Some of the channelized sandstone bodies were also logged laterally in order to capture lateral changes in facies and depositional architecture. No fixed scale was used when logging in the field, because different sections required different scales of drawing to represent the sedimentary structures and architectures.

The first summer (2013) transportation to the study area was by boat, first by Stålbas to the inlet of Van Keulenfjorden and then by zodiac to the camp location. The second summer (2014) a helicopter was used for transport to an already established field camp by Knut William Jørgensen and Andreas Gillebo Kongsgården, at approximately the same location as the year before.

2.2 Post-field work

Post-field work was concentrated on digitalization of logs in a 1:50 scale by the use of Adobe Illustrator (CS6). Additionally, figures and photo interpretations were conducted in Adobe Illustrator and Photoshop (both CS6). Rose diagrams from various paleocurrent measurements from channelized sandstone bodies and interchannel sandstone bodies were created by the use of OSXStereonet 8.9.2. by Richard W. Allmendinger (2011-2013).

3 GEOLOICAL FRAMEWORK:

3.1 Introduction

Svalbard represents an uplifted parts of the shelf, revealing geological provinces ranging from Precambrian to Oligocene. The geological provinces include; metamorphic Precambrian to early Silurian rocks along the west coast and north eastern parts, Devonian grabens in the northern, Late Paleozoic and Mesozoic platform sediments in the central and eastern parts, and Paleogene strata in the Central Basin on central parts of Spitsbergen. The west coast is dominated by exposed basement and the tertiary fold-and-thrust belt (fig. 1.1-3.1) (Dallmann, 1999; Harland et al., 1997; Steel et al., 1985). The oldest rocks of the geological provinces are preserved in the west and northern parts of the archipelago due to the uplift being most extensive in these regions. These rocks have been influenced by several tectonic events, in which the most significant are the Grenvillian (Precambrium), Caledonian (Ordovician-Silurian), and the West Spitsbergen orogeny (Paleogene) (Dallmann, 1999). The pre-Cenozoic sedimentary record of Svalbard includes the development of several basin infill sequences which indicate paleoclimatic changes and the progressive movement of Svalbard from equatorial regions to its current position between 74 and 81 degrees north (Worsley, 2008).

The Cenozoic development of Svalbard, which is the focus of this thesis, includes the development of a trough shaped basin parallel to the north-northwest to south-southeast trending fault and thrust sheet.

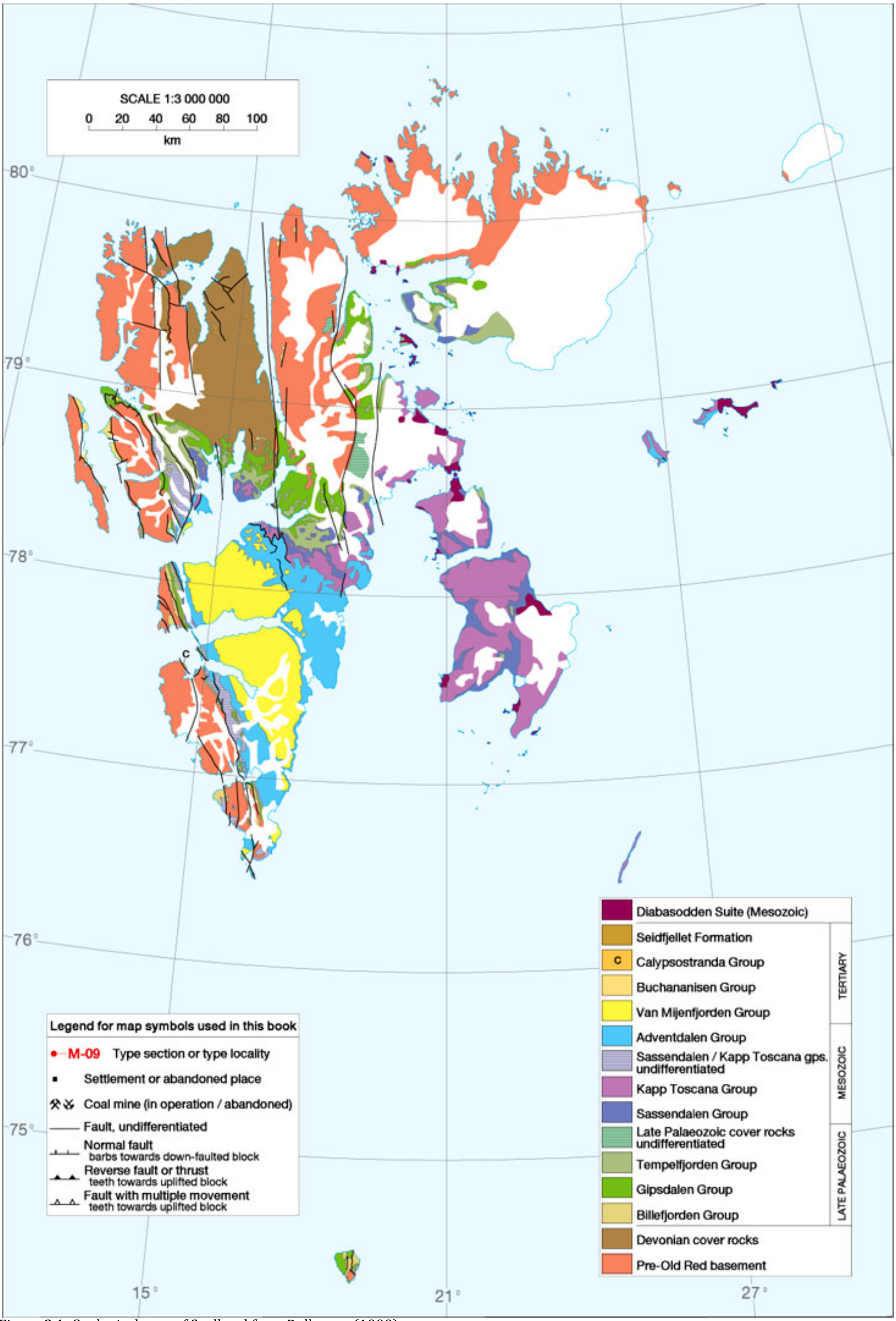

Figure 3.1: Geological map of Svalbard from Dallmann (1999).

3.2 Introduction to the Cenozoic:

3.2.1 The Cenozoic sedimentary system:

The Cenozoic deposits in Spitsbergen are mostly located in the central areas of the island in the area south of Isfjorden (fig. 3.1). The basin consists of a north-northwest to south-southeast trending syncline extending from the West Spitsbergen fold-and-thrust belt in the west (Harland, 1969; Harland et al., 1997) to the Lomfjorden Fault Zone in the east. The opening of the Norwegian-Greenland Sea during the late Cretaceous to Palaeogene lead to the development of an orogenic wedge due to a transpression related dextral shear along the De Geer Fault Zone (Blinova et al., 2009; Faleide et al., 1993). Adjacent to the fold-and-thrust belt the Central Basin developed on top of Caledonian basement (Birkenmajer, 1981). The Central Basin comprises seven formations (Harland, 1969; Harland et al., 1997) That represent deposition during late Paleocene to early Oligocene time, and consists of mixed continental and marine sediments, mainly deposited on coastal plains and wave to tidal dominated delta systems (Steel et al., 1981). The formations which comprises the Van Mijenfjorden Group have been estimated to have a original thickness of 1.5 km in the northeastern and 2.5 km in the southwestern regions (Harland et al., 1997). Later post-orogenic uplift in the Cenozoic resulted in erosion of large parts of the basin, leaving 1.5 km exposed in the west and up to 600 m in the east (Helland-Hansen, 1990). The Aspelintoppen Formation, which is the focus of this paper, are the youngest sediments exposed in the basin, estimated to be deposited from the late Eocene to early Oligocene (Paech, 2001).

3.2.2 Tectonic History:

The opening of the North Atlantic between the Norwegian and Greenland Sea resulted in a dextral transpression (fig. 3.2, W-E profile) during the Eocene to Early Oligocene. This uplift in the late Cretaceous to early Tertiary generated during an early phase of the Norwegian Greenland Sea opening, which resulted in dextral shear along the Hornsundet-Senja Fault Zone between the North American and Eurasian plate (Braathen et al., 1999; Dietmar-Müller and Spielhagen, 1990; Roest and Srivastava, 1989). The uplift comprises a north-northwest to south-southeast trending fold-and-thrust belt forming a 100-200 km eastwards thinning prism, which included a 30 km thinning of the crust (Braathen et al., 1999). Bergh et al. (1997) and Braathen et al.

(1999) subdivided the Cenozoic fold-and-thrust belt into three and later four major structural zones including the fold and thrust belt hinterland. The sub-division are as following (fig. 3.2):

1) The western basement-involved hinterland reflects the thickest part of the eastwards thinning prism. This zone is indicated by no cover strata and consists predominantly of Silurian to Devonian basement rocks, deformed Carboniferous to Permian deposits, and dispersed late orogenic Cenozoic grabens including the Forlandsundet Graben and the Øyrlandet Graben (southern Spitsbergen) (Braathen et al., 1999; Harland and Horsfield, 1974; Steel et al., 1985).

2) The basement-involved western fold-thrust belt include complex deformation. Overall structures include rotated thrust, which was progressively modified during progradation, generating chevron anticlines and synclines as well as large-scale (approximately five km wave length) monoclines (Braathen et al., 1999).

3) The thin-skinned central fold and thrust belt zones are thinning to the east where exposed Permian to Mesozoic strata are characterized by open to tight, upright folds developed over a regional decollement of the Gipshuken formations evaporites. Exposed thrust typically dies out in these folds. The regional decollement is further emphasized by gentle folds in the Paleocene-Eocene sediments of the Central Basin. The transition from central thin-skinned zones to the flat lying foreland zone is indicated by a major thrust ramp (Braathen et al., 1999).

4) The eastern foreland zone is characterized by less deformed subhorizontal cover strata. Deformation includes internal deformation of subhorizontal strata associated with decollment rooted thrust fault and macroscale folding of decollments related to reactivation of pre-existing faults at Billefjorden and Lomfjorden (Braathen et al., 1999).

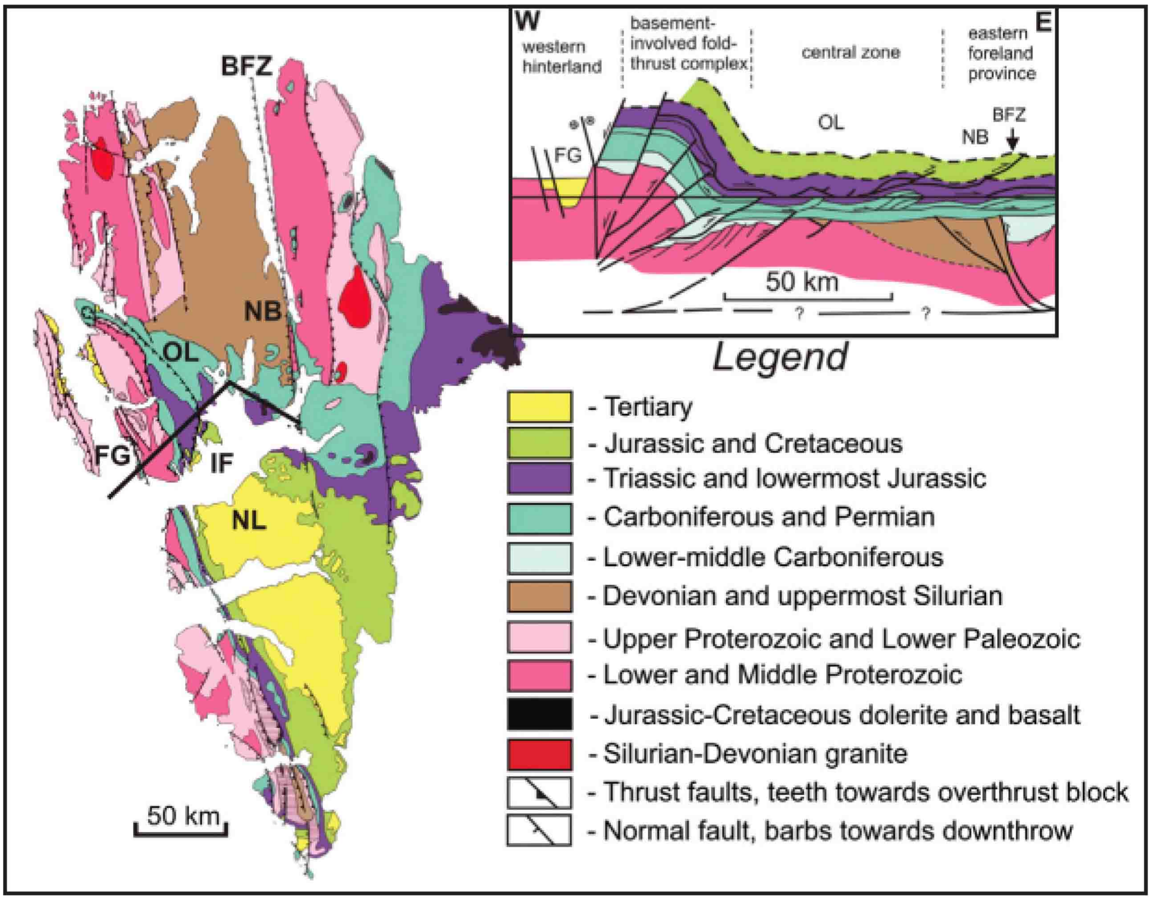

Figure 3.2: Cross section illustrating the different structural zones of the Cenozoic fold and thrust belt on Spitsbergen, Svalbard. BFZ = Billefjorden Fault Zone, FG = Forlandsundet Graben, OL = Oscar II Land, IF = Isfjorden, NB = Nordfjorden block, and NL = Nordenskiöld Land (Blinova et al., 2012).

The evolution of the west Spitsbergen Orogen has been studied by a number of authors (Dietmar-Müller and Spielhagen, 1990; Maher et al., 1995; Manby and Lyberis, 1996). One of the most recent models suggested by (Braathen et al., 1999) consists of a five-stage kinematic evolution.

The early stage (stage one) of the evolution includes a late Cretaceous-early Paleocene north-south contraction orientated oblique to the orogeny, prior to uplift. A counterclockwise movement from strike-slip to contraction was initiated as the North Atlantic plate movement changed (Roest and Srivastava, 1989). This resulted in NNE-SSW bedding parallel shortening and the development of basement involved fold-thrust complex demonstrated by folds and detachment thrusts. The northward compression and crustal shortening initiated the growth of a low-taper critical-supercritical wedge (Braathen et al., 1999).

During the early to middle-Paleocene the second stage continued with uplift and shortening in an ENE-WSW direction. This was promoted by thick-skinned thrust and rotations of pre-existing thrusts in the basement-involved fold and thrust belt zone (fig. 3.2). In central zones thrust progradation resulted in in-sequence skinned piggy-back thrusting, while eastern foreland provinces experienced layer parallel shortening and decollement thrusting. In the uplifted hinterland movement caused development of the Svartfjellet-Eidembukta-Daudmannsodden lineament (Braathen et al., 1999).

Shortening in the same direction continued in the third stage, with further rotation of pre-existing faults and thick-skinned thrusts in basement-involved fold-and-thrust belt zones. Central zones experienced continued in sequence thrusting, while the eastern foreland province layer parallel shortening and decollement thrusting proceeded. The increased eastward thrusting in stage three and four is thought to have developed as the hinterland was thickening because of strike-slip duplexing. This generated a supercritical wedge, which later became stable due to eastwards progradation and overall lengthening of the wedge. The contractional event in the Svartfjellet-Eidembukta-Daudmannsodden hinterland lineament was characterized by a sinistral strike-slip overprint (Braathen et al., 1999).

Shortening continued in a northeast-southwest direction in the fourth stage, indicating temporal change in the tectonic transport direction. The basement-involved fold-and-thrust belt is here defined by strike-slip faults, consistent with the orogen-oblique movement in combination of a dextral transpressional setting of this stage (four). Both in the central and foreland zones out-of-sequence thrusts are identified, decapitating pre-existing faults. In addition large-scale monoclines are generated by reverse reactivation of pre-existing faults. Similar to the basement-involved fold and thrust belt movement the hinterland lineaments experienced a dextral strike-slip movement. Along with the dextral strike-slip movements in the hinterland a adjacent local transtensive setting is likely to have initiated development of the Forlandsundet Graben (Braathen et al., 1999).

Wedge adjustment of stage three and four are likely to have developed because of the out-of-sequence thrusting in the central zones and thinning of the hinterland wedge because of transcurrent faulting (Braathen et al., 1999).

The last stage of the Central Basins tectonic evolution (stage five) is defined by an east-northeast to west-southwest Late Eocene-Oligocene extension, which eventually led to collapse and basin formation. Continued out-of-sequence thrusting and truncation of inversion monoclines in the foreland characterize central and foreland zones. Extensional faults in the hinterland developed as the shortening terminated and the extension started generated basin formation and the last adjustment of the wedge resulting in a critical taper angle (Braathen et al., 1999).

3.2.3 The Central Cenozoic Basin:

The Central Cenozoic Basin of Spitsbergen, Svalbard comprises an asymmetrical shaped basin, originally comprising an 2100 m thick Paleocene to Early Eocene clastic succession, in addition to an over 1400 m thick Eocene to Early Oligocene succession, together forming the Van Mijenfjorden Group (Bruhn and Steel, 2003). These successions show an overall thinning from the west towards the east. The basin developed as an asymmetrical foreland basin adjacent to the West Spitsbergen fold-and-thrust belt (Bruhn and Steel, 2003; Dietmar-Müller and Spielhagen, 1990; Helland-Hansen, 1990; Steel et al., 1985). The location of the basin close to the hinterland and it's asymmetrical profile supports the foreland basin interpretation (Helland-Hansen, 1990). Despite this the sedimentary infill is not consistent and the tectonic regime of the basin development is of a transpressional origin rather than a normal compressional. Sedimentary infill is here believed to be influenced by a significant shift in source area during Late Paleocene/ Eocene (Bruhn and Steel, 2003; Steel et al., 1985). Due to these reasons the basin model of the Central Basin does not correspond with the general conception of a foreland basin consistently building out by hinterland-derived sediments.

Early basin infill just above the Late Cretaceous unconformity indicates a different sediment transport direction than the rest of the succession. This is suggested to be because of a minor elevation of north Spitsbergen in Late Cretaceous, resulting in a short period of sediment infill from the north (fig. 3.3).

The Paleocene succession of the Central Basin consist of an overall transgressive phase (fig. 3.3), generating up to a 700 m thick succession transported from the east and northeast. The succession comprises the Firkanten, Basilika and Grumantbyen formations consisting of delta-plain to shoreface and shelf deposits. Early Eocene to Oligocene deposits records the main infilling of the Central Basin (fig. 3.3). The succession comprises an overall regressional succession of basin-plain turbidites of the Frysjaodden Formation passing through slope into shelf and shoreline to facies of the Battfjellet Formation. The latter partly interfingers with coastal-plain and alluvial deposits of the Aspelintoppen Formation. Together these formations comprises an up to 1400 m thick sedimentary succession that was mainly sourced from the west (Bruhn and Steel, 2003; Helland-Hansen, 1990; Kellogg, 1975; Steel et al., 1985; Steel et al., 1981).

The change in sediment transport direction from the Paleocene to Eocene succession is widely discussed. Bruhn and Steel (2003) suggested that the sudden reversal in sediment transport direction was due to an eastward migration of the periphiral bulge coupled with the eastward growth of the fold-and-thrust belt. This migration was probably generated by a tectonic change from a Paleocene extensinal/ transtensional to an Eocene transpressive setting (Braathen et al., 1999).

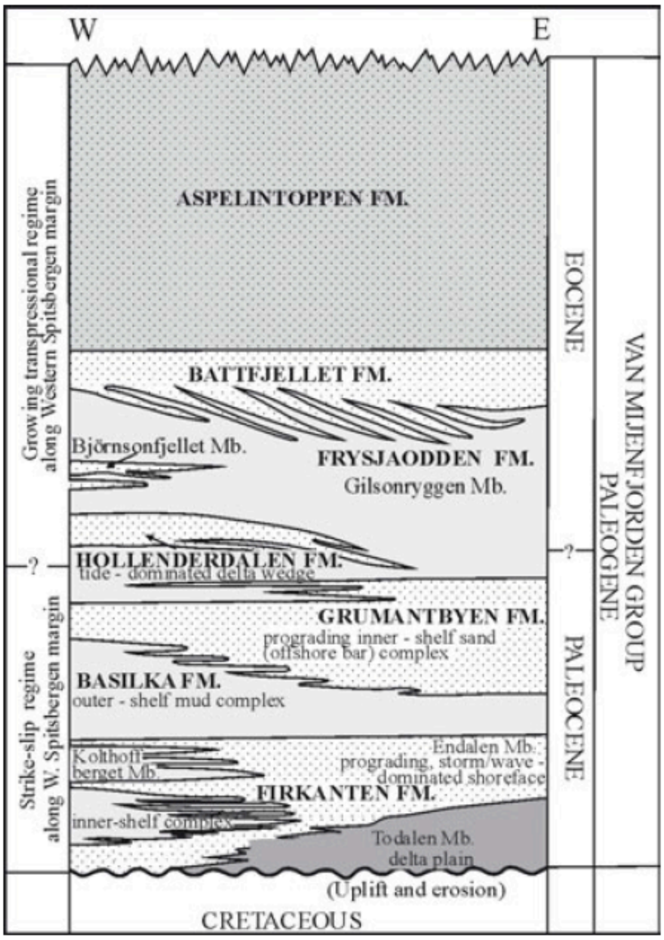

Figure 3.3: Stratigraphy of the Central Cenozoic Basin (Steel et al., 1985)

3.2.3.1 Firkanten Formation:

The Firkanten Formation is comprised of the first deposits of the Central Basin situated just above the Late Cretaceous unconformity. The formation thickens westwards from 80 – 200 meters, with the original depocentre located west of the present basin axis (Bruhn and Steel, 2003).

Braided river conglomerates of the Grønfjorden Bed form a lag that represent the basal deposits. These deposits are located directly on top of Late Cretaceous shelf deposits, thus representing a major depositional hiatus. Overlying the Grønfjorden Bed is the Todalen Member which consists of a fluvial dominated coal-bearing delta-plain package that can be traced laterally into delta-front sandstones (Bruhn and Steel, 2003). In the upper parts of the Todalen Member, marginal marine deposits interfingers with wave-dominated delta front, barrier bar and shoreface sandstones of the Endalen Member (Harland et al., 1997; Steel et al., 1985). In the top of the latter formation outer shelf mudstones of the Kalthoffberget Member interfinger with the Endalen Member, recording an overall transgressive trend. Despite the overall transgressive trend several minor regressive phases occur. The most prominent of these regressive trends is the transition from shallow marine to continental deposits in the Endalen Member.

Nagy et al. (2001) established a Selandian age of the Kalthoffberget Member based on foraminifera assemblages. Fission track dating of apatite grains by Blythe and Kleinspehn (1998) indicates a Danian age for the Endalen and Todalen members (Bruhn and Steel, 2003; Gjelberg, 2010).

3.2.3.2 Basilika Formation:

The lower Basilika Formation is overlying the Firkanten Formation and consists of dark grey to black shale and siltstone of Late Paleocene age. These deposits are interpreted as deep marine to outer shelf in origin, indicating a continued deepening upwards trend throughout the Paleocene (Bruhn and Steel, 2003; Steel et al., 1985).

The formation is thickest in the basinal regions in the southwest and gradually thins from tens of meters to a few meters towards northeast (Kellogg, 1975). In the top 45 m of the western segment of the formation silt and sandstone 50-150 centimeter (cm) thick interfingers the fine-grained deposits. These coarser sediments are suggested to be distal deposits of the overlying and partly interfingering Grumantbyen Formation. The fining and deepening upwards trend of deep marine shales diminished in a zone located in the deepest basal parts of the Basilika Formation. This zone indicates a change in depositional style from an overall transgressive to a regressive shoaling upwards trend. .

In total the Basilika Formation comprises of an up to 350 m thick succession thinning to 20 m from the southwest to the northeast (Harland et al., 1997). The late Paleocene age was determined from foraminifera found in mudstones of the Basilika formation (Nagy et al., 2001).

3.2.3.3 Grumantbyen Formation.

The Grumantbyen Formation interfingers as well as overlies the Basilika Formation and is defined by the first appearance of greenish highly bioturbated sandstone sheets at first appearance. These deposits are interpreted as a "shallow offshore bar complex" consisting of five major sandstone sheets, which are further divided into six minor-scale sequences (Bruhn and Steel, 2003). The formation is approximately 450 m thick in the east-northeast regions of the basin and gradually thins westwards to approximately 200 m in the west-southwest (Dallmann, 1999).

The sandier deposits discussed above (3.2.3.2 Basilika Formation) are interpreted as distal parts of the Grumantbyen formation represented in the two lower sandstone sheets. Tempestites and trace fossils including *Cruziana*, *Zoophycos* and *Nerites* recognized in the sandstone sheets emphasize the distal shelf environmental origin (Bruhn and Steel, 2003).

Upward in the succession the minor sequences become thicker, resembling the regressive phase of the Grumantbyen Formation. These deposits comprise the upper three sandstone sheets developing distinct coarsening and shallowing upward trends in the upper part of the Grumantbyen Formation. Individual sequences range from two-15 m in thickness and consist of hummocky cross-stratification, planar laminated and wave rippled sandstones indicating a more proximal inner shelf setting (Bruhn and Steel, 2003).

3.2.3.4 Frysjaodden Formation

The Fysjaodden formation consists of uniform olive to dark-grey shale, occasionally with interbedded silt and sandstones of turbiditic origin (Steel et al., 1981). The formation is situated above the Grumantbyen Formation and below the first sandstone sheets of the Battfjellet Formation. The thickest part of the formation are located south of Van Mijenfjorden and thin north and eastwards to Nordenskiöld Land from 400-200 m, respectively.

The Frysjaodden Formation was deposited during the Late Paleocene/Early Eocene overthrusting, which resulted in a change in sediment input from the west compared to the underlying formations eastern trending sediment input (Dallmann, 1999; Helland-

Hansen, 1990). Shale and interbedded turbidite beds are believed to have originated from a deltaic source in the west which correspond to the overlying Battfjellet Formation (Grundvåg et al., 2014a; Harland et al., 1997; Steel et al., 1985).

3.2.3.5 Hollendardalen Formation

The Hollendardalen Formation consists of tidal-dominated, deltaic sandstone wedges that build from the west thinning towards the east and eventually pinching out into the Frysaodden Formation (Dalland, 1979). It is situated above the Grumantbyen and below the Gilsonryggen formations (Steel et al., 1985).

3.2.3.6 Battfjellet Formation

The Battfjellet Formation consists of deltaic wave-influenced sandstones and siltstones gradually coarsening upwards from the underlying Frysjaodden Formation. Together with the underlying Fysjaodden and the overlying Aspelintoppen formations, the Battfjellet Formation represents the third and last depositional cycle of the Central Basin. The boundary between the Frysjaodden and Battfjellet formations are transitional (Helland-Hansen, 1990), and the formations interfingers with the lower part of the overlying Aspelintoppen Formation.

This depositional cycle are of early to mid Paleocene age and developed in concern with the West Spitsbergen Orogeny. This lead to a strongly regressive development aided by high sedimentation rates and an eastwards migrating depocentre. This resulted in the formation of several shelf-margin-scale clinothems, which can be observed to build out eastwards. Some of the clinothems are possible to trace laterally from the coastal plain facies in the most proximal setting (i.e. Aspelintoppen Formation) to distal shelf, shelf edge, slope and basin floor in most distal setting (i.e. Fysjaodden Formation). Within the shelf-segment of the clinothems, stacked upwards-coarsening parasequences of the Battfjellet Formation show no distinct vertical trends and rather varies in number at different locations (Helland-Hansen, 1990; Helland-Hansen, 2010). This suggests that the Battfjellet Formation consists of overlapping delta lobes which evolution was strongly controlled by autogenic processes (Grundvåg et al., 2014a; Helland-Hansen, 2010).

3.2.3.7 Aspelintoppen Formation

The Aspelintoppen Formation stretches from the Eocene and possibly into Early Oligocene, and represent the continental counterparts of the deltaic Battfjellet Formations (Plink-Bjørklund, 2005; Steel et al., 1985).

The boundary between the Battfjellet and Aspelintoppen formations are defined by the first occurrence of coal or fine-grained shales over the last coarsening upwards parasequences of the Battfjellet Formation (Dallmann, 1999). The latter formation represents the last sediment infill of the Central Basin. The deposits comprises delta plain to fluvial channel sandstones, lacustrine and floodplain shale, and thin coal deposited in mires and swamps. Individual sandstone bodies record both upwards-coarsening and upward-fining trends.

The formation is dominated by alternating floodplain sandstone sheets and shales that roughly comprise over 2/3 of the formation. Sandstone beds often include a variety of deformation structures such as large folds and convolute lamination or minor spoon shaped deformation structures, which makes it significantly more difficult to determine sedimentary structures (Steel et al., 1985). It is suggested by Steel et al. (1985) among others that frequent earthquakes caused repeated liquefaction and blurring of sediments before they became consolidated.

Plink-Bjørklund (2005) have suggested a three-stage depositional model for the lower Aspelintoppen Formation based on her field studies at Brogniartfjella. The model is based on the concept of incised valleys formed by relative falling sea-level. The infill of these valleys is characterized by a first stage of low-stand fluvial deposits followed by transgressive estuarine and finally high-stand estuarine deposits. Eight of these coastal-plain incised valley sequences, ranging from seven-44 m in thickness, were distinguished. Although this may be true for some locations in the lower Aspelintoppen and lower Aspelintoppen upper parts of the Battfjellet formations no features resembling incised valleys were recognized in the present study.

Early studies of the Aspelintoppen formations paleoflora assemblages indicates a temperate climate (Manum, 1962). A similar conclusion was recently carried out by Clifton (2012).

This extensive study of the Aspelintoppen Formations paleoflora at Brogniartfjella concluded that angiosperm leaf remains comprising 22 morphotypes dominated the formations flora. A number of the same paleoflora assemblages are also observed in the Paleocene floras of North America and the British Tertiary Volcanic Province. A. J. Clifton (2012) pointed out that the widespread of paleoflora during Paleocene suggested a retreat of taxa during Eocene, which could linke to changes in global temperature and/ or precipitation. As mentioned above this paleoflora whould be similar to the present temperate Canadian arctic environment.

4 SEDIMENTARY LITHOFACIES AND FACIES ASSOCIATIONS:

4.1 Introduction:

The sedimentary strata studied on the western side of Brogniartfjella have been divided into 17 sedimentary lithofacies based on their lithological features including: grain-size; sedimentary structures; bounding surfaces; color; trace fossils; and degree of bioturbation. Lithofacies descriptions and interpretations are provided in table 4.1, where they are arranged from highest to lowest flow regime. Figure 4.1 provides associated pictures. The lithofaceis are further grouped into 10 facies association sub-groups, which represent different depositional sub-environments. The 10 sub-groups are grouped into three facies associations, representing deposition in three gross environments; 1) fluvial channel settings, 2) interchannel floodplain settings, and 3) shallow marine to marginal marine settings (see Table 4.2).

Table 4.1: Lithofacies:

Facies	***Facies name***	***Lithology***	***Structures***	***Thickness (m)***	***Color***	***Architecture***	***Interpretation***
F1 (figure 4.1, A)	Trough cross-stratified conglomerate	Pebble dominated conglomerate with coarse to very coarse-grained well to moderate sorted sandstone matrix	Erosional scoured, low angular to sub angular trough cross-stratified conglomerates, with abundant pebbles, a high degree of organic detritus and rip-up mud clasts. Beds often partly deformed.	From decimeters (dm) thick beds within up to 1.2 m thick units.	Brown red to yellow	Lenticular bodies with high relief concave-upwards lower boundaries, and straight undulating to concave-upwards, upper boundaries.	Deeply incised trough-shaped scours infilled by three-dimensional dunes within trunk channel-belts. Filled by the migration of bars, or by sediments settling during waning-flood conditions.
F2 (figure 4.1, B-C)	Trough cross-stratified sandstone	Laminated medium to very coarse-grained well-sorted sandstones with occasional pebbly zones.	Normal graded, trough cross-stratified, erosional scoured sandstones, occasionally with pebbles. Beds often partly deformed. High degree of organic detritus and rip-up mud clasts.	0.2 to 4 m thick units, Sandstone beds; 0.1 to 2.0 m thick.	-	Lenticular bodies with concave-upwards to straight lower boundaries and straight to gradual upper boundaries.	Channel infill by aggradation of three-dimensional dunes in various bar settings. Deposition of sand by high velocity unidirectional currents.
F3 (figure 4.1, D-E)	Massive sandstone	Very-fine to coarse-grained sandstones	Massive, non-structured to weakly laminated beds often with organic detritus and coal clasts.	0.25 to 1.5 m thick units.	-	Lenticular or transitional to undulating bodies. Erosive lower boundaries and straight non-erosive upper boundaries	Migration of dunes in major distributary, trunk or minor crevasse splay channels and/ or sheets.
F4 (figure 4.1, F-G)	Soft-sediment deformed sandstone	Very fine to very coarse grained sandstones	Soft-sediment deformation causing overturned beds, folded lamina to massive beds and small spoon shaped deformation structures.	0,2 to 4,0 m thick units.	Brown yellow to grey.	Lenticular bodies with gradual, erosive and straight non-erosive upper and lower boundaries.	Secondary structure developed as liquefied sediments deform from seismic activity or by shear stress.

F5 (figure 4.1, H-I)	Planar parallel-stratified sandstone	Fine to coarse-grained sandstones with occasional pebbly zones	Planar parallel-stratified sandstones, with upper surfaces partly deformed by water escape structures.	0.2 to 2.0 m thick units.	Brown to grey	Lenticular bodies with erosional undulating to straight upper and straight non-erosive to gradual lower boundaries.	Deposition by upper flow regime (UFR) unidirectional currents as tractional carpets or UFR bars by migration of low-amplitude bed waves.
F6 (figure 4.1, J)	Sigmoidal cross-stratified sandstone.	Fine to medium grained sandstones.	Normal graded sigmoidal cross-stratified sandstones.	0.2 to 0.3 m thick units	Light grey to grey blue	Lenticular to sheet-shaped bodies with straight non-erosive upper and straight non-erosive to concave-upwards erosive lower surfaces. Cross sets are gently dipping	Migration of two-dimensional dunes by unidirectional currents. Reflects deposits of the transitional phase between simple bars and upper flow regime planar beds. Typical in flood-dominated and in tidal-influenced systems.
F7 (figure 4.1, K-L)	Tangential cross-stratified sandstone	Normal graded fine to medium-grained sandstones.	Normal graded tangential planar cross-stratified sandstones,	0.2 to 1.0 m thick units.	Light grey to grey blue	Lenticular to sheet-like bodies with straight non-erosive to slightly undulating lower and upper boundaries. Gently to moderately dipping foresets.	Migration of two-dimensional dunes deposited by lower flow regime unidirectional currents.
F8 (figure 4.1, M)	Planar cross-stratified sandstone	Medium to coarse-grained sandstones, with occasionally occurring pebbles in coarse-grained sandstones.	Normal graded, tabular cross-stratified sandstones ,with occasional pebbles, organic detritus and rip-up mud clast. Beds often partly deformed.	0,25 to 1,55 m thick units.	Brown red to yellow	Lenticular bodies with erosional scoured concave-upwards to straight non-erosive lower boundaries. Straight non-erosive and occasional undulating upper boundaries. Moderately to steeply dipping foresets.	Deposition and migration of two-dimensional dunes by lower flow regime unidirectional currents.
F9 (figure 4.1, N)	Low angular cross-stratified sandstone	Fine to coarse-grained sandstone, with occasional pebbly zones.	Normal graded, low angular cross-stratified beds, with occasional pebbles and large amounts of detritus and rip-up mud clasts. Beds often partly deformed.	0.2 to 1.0 m thick units.	-	Lenticular bodies with straight to non-erosive lower or undulating erosive lower boundary, and straight non-erosive upper boundary.	Two-dimensional dunes deposited by lower flow regime unidirectional currents.

F10 (figure 4.1, O)	Planar parallel-stratified very fine grained sandstones	Very fine-grained sandstones	Planar-parallel-stratified sandstones, penetrated by roots when observed in the fully continental deposits.	0.1 to 0.25 m thick units.	Brown yellow to grey	Amalgamated sheet to lenticular units of sandstone and shale with straight upper and straight to gradual lower boundaries.	Upper bar deposits, deposited by high velocity unidirectional currents at low water stage.
F11 (figure 4.1, P-Q)	Combined flow ripple laminated sandstone.	Very-fine to fine-grained sandstones	Superimposed ripples	0.1 to 0.25 m thick units.	Light grey to grey.	Sheet to lenticular shaped amalgamated or heterolithic beds with straight non-erosive upper and lower boundaries.	Upper bar deposits, deposited by a combination of oscillation and unidirectional flow.
F12 (figure 4.1, R-T)	Wave ripple cross-laminated sandstone.	Very-fine to medium- grained sandstones.	Symmetrical wave ripple cross-laminated sandstones.	0.5 to 25 cm thick units.	Light grey.	Sheet to lenticular shaped amalgamated or heterolitic beds with straight non-erosive upper and lower boundaries.	Deposited from oscillation and combined flow currents of relatively low velocity currents.
F13 (figure 4.1, U-V)	Current ripple cross-laminated sandstone.	Very fine to medium-grained sandstones, often penetrated by charred roots.	Asymmetrical unidirectional current ripple cross-laminated sandstones.	0.05 to 1.0 m thick units.	Yellow brown, light bronze and grey.	Sheet to lenticular sandstone bodies with straight to erosive upper and gradual to straight lower boundaries.	Upper bar deposits, deposited by unidirectional currents.
F14 (figure 4.1, W)	Climbing ripple laminated sandstone.	Very fine to medium grained sandstones, often penetrated by charred roots.	Gently climbing ripples to highly aggradational super critical climbing ripples similar to wavy lamination.	0.1 to 0.5 m in thick units.	-	Sheet-like-units	Deposited when sediment supply exceeds stream capacity, resulting in highly aggradational ripples.
F15	Shale	Silty mudstone with occasional very-fine gained sandstone.	Irregular to flakey lenticular shaped lamination and rippled lensoid sandstones.	0.02 to 0.1 m thick units.	Dark to light grey.	Heterolithic flaser laminated shale and non-laminated mudstone.	Deposited by suspension during flooding of channel banks. Very fine sandstone lenses part of distal crevasse splay sheets.

F16 (figure 4.1, Y-Z)	Coal	Coal, with occasional shale and siltstone.	Massive to flaky appearance.	0.05 to 0.2 m thick units.	Glossy to matt black	Thin sheets or small lenticular shaped beds. Commonly eroded.	Developed by compaction of *in-situ* peat.
F17 (figure 4.1, X)	Paleosol	Shale, siltstone and very-fine grained sandstone.	Soft-sediment deformed to heterolithic shale, siltstone and very fine sandstones, including abundant sideritic nodules and various root traces.	0.05 to 0.2 m thick units.	Dark to light brow-red	Chaotic soft-sediment deformed to massive appearance.	Developed by chemical and physical degradation under sub-aerial exposure.


A
B
C
D
E
F
G
H
I

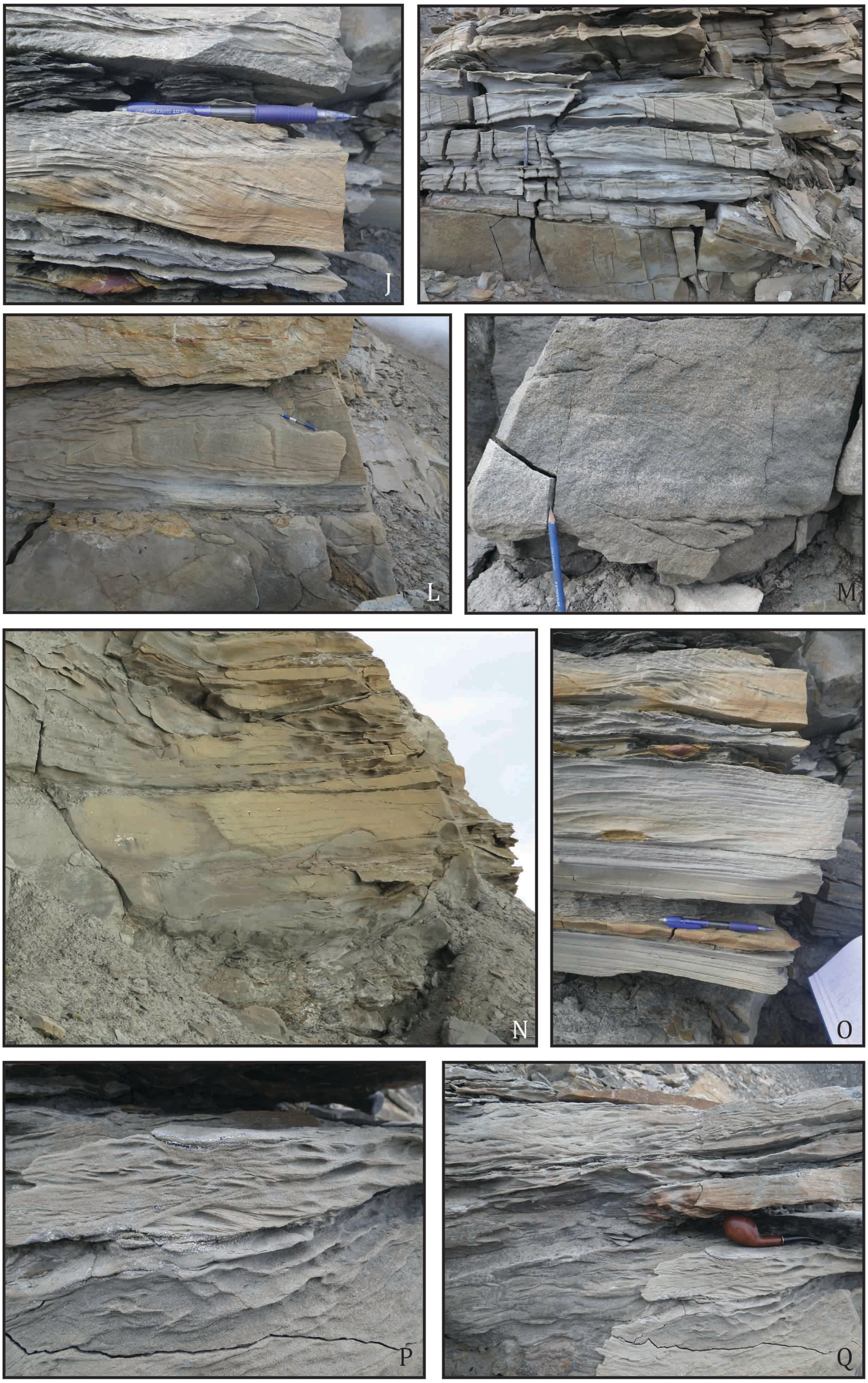
J
K
L
M
N
O
P
Q

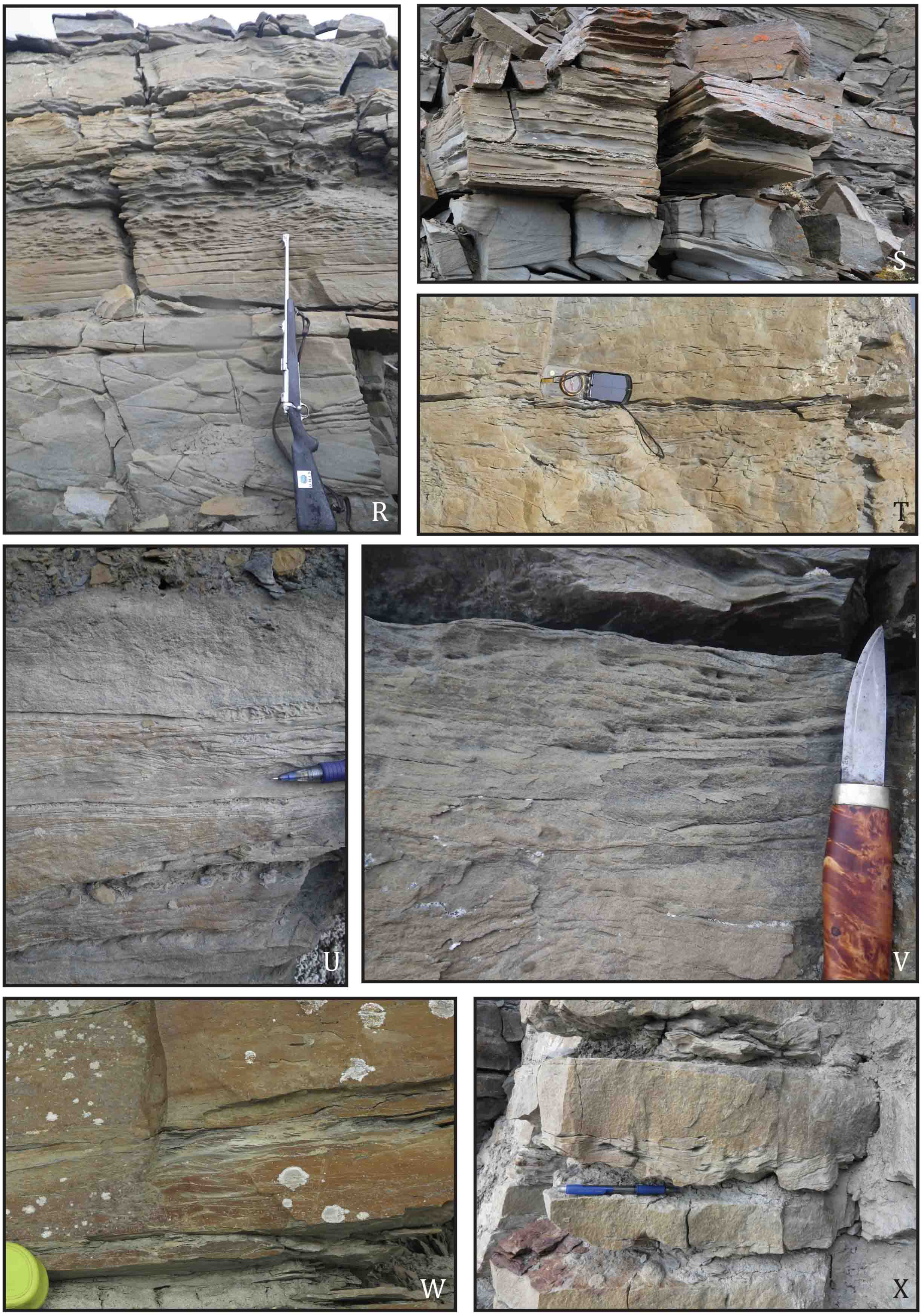
R
S
T
U
V
W
X

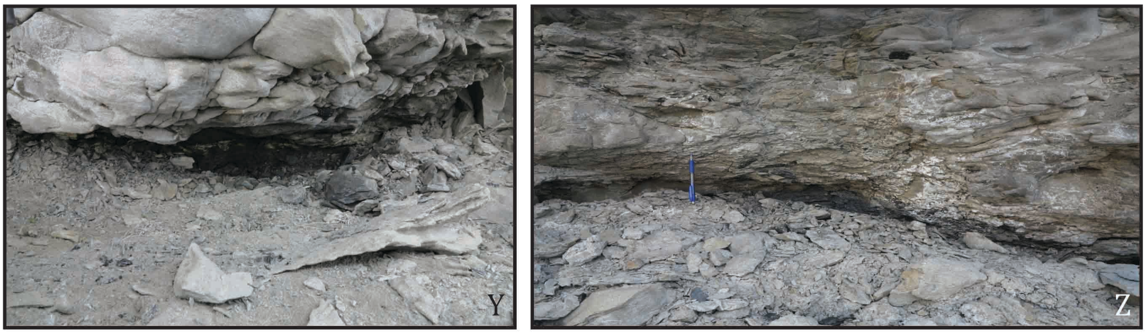

Figure 4.1: Lithofacies examples: A) Trough cross-stratified conglomeratic basal lag deposits (F1). B-C) Trought cross-stratified coarse to very coarse-grained sandstone deposits (F2). D-E) Massive (F3) lower and upper beds in fluvial channels (D) and interchannel (E) deposits. F) Convolute laminated (F4) interchannel sheet sandstones. G) Large soft-sediment deformed fold (F4) in fluvial channel deposits. H) Coarse grained planar-parallel stratified sandstone deposits (F5) in fluvial channel. I) Coarse grained planar parallel stratified tidal bar deposits (F5) of the upper Battfjellet formation. J) Sigmoidal cross-stratified tidal bar deposits (F6) of the upper Battfjellet formation. K-L) tangential cross-stratified sandstones (F7) in interchannel (L) and channel deposits (K). M) Planar cross-stratified sandstones (F8) related to interchannel sheet sandstones. N) Low angular cross-stratified sandstones (F9) in lower parts of channelized sandstone body. O) Very fine to medium grained planar-parallel stratified interchannel sandstone sheet deposits (F10). P-Q) Compound ripple cross-stratified sandstones (F11) in the lower Aspelintoppen – upper Battfjellet formation transition tidal influenced deposits. R-S) Wave-ripple cross-stratified sandstones deposits (F12) in beds of upper Battfjellet formations heterolitic. T) Wave-ripples on top of interchannel sheet sandstone deposit. U-V) Current-ripples in heterolithic levee deposits. W) Climbing ripple cross lamination deposits (F14) in interchannel sheet sandstone. X) Paleosol (F16) with siderite concretions and fine-grained sediments interbedded in thin amalgamated sandstone sheets deposits. Y-Z) Coal layers (F17) underneath channelized sandstone body (Y) and interchannel sheet sandstone deposits (Z).

4.2 Facies association:

Table 4.2: Facies associations:

Facies Association:	**Facies association sub-groups:**	**Lithofacies:**	**Depositional Environment:**
FA1	FA1.1 FA1.2	F1, F2, F3, F4, (F10, F13) F1, F2, F4, F5, F8, F9, (F11, F13)	Fluvial channels
FA2	FA2.1 FA2.2 FA2.3 FA2.4 FA2.5 FA2.6	F15, F16, F17, (F13) F13, F14, (F4, F8) F10, F13, F14, (F3, F4) F2, F3, F4, F5, F9, (F13, F14) F3, F4, F13, F14, (F9, F10, F11) F2, F4, F9, F11, F13, F14	Interchannel floodplain
FA3	FA3.1 FA3.2	F2, F5, F6, F7, F8, F11, (F9) F12, F13, F14, F15, F16	Shallow to marginal marine

4.2.1 Facies association 1: Fluvial channel fill deposits:

Facies association one consists of two sub-facies associations based on the geometry and lithofacies stacking patterns within the channels.

FA1.1: Erosional-based, multistorey trunk channel sandstones:

Description:

Facies association sub-group 1.1 (FA1.1) comprises of yellow/brown to grey, erosional based, fine to very coarse-grained sandstone and occasional conglomerates. FA1.1 preserve mostly fine to very coarse-grained trough cross-stratified sandstone (F2), medium to coarse-grained soft-sediment deformed sandstones (F4) and trough cross-stratified pebble dominated conglomerate (F1) (as illustrated in fig. 4.2). Occasionally fine to medium grained massive sandstones (F3) occur in the top meters of the sequences (fig. 4.2, B). Conglomeratic trough cross-stratified beds (F1) up to 1.0 m thick are common within scours, but are occasionally replaced by medium to coarse-grained trough cross-stratified sandstones (F2) (fig. 4.2). Scour infills consist of a coarse to very coarse-grained sandstone matrix, abundant mud clasts, organic detritus fragments and pebbles, with pebbles longest axis seldom exceeding 40 millimeters (mm). Medium to coarse-grained trough cross-stratified sandstones (F2) and soft-sediment deformation structures (F4) dominate the rest of the channel fill. Occasionally very fine- to fine-grained planar-parallel (F10) and current ripples cross-laminated sandstones (F13) ranging from 0.25-1.5 m are observed above sandy channel fill deposits. Stacked channel fills form sequences with faint to non-existing fining-upwards trends, ranging in thickness from 6.0-10.0 m, with individual units ranging from 0.5-3.0 m. The trough cross-stratified and soft-sediment deformed (F2 + F4) intervals contain several internal erosive surfaces. Width estimates of the sandstone bodies are non-conclusive because of poor outcrop quality. In a few locations where width estimations of larger channel bodies could be carried out measurements typically ranged from 70-200 m.

The channel fill's generated lenticular to sheep shaped bodies, with concave-upwards lower boundaries generating erosional reliefs ranging from approximately 1-3m.

The scoured lower surfaces are less pronounced than the distributary channels (further described below), giving a lenticular and occasional sheet shaped geometry where reliefs are as low as one meter (fig. 4.2, A and 4.3, C).

In most cases, the channelized sandstone bodies are eroding into very fine- grained sandstones, siltstones and shales. The shale contain a large amounts of coal fragments, occasional coal layers, siderite nodules and a variety of horizontal and vertical burrows (further described in FA2.1). Trace fossils are described and interpreted in chapter 5.

Interpretation:
The erosional bases, lenticular geometry, multiple scoured surfaces, unidirectional flow direction, traction-generated structures and pebbly basal surfaces with occasional mud clasts and organic fragments strongly suggest that this facies association is of fluvial multi-storey channel origin. The absence of lateral accretion packages suggests that the channels are straight to low sinuous. The abundance of leaf prints and organic fragments found in the adjacent and overlying (fig. 4.1, Y-Z) floodplain deposits (FA 2) points to stable, highly vegetated riverbanks. The absence of marine trace fossils and indicators of tidal influence suggests deposition in fully continental fluvial channels.

The lenticular (fig. 4.2, B) to sheet-like geometry (fig. 4.2, A), thickness and assumed width extending well over 200 m suggests that these trunk channel bodies fit within the broad ribbon to narrow sheet category of Gibling (2006) classification of fluvial-channel bodies. These channels are therefore assumed to be entry points and may pass downflow from narrow sheets into ribbons and further downstream into distributary channels. Another possibility is that narrow sheets represent sinuous channels close to the delta front, where lateral accretion is promoted by low river-system gradients. Secondary soft-sediment deformation structures could make it difficult to observe lateral accretion packages if they are present (fig 4.2).

The abundance of high velocity unidirectional current structures (F1+F2), homogeneity of vertical grain-size trends and lack of lateral accretion surfaces strongly suggests that vertical accretion predominates. This along with the lack of pronounced fining-upwards trends indicates rapid infill due to high sedimentation rates, promoting repeated events of channel erosion as reflected by the multiple internal erosion surfaces. As the channel filled up this eventually lead to channel avulsion. The planar sheet geometry of internal beds, including trough cross-stratified (F2), massive (F3) and soft-sediment deformed (F4) coarse to very coarse grained sandstones are interpreted as downstream migrating transverse bars (fig 4.1, A-G). These bar deposits dominate the channel fill and are suggested to have filled up the entire channelized sandstone body, developing the constant vertical grain-size trend.

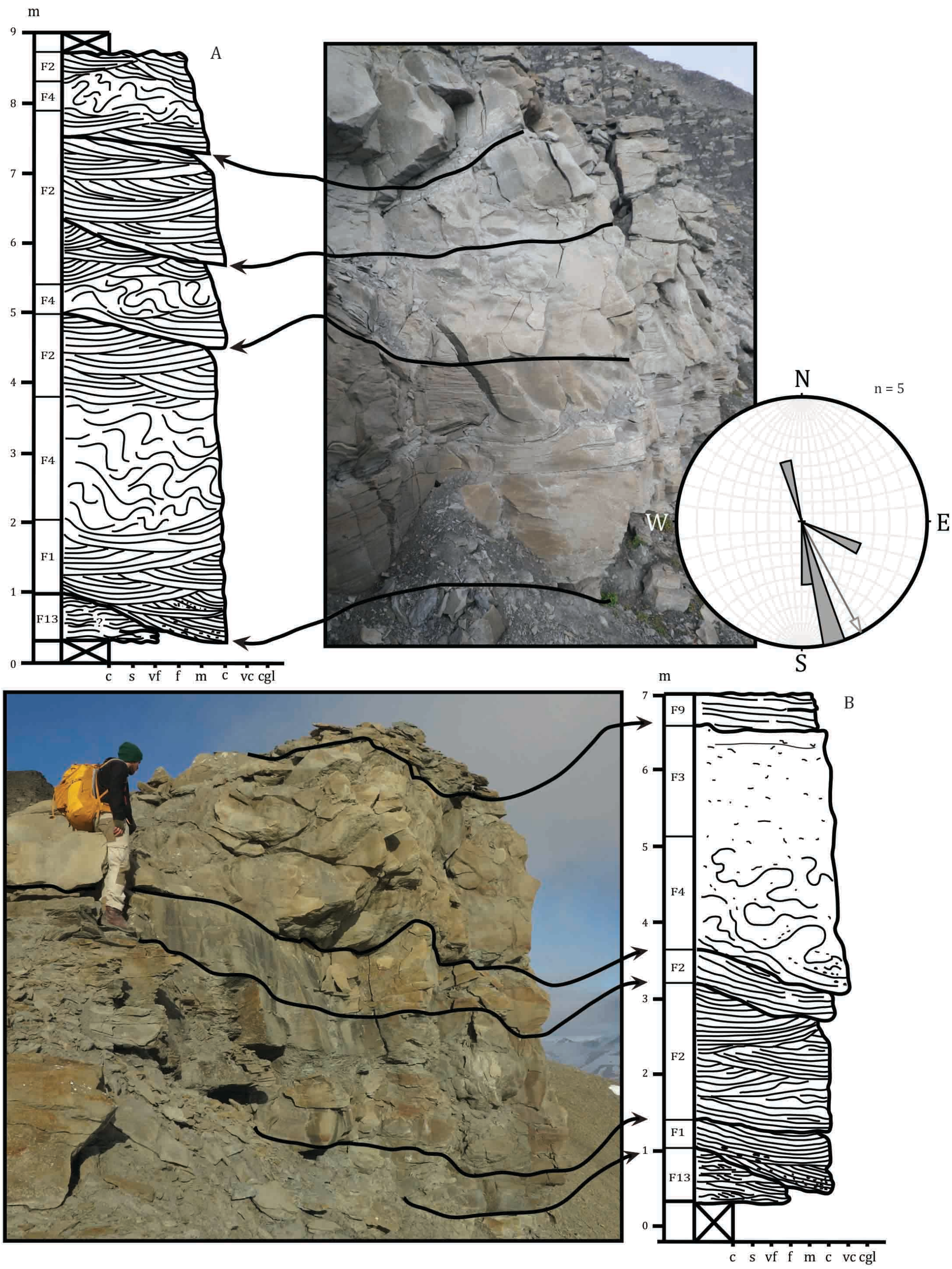

Fig 4.2: Multistory trunk channels. A) Fluvial channel deposits dominated by trough cross-stratified sandstones and interbedded horizons of soft-sediment deformed. B) Fluvial channel deposits with lower parts dominated by trough cross-stratified sandstones and upper parts dominated by soft-sediment deformation structures and massive sandstone. Rose diagram indicates paleocurrent measurements for all the identified trunk channels.

FA1.2: Erosinal-based, distributary channel fill deposits:

Description:

Facies association sub-group 1.2 (FA 1.2) consists of upward fining, fine to very coarse-grained sandstones successions with occasional conglomerate basal lag deposits. The upwards-fining successions range from 2.0-4.35 m in thickness. Facies association sub-group 1.2 (FA 1.2) is fairly similar to FA 1.1, but has some wider range of lithofacies assemblages and is more abundant in numbers than the larger trunk channel sandstone bodies. Geometries of these channel bodies include concave-upwards high relief erosional scoured lower boundaries, and with straight non-erosive upper boundaries. These channel bodies are observed with pinching terminations into adjacent heterolithic sandstones (FA 2.3). Internal architecture includes lenticular to sheet shaped units with low relief concave-upwards erosional lower boundaries and straight non-erosive to partly eroded upper boundaries.

Thinner channelized bodies (2.0-3.0 m in thickness) observed are possible to trace laterally, and do not exceed widths over 50 m. Conglomeratic trough cross-stratified basal (F1) deposits are only observed in one of these sandstone bodies suggesting that such deposits are of minor importance for these types of channels (fig. 4.3). Paleocurrent measurements conducted on a number of channelized bodies within this thickness interval range from approximately 050-230 degrees (fig. 4.3), indicating a wide distribution of paleocurrent directions. Measurements were conducted mostly on ripples foresets, dune-scale foresets, and by apparent measuring of channel body axis.

The thicker lenticular sandstone bodies range from 3.0-4.35m in thickness. Facies stacking patterns of these channel bodies are dominated by trough cross-stratified medium to coarse-grained sandstones (F2) and soft-sediment deformation structures (F4), similar to the trunk channels. Soft-sediment deformation structures are expressed as chaotic folded to massive horizons and large singular folds and overturned beds. Unlike the trunk channel bodies some of the distributary channel bodies include low angular cross-stratified medium to coarse-grained (F9) and planar-parallel stratified fine to coarse-grained sandstone (F5) beds. The planar-parallel stratified beds included spoon-shaped deformation structures in the top decimeters of the bed. In places, pebble lags dominated by well to sub rounded quartz grains are observed in the base of troughs, in soft-sediment deformed units or planar-parallel stratified layers (fig. 4.3, B-C).

Lenticular sandstone bodies between 2.0 and 3.0 m in thickness show a larger variability of lithofacies assemblages. Two channelized sandstone bodies located in the lower 50 m of the Aspelintoppen Formation consist of medium to coarse-grained tabular cross-stratified beds (F8), soft sediment deformed beds, including rip up clasts, and upper beds dominated by very fine to fine-grained sandstones with current ripple cross-lamination (F13), combined flow ripple cross-lamination (F11) and soft-sediment deformation (F4) structures. The rest of the beds observed are entirely dominated by soft-sediment deformation structures similar to the ones described above, and include abundant basal mud-clast and organic fragments.

Intepretation:

The erosinal scoured concave upwards sandstone bodies with apparent fining upwards trends and limited lateral extent are interpreted as mostly single story fluvial channels (thinner channel bodies). The larger facies variety, paleocurrent distribution and single storey appearance of the thinner channel bodies between 3.0-2.0 m suggests that they represent different channel types. Apart from the thinner channel bodies six thicker bodies are observed. These bodies contain multiple internal scoured surfaces pointing too a multistory fluvial channel origin (thicker channel bodies). The thicker channelized sandstone bodies between 3.0-6.0 m are suggested to represent major distributary channels.

The facies stacking patterns, channel geometries and the radial distribution of paleocurrent directions emphasize the distributary nature of most of these channels (Nichols and Fisher, 2007). The dominance of concave upward scoured trough cross-stratified sandstone (F1, F2) units, with occasional pebble lag, coal fragments and mud clasts in the base of channels bodies indicate moderate to high-energy flow conditions. Occurrence of two-dimensional dune structures indicates lower flow velocity conditions, which coincides with the distributary channel interpretation. The coarser deposits near the channel bases are interpreted as basal lag deposits. The absence of lateral accretion beds, dominance of homogenic sandstone fill, and their lenticular geometry suggests that channel infill was generated by migration of highly aggradational transverse dunes. The range of soft-sediment deformation structures (F4) interbedded in these channel bodies are generated by processes, all of which are assumed to be syn- or post-depositional structures. Channel bodies with lateral continues units dominated by soft-sediment deformation are suggested to indicate tectonic activity (Kundu et al., 2011), while larger singular features like folds and overturned beds probably are developed by channel bank slides caused by channel bank instabilities generated by major tectonic events, or simply by high shear stress on the channels bottom (fig. 4.3, C). Smaller deformation structures observed in planar-parallel laminated beds are suggested to have developed as water migrates out of the water saturated sediments, developing distinct spoon-shaped deformation structures (fig. 4.3, A).

Channel bodies dominated by planar cross-stratified sandstones (F8), located in the first 50 m of the formation, are suggested to represent terminal distributary channels close to the delta front associated with tabular cross-stratified sandstones interpreted as potential mouth bar deposits (Olariu and Bhattacharya, 2006). The remaining channels show lithofacies stacking patterns dominated by soft-sediment deformation (F4) and occasionally low angular cross-stratified sandstones (F9) suggesting deposition during major floods as larger crevasse splay channel features.

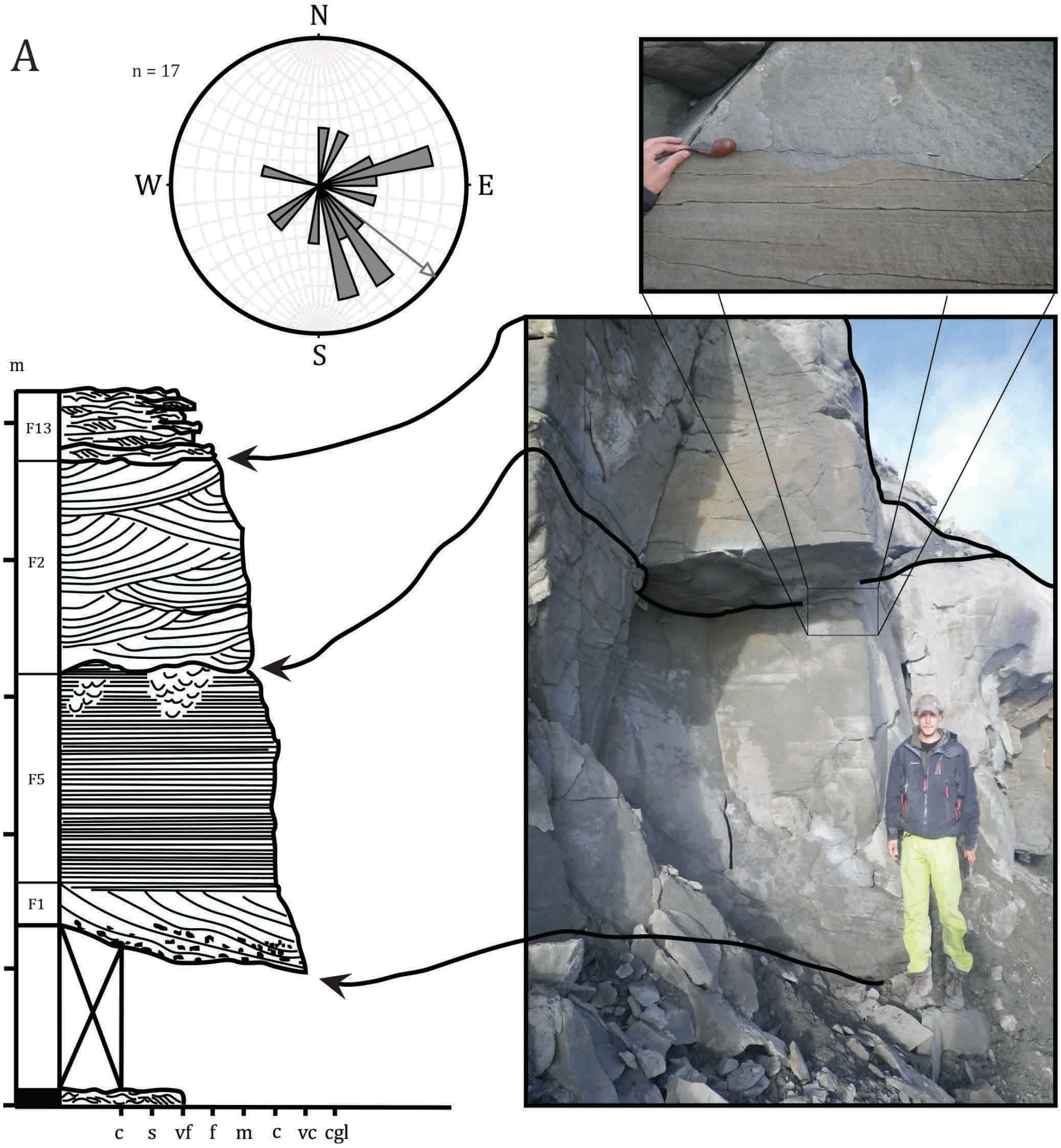
A
n = 17
N
E
S
W
m
F13
F2
F5
F1
0
1
2
3
4
5
c
s
vf
f
m
c
vc
cgl

B

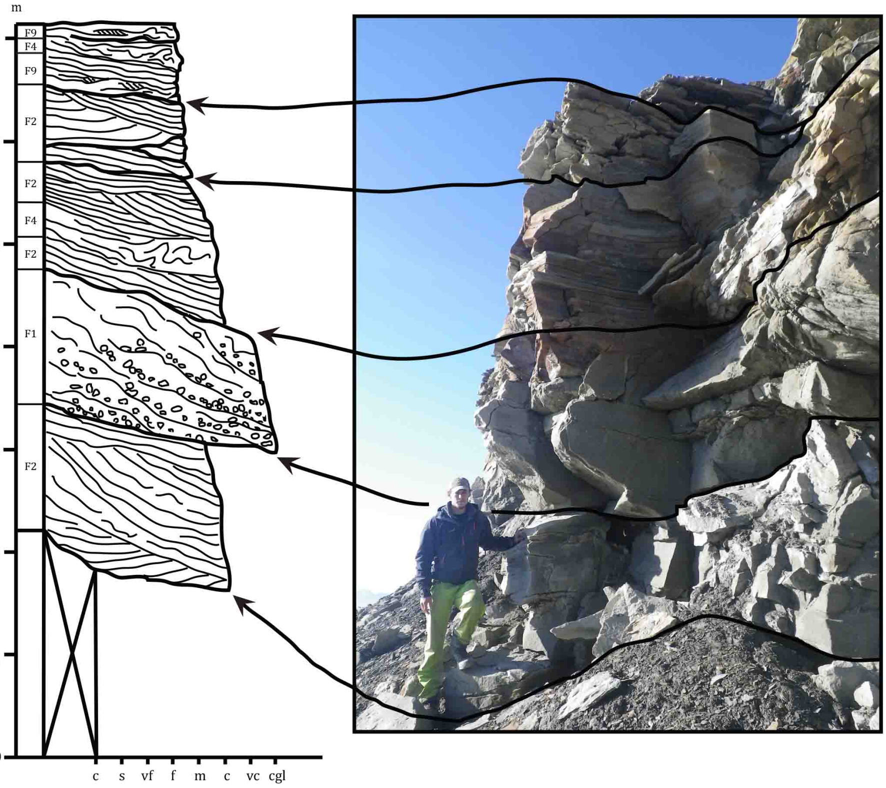

C

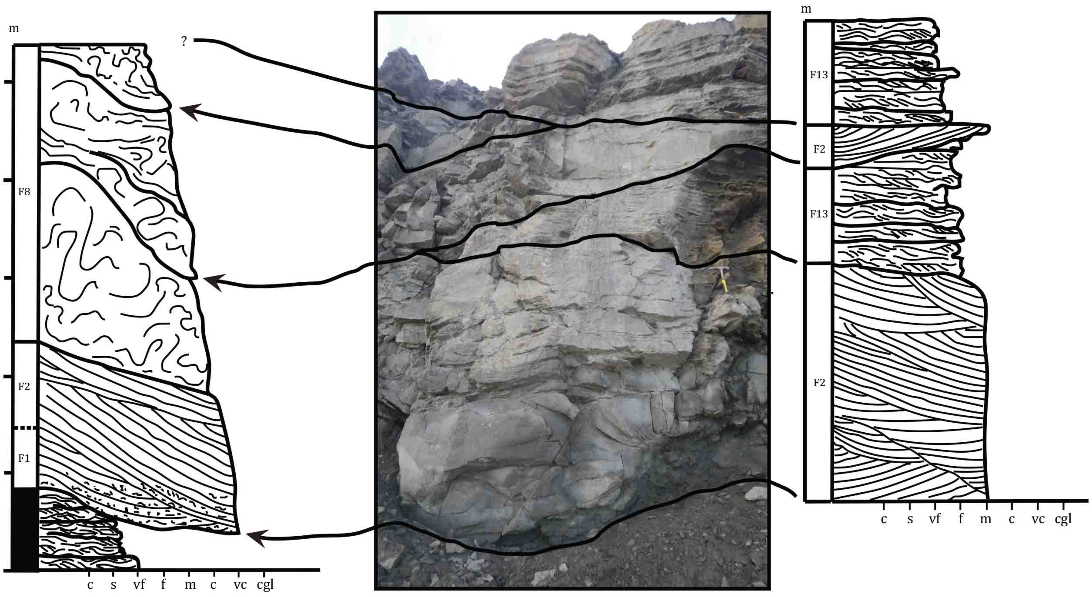

Fig 4.3: Multistorey and possibly single story distributary channels. A) Two story channel, including conglomeratic basal lag overlain by UFR planar parallel stratified sandstones which is partly eroded by a upper through cross stratified unit. B) Two to Three story channel including a lower unit dominated by trough cross-stratified coarse grained sandstones eroded by a overlying basal cross-stratified conglomerate which continues into a top unit dominated by trough cross stratified very coarse to coarse grained sandstones and occasional soft-sediment deformed intervals. C) Single to two story channel consisting of a lower basal through cross-stratified unit including large amounts of coal fragment passing into soft-sediment deformed rocks which dominated the channel body. Individual storys or sandstone units pinch into adjacent heterolithic levee deposits of FA 2.3. Rose diagram indicates paleocurrent measurements for all distributary channel bodies recognized.

4.2.2 Facies association 2: Interchannel deposits:

Facies association two (FA2) consists of heterolithic deposits of alternating shales and very fine to medium grained sandstones. The fine to medium grained sandstones occurs as extensive sheets characterized mainly by coarsening upward and subordinate fining upward trends.

Scree covered intervals by debris make up the largest portion (close to 40-50%) of the Aspelintoppen Formation at Brogniartfjella. These intervals are assumed to be dominated by less cohesive shale, siltstone and thin coals. When looking along the mountainside, the scree-covered intervals appear as segments of gentle slopes between the successive sandstone cliffs. Because of the scree cover it is hard to determine the exact distribution of these deposits. From the present observation carried out at the western part of Brognartfjella it is reasonable to say that FA2 is by far the most abundant of the sandstone dominated facies associations. This has also previously been reported by (Dreyer and Helland-Hansen, 1986).

In order to better categorize the interchannel deposits, these deposits are grouped into six facies association sub-groups; 1) distal floodplain deposits, 2) distal crevasse splay sheet deposits, 3) heterolithic levee deposits, 4) crevasse splay channel deposits 5) proximal crevasse splay sheet deposits, 6) interdistributary bay fill deposits.

FA2.1: Distal floodplain deposits.

Description:
The facies association mainly consists of shale, siltstones and locally, lenses of very fine-grained sandstones (fig 2.3 A-B). These intervals range from 1.0-6.0 m in thickness and alternate with sandstone bodies, and are commonly covered by scree.

The best exposures occur just above and underneath channelized sandstone bodies (FA 1). The following descriptions are therefore based on these limited exposures (fig 2.3, A-D). The fine-grained (F15) intervals typically contain abundant amounts of fragmented organic detritus, plant imprints, root traces, siderite and pyrite concretions (fig. 4.1, X and 4.4, D) and thin (2-10 cm) coal layers (F16) (fig. 4.4, A, C). Less frequently observed are immature soil profiles (F17) (figure 4.1, X, 4.4, D), which mostly occur underneath channel bodies, and are characterized by a red brown color.

In places, 5 to 50 cm thick sheets or wedges (FA 2.2) of very fine- to fine-grained, current ripple cross-laminated sandstones (F13) and soft-sediment deformation structures (F4) (figure 4.4, A-B) occur within the fine-grained intervals (F15) (further described (FA2.2). The lateral continuity of these fine-grained intervals often exceeds the outcrops width (figure 4.4, A).

Trace fossils observed in this facies associations include; *Arenicolites*, *Archaenossa*, *Cylindricum*, *Helminthoidichnites*, *Koupichnium*, *Planolites* and *Scoyenia* (see chapter 5).

Interpretation:
The abundance of fine clay and silt material suggests deposition from suspension.
The fine grain-size, lamination of sediments and deposition by suspension lateral extent of this facies association suggests that these sediments were deposition within a low energy environment. The occurrence of immature soil profiles, organic detritus, root traces and plant imprints suggest that the sediments were a sub-aerially in periods. Thus it is suggested that this association was deposited in a floodplain setting. The suspended material is brought to the floodplain by overbank flooding of nearby fluvial channels, which probably left the floodplain under water for longer periods of time.

The paleosols (F17) are generally poorly developed and include large quatities of siderite and iron nodules (fig. 4.1, X and 4.3, A, D). This indicates that the floodplain was poorly drained. Paleosol maturity tends to reflect the distance from the active channel or the frequency of flood episodes (Willis and Behrensmeyer, 1994). Trace fossils assemblages resemble a mix of the *Scoyenia* and *Mermia* ichnofacies. The *Mermia* ichnofacies was introduced by Buatois and Mángano (1998) to make a separate ichnofacies for freshwater aquatic trace fossils. The presence of the *Mermia* ichnofacies in the investigated succession supports previous suggestions that areas of the floodplain remained under water for longer periods of time (Grundvåg et al., 2014a; Uchman, 2004). At Brogniartfjella, marine influence as observed in some studies (Grundvåg et al., 2014b; Plink-Bjørklund, 2005; Uchman, 2004), are limited to the lower parts of the formation and only occur sporadically.

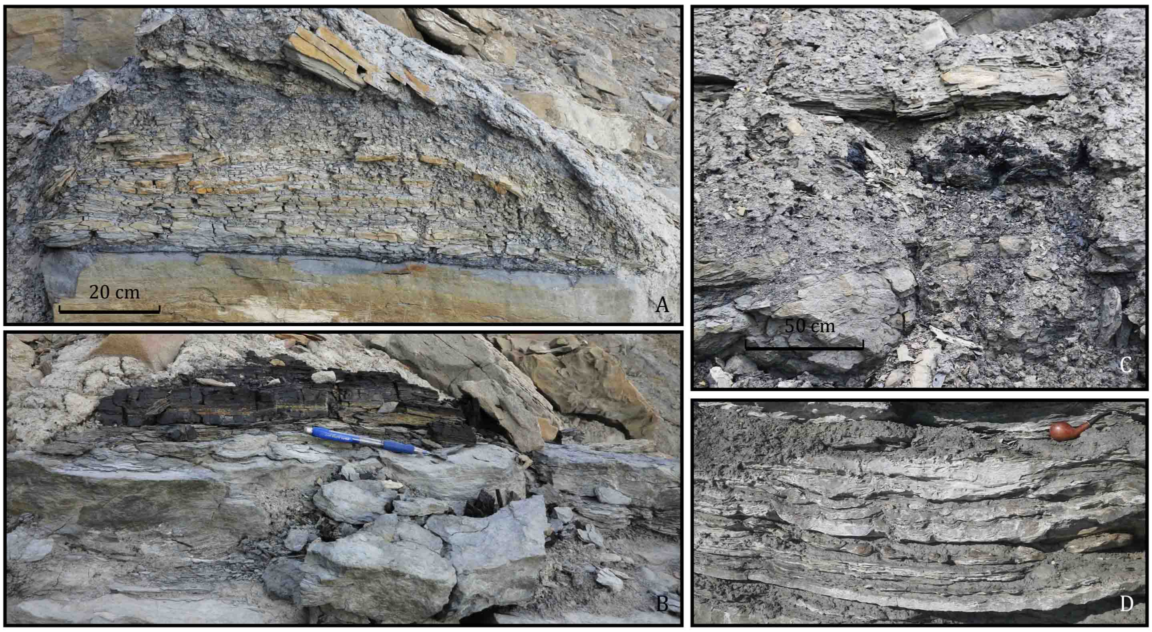

Fig 4.4: Shale and mudstone dominated deposits. A) Organic rich shale with siltstone to very fine grained sandstone lenses, overlying isolated sandstone body of FA 2.2 or amalgamated sandstone body of FA 2.5. B) Shales interval with overlying coal layer. C) Shales dominated interval including coal lenses, underlying channelized sandstone body. D) Thin bedded heterolitic sandstone sheets with thin shale layers including siderite concretions.

FA2.2: Distal crevasse splay or levee sheet deposits.

Description:

Facies association 2.2 consists of thin normal graded siltstones and very fine-grained sandstone lenses that form heterolithic sheet-like units ranging from 5-50 cm in thickness.

These fine-grained silt and sandstone lenses alternate with the shale-dominated units of FA 2.1 (fig. 4.5, A). Thicker, tabular beds occur in some of the thicker units. Beds typically pinch out into surrounding shale (fig. 4.5, A). The upper bounding surfaces of the heterolithic sandstone sheets are sharp and weakly undulating, and the lower surfaces are sharp straight to low relief concave upwards. Sedimentary structures within the sandstones include current ripple cross-lamination (F13), climbing current ripple cross-lamination (F14) (figure 4.5, B) and soft-sediment deformation structures (F4). Less frequently observed are dune-scale tabular cross-stratified beds (F8). The orientation of current ripple foresets is often random with a wide range of paleocurrent directions, although with a minor tendency towards the southeast.

Bioturbation is restricted to root traces, leaf imprints including leaf undermining and sporadically occurring *Arenicolites*, *Scoyenia* and *Cylindricum* (see chapter 5).

Interpretation:

The thin fine-grained heterolithic sandstone sheets dominated by current ripples, which occur in shale dominated intervals, and include root traces, leaf imprints and sporadically occurring *Scoyenia* ichnotaxa are suggested to be related to distal crevasse splays or levees, reaching far out on the floodplain.

The sheets are generated by deposition of migrating ripples (F13+F14) and possibly minor dunes (F4+F8) over the floodplain. Dunes are not commonly observed, but some of the soft-sediment deformed sandstone sheets, may have included dune-scale stratification before the secondary deformation occurred. This associations' occurrence within the fine-grained floodplain deposits (FA 2.1) suggests deposition by sheet-floods reaching far out on the floodplain.

The low relief concave-upwards lower surfaces are interpreted as minor erosion by the initial flooding episode transporting the sediments to the floodplain. These minor depressions will act as sediment tracts during seasonal floods for sediment transport out on the floodplain. These sedimentary units are suggested to correspond to Smith et al. (1989) second to last stage in their three stage model for the evolution of crevasse splay systems. This stage consist of elongated bodies with lower channel density, lower channel width/ depth ratios including thin lateral extensive levees of finer sediments (further described in chapter 6). Some of these deposits are suggested to prograde into interdistributary bays as smaller mouth bars (further described in FA 2.6).

Trace fossils include Root traces and Leaf traces including leaf underminings. These trace fossils established under calmer periods between floods. The occasionally occurring *Scoyenia* and *Cylindricum* trace fossil is suggested to develop in areas where sediments are deposited into standing water.

Figure 4.5: Isolated sheet sandstones. A) Very fine-grained ripple dominated distal sandstone sheets, with overlying coal horizons. B) Approximately 0.5 m thick very fine- to fine-grained sandstone sheet dominated by current ripples structures. Tobacco pipe for scale (5 cm).

FA2.3: Levee deposits

Description

Facies association 2.3 comprises heterolithic units that consists of thin-bedded siltstones, normal-graded very fine to fine grained sandstones and interbedded shale. These deposits develop heterolithic sheet-like units that rang in thickness from 0.5 to 4.0 m. Individual sandstone beds sets ranges from 5.0 to 20.0 cm, and shale units from bed sets ranging from 0.5 to 2.0 cm in thickness.

Sedimentary structures are mostly present in the very fine to fine grained sandstones and include current ripple cross-laminated (F13), plane-parallel stratification (F10) to slightly undulating lamination (F14) and subordinate occurrence of massive (F3) and soft-sediment deformed beds (F4) (fig. 4.6, A-C). Basal bounding surfaces are sharp and non-erosive to undulating and erosive, whereas the top surfaces are typically sharp to transitional. The shale include abundant siderite concretions and organic detritus.

The normal graded sandstone beds typically promote massive or soft-sediment deformed lower parts (F3+F4), followed plane-parallel (F10) and current rippled (F13+F14) parts. In proximity to the channels (FA1), this facies association tends to become more sandstone-dominated. Vica versa, tracing the heterolithic sheets laterally from the channel margins, they commonly pinch out and shale intervals become more abundant. The heterolithic units commonly show coarsening upwards grain-size trends, and are typically topped by thicker floodplain shales (FA 2.1) or eroded by channelized sandstone bodies (FA 1).

Trace fossils observed in the heterolithic deposits include; surfaces penetrated by carbonaceous root traces, *Arenicolites*, *Scoyenia* and occasionally *Skolithos* (described in chapter 6), as well as leaf imprints and sideritized horsetail plants (fig. 4.6, B-C). The root traces, leaf imprints and horsetail plants occur regularly in the top parts of sandstone beds and interbedded shale.

Interpretation:
The heterolithic units of alternating thin-bedded sandstones and shale are interpreted to represent prograding to aggrading levees, deposited by flooding episodes on and across fluvial channel levees. Normal grading of individual beds suggests that the deposits were laid down from density currents.

Massive and soft-sediment deformed beds were generated from pulses of sediment spill-over from the channel banks. These flows travel downslope along the levee and may slightly erode earlier deposits. As the flow decelerates plane-parallel and current ripple cross-laminated sandstone deposits form and eventually as the flow has decelerated sufficiently suspended fine-grained material fall out of suspension generating normal graded beds. These type of deposits have earlier been documented by among others Farrell (2001), which described them as Bouma-like sequences (Bouma, 1964).
Each of the normal graded sandstone beds was interpreted by Farrell (2001) to represent deposition from waning flows that was initiated by successive river floods. Each normal graded sandstone bed is subsequently, typically separated by shale units containing root traces, siderite concretions, horsetail plant and leaf imprints indicating calmer periods of time. The shale units containing siderite concretions are interpreted as immature paleosols, related to poorly drained areas.

Limited erosion, abundance of current ripple cross-laminated beds, the thickness of the deposits and the limited vertical distance between each rooted horizon, with related immature paleosols, suggest that flooding episodes occurred frequently. Units where shale is absent are interpreted as proximal levee deposits, while units where shale are more abundant coincide with more distal levee deposits. The occurrence of horsetail plants could indicate that parts of the levee were flooded by shallow water for longer periods.

Paleocurrent measurements conducted in the levee deposits (fig. 4.6) indicates that the sediment filled flood generated pulses, generated fan shaped patterns, with ripples propagating parallel, perpendicular to or against the channel where the current propagated from.

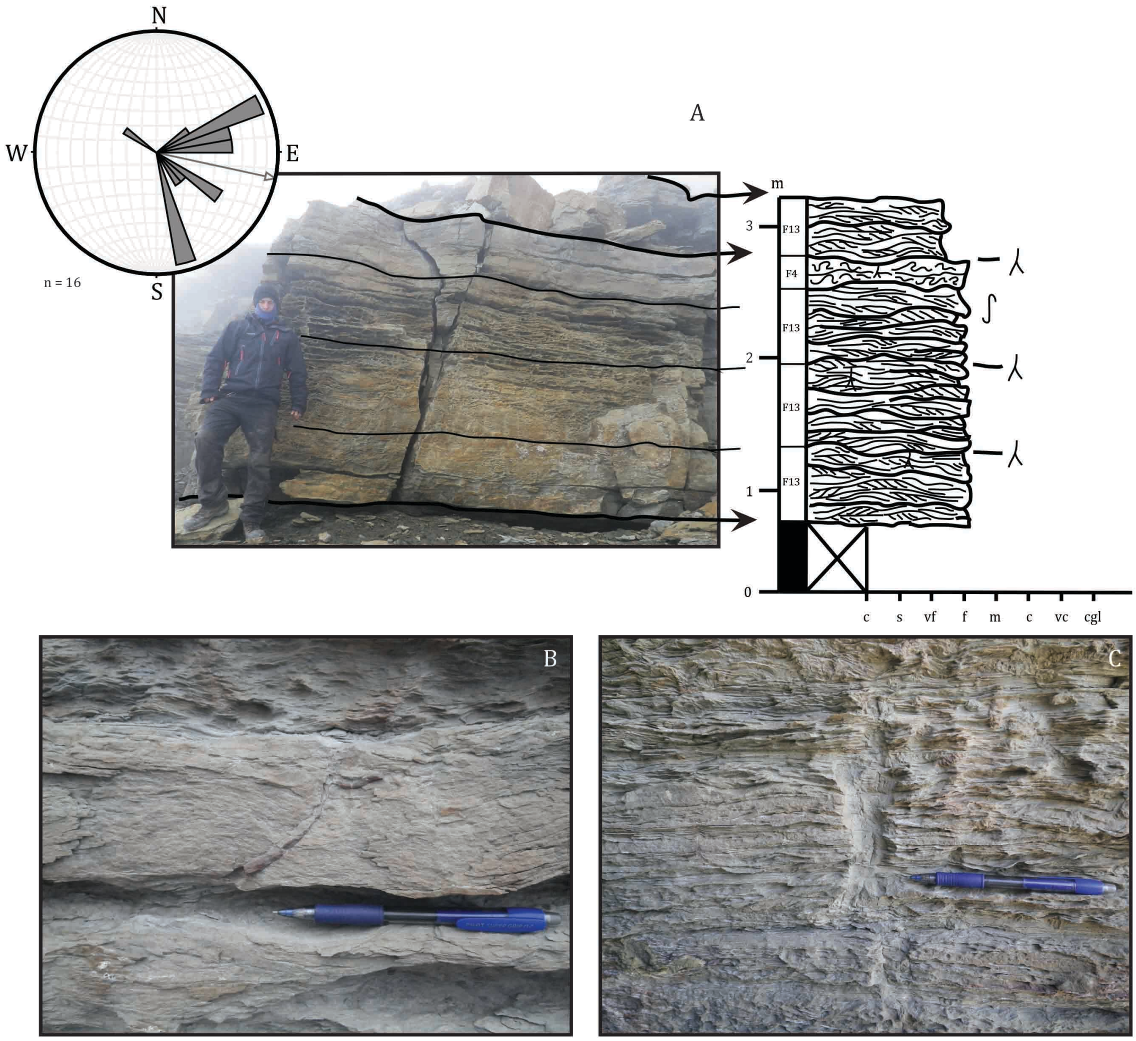

Figure 4.6: Heterolithic levee deposits. A) Heterolithic sandstone sequence approximately 2.5 m thick with no apparent vertical grain-size changes accept in the uppermost 30-40 cm where there is a small fining-upward -trend. B) Close-up picture of heterolithic unit showing current ripple (F13), highly aggradational climbing ripples (F14), possibly wave ripples in the uppermost sediments (F12) and sub horizontal horsetail plant, typical for this facies association. C) Close-up picture of heterolithic units consisting of current ripple and planar parallel laminated very fine-grained sandstones. The sediments lamina is also partly disturbed by roots penetrating the sediments. Rose diagram indicates the paleocurrent directions measured in selected heterolithic units distributed over most parts of the Aspelintoppen Formation.

FA2.4: Crevasse channel deposits:

Description:

Facies association 2.4 consists of 0.3 to 2.2 m thick fine- to coarse- grained fining-upward sandstone bodies. The sandstone beds range from 0.3 to 1.5 m in thickness, and have concave upward bases and straight non-erosive upper boundaries. The upper boundaries are often sharp to overlying floodplain shale (FA 2.1) and proximal crevasse splay sheets (FA 2.5). The sandstone units form ribbon shaped bodies with wings that pinch out into adjacent floodplain shales (FA 2.1) or levee deposits (FA 2.3) (fig. 4.7). Sandstone bodies occur for most cases as single storey bodies, but some of the largest bodies include up to two storys. Basal deposits tend to be dominated by massive (F3) to soft-sediment deformed (F4) fine to coarse grained sandstones, including mud-clasts and plant detritus, but dune-scale low angle cross-stratified (F9), trough cross-stratified (F2) and planar cross-stratified (F5) fine to coarse-grained sandstones are also observed. Towards the top of the fining-upward units, current (F13) and climbing current (F14) ripple cross-laminated sandstone beds are abundant. These generate several centimeters thick heterolithic units similar to the once associated with distributary and trunk channel levee deposits (FA2.3).

The fining-upwards sandstone units are often observed eroding into heterolithic levee and floodplain shale deposits and locally include several units stacked on top of each other (fig. 4.7). Sandstone bodies are laterally well exposed and can be traced out at many locations. The lateral exposure of the axis of these lenticular-shaped units, in addition to foresets in dunes and ripples, makes it possible to measure apparent paleocurrent direction within the units. The paleocurrent directions indicate a large range in paleocurrent directions, and can differ as much as 180 degrees from one another (fig. 4.7).

Carbonaceous root traces are often observed penetrate the overlying current rippled sandstones and shale deposits, locally disrupting the top most lamination.

Interpretation:

The erosional based ribbon shaped sandstone bodies are interpreted as ephemeral crevasse channels developed by flooding episodes breaching the banks of trunk or larger distributary channels (FA 1).

Massive (F3) and soft-sediment deformed (F4) deposits with associated mud-clasts and plant detritus are interpreted as sediments derived from the initial riverbank breach, as well as basal lag deposits. Above the basal deposits, the various cross-stratified sandstones (F2, F5, F9) indicate migration of bars deposition during peak flood. Current and climbing current ripple cross-laminated beds (F13 + F14) indicate deposition by several pulses of suspended sediments under waning flow conditions. Overlying shale intervals indicate channel abandonment and where probably deposited in standing bodies of water. It is within the rippled sandstone and laminated shale layers the rooted horizons occur, marking periods of emergence between floods (Farrell, 2001).

The paleocurrent direction measurements conducted proposes that these channels builds out perpendicular to the larger channel units, which have a mean paleocurrent direction towards the southeast.

The evolution of the crevasse channels is further discussed in chapter 6, under type 1 channels.

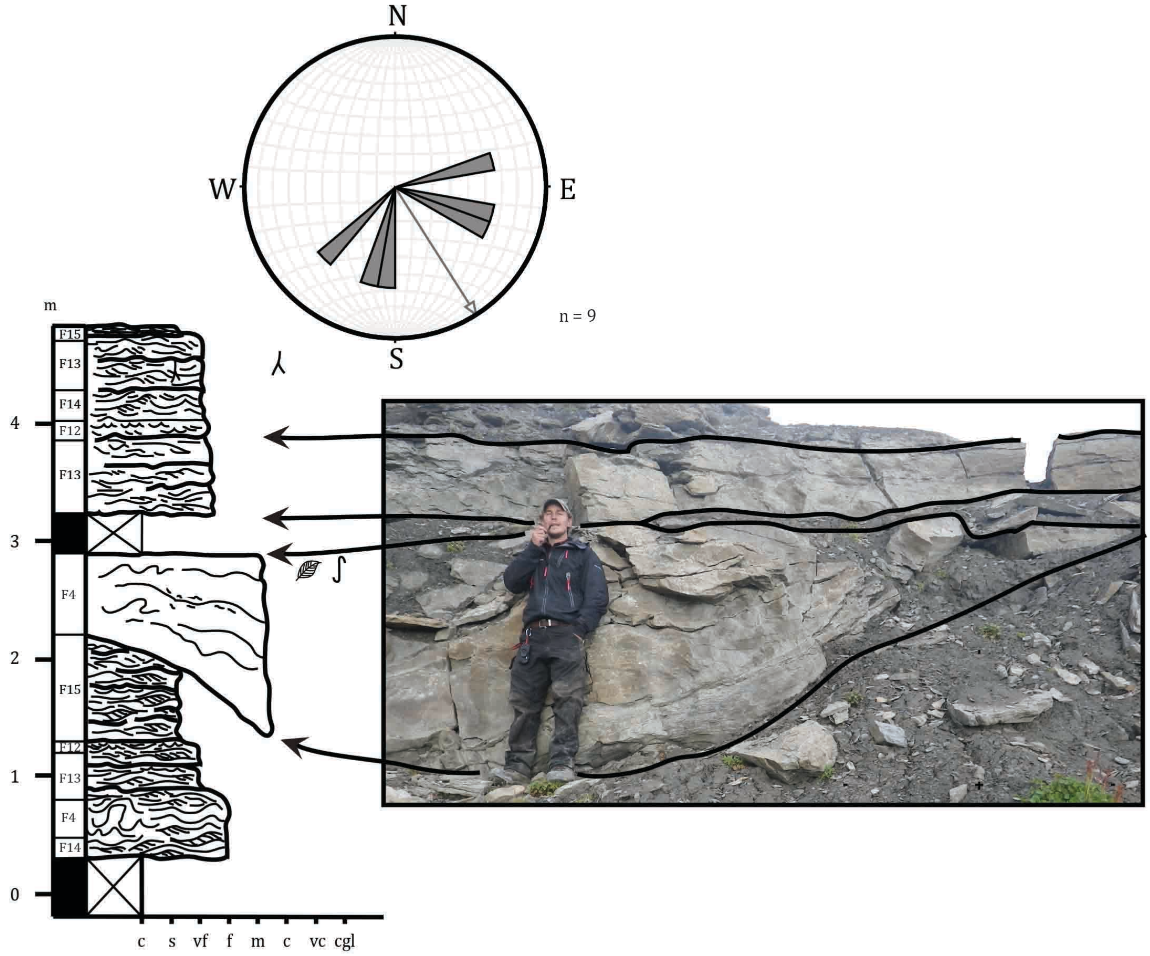

Figure 4.7: Fining-upwards erosional based crevasse channel. It comprises massive to weakly cross-stratified medium to coarse grained sandstones, and erode down into underlying floodplain shale (FA 2.1) and crevasse splay deposits (FA 2.5). Rose diagram represents scattered measurements of crevasse splay channels of the Aspelintoppen Formation.

FA2.5: Proximal crevasse splay deposits.

Description:

The facies association consist of alternating layers of normal graded very fine to medium grained sandstones and thin interbedded shale layers. The sandstone beds range from five to 50 cm in thickness, and typically form sheet-like units up to five m thick. The beds are bounded by undulating and erosional based lower surfaces, with reliefs rarely exceeding some few centimeters. Upper bed surfaces are normally transitional from sandstones into floodplain shale (FA 2.1).

These sheet-like normal graded sandstone beds are often lateral extensive and are often observed pinching into surrounding floodplain shale. These sandstone beds typically comprise massive (F3), soft-sediment deformed (F4), planar-parallel (F11) or low angular cross-stratified (F9) sandstones in the lower parts of each bed. The upper part typically consists of fine grained sandstone and siltstone, and includes a variety of structures: current ripple cross-lamination (F13), gently to supercritical climbing ripple cross-lamination (F14), planar-parallel lamination (F10), soft-sediment deformation (F4) and less frequently wave ripple cross-lamination (F11).

Units of alternating normal graded sandstone beds and interbedded shale typically generate coarsening upward trends, with each normal graded sandstone bed getting successively thicker and coarser upwards (fig. 4.8, A). Less frequently observed are fining upward units (fig. 4.8, B). Locally these coarsening and fining upward units develop composite units of coarsening upward trends in the lower part and fining upward trends in the upper part (see log in appendix). These packages are typically located in the lower half of the logged section, and form up to several meters thick coarsening upward units with overlying fining upward units up to a couple of meters thick.

Moving upwards in the logged section, beds of this facies association becomes increasingly coarser from very fine to fine grained sandstones to some beds as coarse as medium-grained sandstone. Composite units of coarsening and fining upward trends are here less prominent, and units tends to be thinner, typically ranging from 1.0 up to 3.0 m in thickness (see log in appendix).

Bioturbation in this facies association is estimated to be of a moderate degree, compriseing the following trace fossils; Root Traces, Leaf Trace with Leaf Undermining, *Arenicolites*, *Archeonossa*, *Scoyenia* and *Skolithos*.

Interpretation:
The alternating normal graded sandstone beds and interbedded floodplain shales developing predominantly coarsening upward units and more rarely fining upward units, which are interpreted as proximal parts of crevasse splay systems.

Crevasse splays are thought to have generated the sheet-like normal graded sandstone beds as high water or floods breaches and exceed height of the levees.

The associated coarsening and fining upward units are suggested to develop, as crevasse splays systems are prograding (fig. 4.8, A) or retrograding (fig. 4.8, B) from their related source respectively (Elliott, 1974). Progradation occurs because crevasse splays successively reach farther out on the floodplain, while retrogradation occurs as the flood velocity decreases, as water levels are lowering, leading to less sediments being transported through the related crevasse (Elliott, 1974). The thicker coarsening upward units in the lower parts of the logged section

Massive (F3), soft-sediment deformed (F4) and low angular cross-stratified bed (F9) is associated with migration of dunes on to the floodplain. Current ripple cross-laminated (F13) and climbing current ripple cross-laminated (F14), with locally occurring planar-parallel (F10) and soft-sediment deformed (F4) beds develop similar to the ripple dominated bed described in FA 2.3. The current rippled, planar parallel laminated and soft sediment deformed sandstone beds of this facies association differs from the ones observed in FA 2.3 as they are coarser grained and have much less consistent vertical grain-size trends. The are subsequently important features of the interpretation of crevasse splays (Farrell, 2001). The coarser grained crevasse splay sandstones occurring in the upper part of the formation (see log in appendix) are suggested to either be deposited closer to the related central channel (FA 1), or to indicate more proximal areas of the fluvial system. The lower-lying floodplain constitutes higher amounts of accommodation space than the levees (FA 2.3) and would therefore be more prominent for accumulating sediments during flooding episodes. This is observed from the thicker crevasse splay complexes occurring in the lower parts of the logged section (see log in appendix).

The alternating crevasse splay deposits of this facies associated are linked to low-sinuous fluvial channels (described in FA1.1) and locally develop relatively thick sandstone-dominated splay complexes, with multiple branched crevasse splay channels. These are comparable with similar systems reported by Smith et al. (1989), Farrell (2001) and Stouthamer (2001).

Wave rippled cross-stratified (F11) beds observed in the upper part of some beds indicates that deposits were partly covered by water in order for these types of structures to occur. The occurrence of *Scoyenia* ichnofacies trace fossils support this interpretation, while the occurrence of Root traces, Leaf Trace with Leaf Undermining indicating that these deposits are mostly of fluvial origin and not influenced by marine processes.

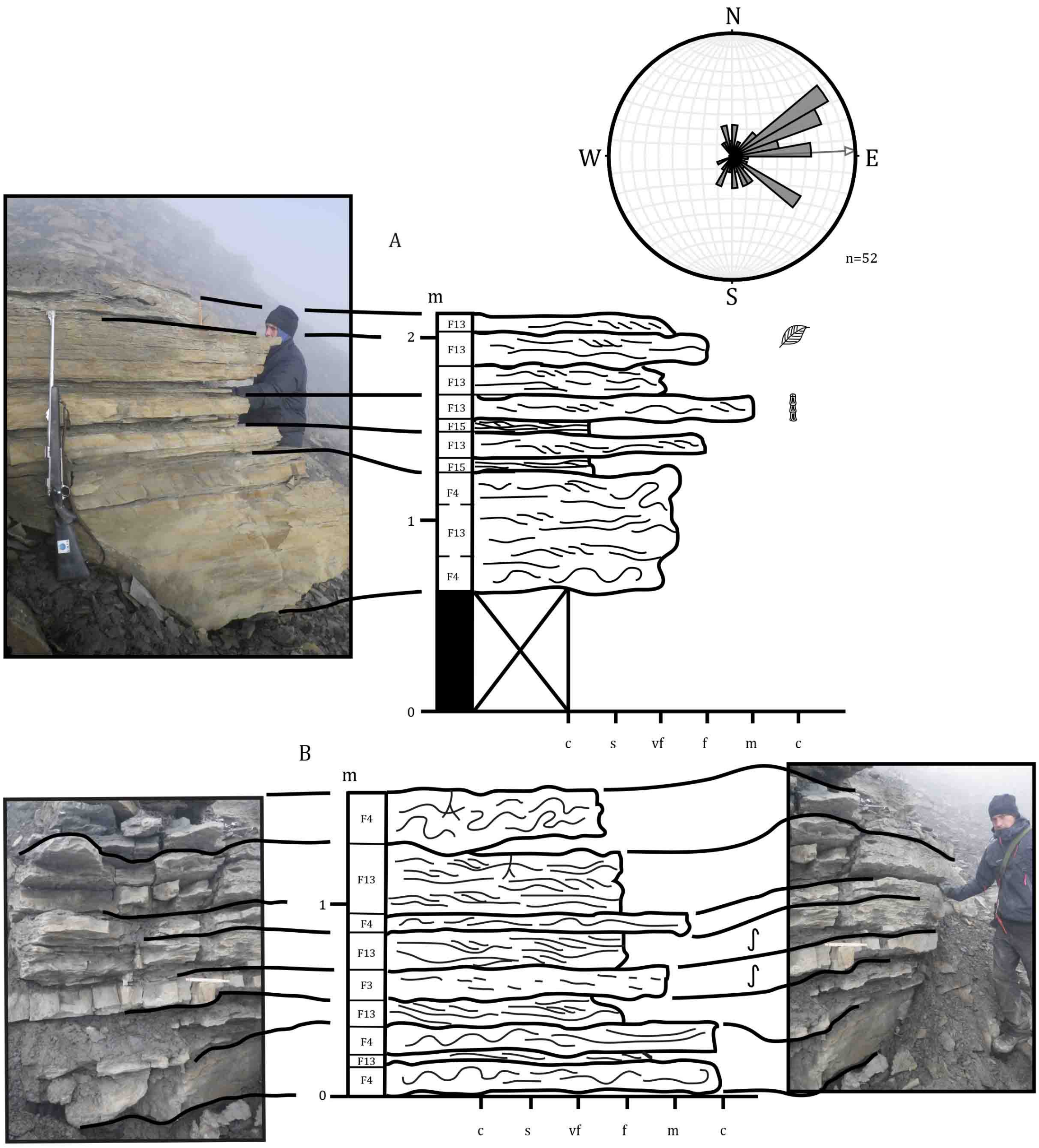

Figure 4.8: Proximal crevasse splay deposits. A) Alternating sheet-like sandstone beds and interbedded shale are indicated by up to 20 cm thick sandstone sheets on top of an approximately 50 cm thick crevasse splay channel sandstone bed. Beds are dominated by

current ripple (F13) structures. The weak coarsening upward trend indicated from the lower to the middles sheets indicates crevasse splay progradation. B) Alternating sheet-like sandstone beds ranging form approximately five to 25 cm in thickness, dominated by current rippled (F13), soft-sediment deformed (F4) and occasional massive (F3) sandstones, showing an overall FU-trend indicating retrogradation of crevasse splay system. Rose diagram indicated paleocurrent measurements conducted on amalgamated deposits over the whole length of the Aspelintoppen Formation.

FA2.6: Interdistributary bay fill deposits.

Description:

Facies association 2.6 (FA 2.6) consists of 1.0-2.5 m thick very fine to medium-grained units where individual beds range from 10-60 cm in thickness.

These beds are stacked developing sequences with overall coarsening upward and thickening upward trends. The lowermost beds comprise current ripple cross-laminated (F13), supercritical to gently climbing current ripple cross-laminated (F14) and soft-sediment deformation structures (F4), and occasional wave ripple cross-stratified very fine-fine grained sandstones (figure 4.9, B). The upper beds are commonly up to 60 cm thick and consist of trough cross-stratified (F2) low angular cross-stratified (F9), and soft sediment deformed sandstones (figure 4.9). The lower current ripple dominated sandstones promote sharp and straight non-erosive upper and lower boundaries, while upper dune-scale cross-stratified sandstones promote straight non-erosive upper and straight to low relief concave upward bases.

Wave ripple cross-lamination (F11), current ripple cross-lamination (F13), carbonaceous root trace and sideritized horsetail plants are also observed on top of coarsening-upward units. Bed boundaries are often sharp and non-erosive in the lower parts and sharp to slightly undulating in the upper parts. Sandstone beds are commonly separated by centimeters thick silt and shalestones. Recognized trace fossils include *Scoyenia* and *Skolithos*, *Cylindricum*, *Helminthoidichnites*, *Lockaia*, and possibly *Atrophod* tracks.

Interpretation:

The coarsening and thickening upward units is interpreted as minor mouth bar systems prograding into interdistributary bays (Elliott, 1974). Typically, because they are prograding, the mouth bars will develop clear coarsening upward trends with successively thicker and coarser beds upward. Water depth are possible to estimate from the thickness of the associated deposits (Bridge, 2009), and will for these sequences range from 1.0-2.5 m in thickness. It is important to emphasize that these estimated depths will only reflect the minimum depth of the depressions. Sediments transported was promoted by river floods feeding water and sediments into crevasse splay channels, which scoured both crevasse splays on the floodplain and minor mouth bars in interdistributary bays.

Finer grained ripple cross-laminated sandstones are interpreted to be deposited under waning flow conditions, by pulses of suspended material get deposited by migration of current ripples. Coarser dune-scale cross-stratified sandstones are interpreted as dunes migrating from the proximal parts of the mouth bars into the embayments, possibly with the initial flow partly eroding into underlying deposits.

Trace fossil assembledges are typical for the *Mermia* ichnofacies (Buatois and Mángano, 1998). The *Skolithos*, *Lockaia* and occasional atrophod tracks are associated with marginal lacustrine trace fossils of the *Scoyenia* ichnofacies. Both these ichnofacies assembledges indicate lacustrine fresh water conditions. This facies association is hard to distinguish from the coarsening upward units of FA 2.5 but differs with absent or less pronounced fining upward bed sets and the occurrence of the *Mermia* ichnofacies.
Paleocurrent measurements were conducted in the intervals in-between channelized sandstone units. The recorded paleocurrent direction indicates a radial distribution with directions ranging between 45 and 180 degrees, and a mean paleocurrent direction towards the southeast.

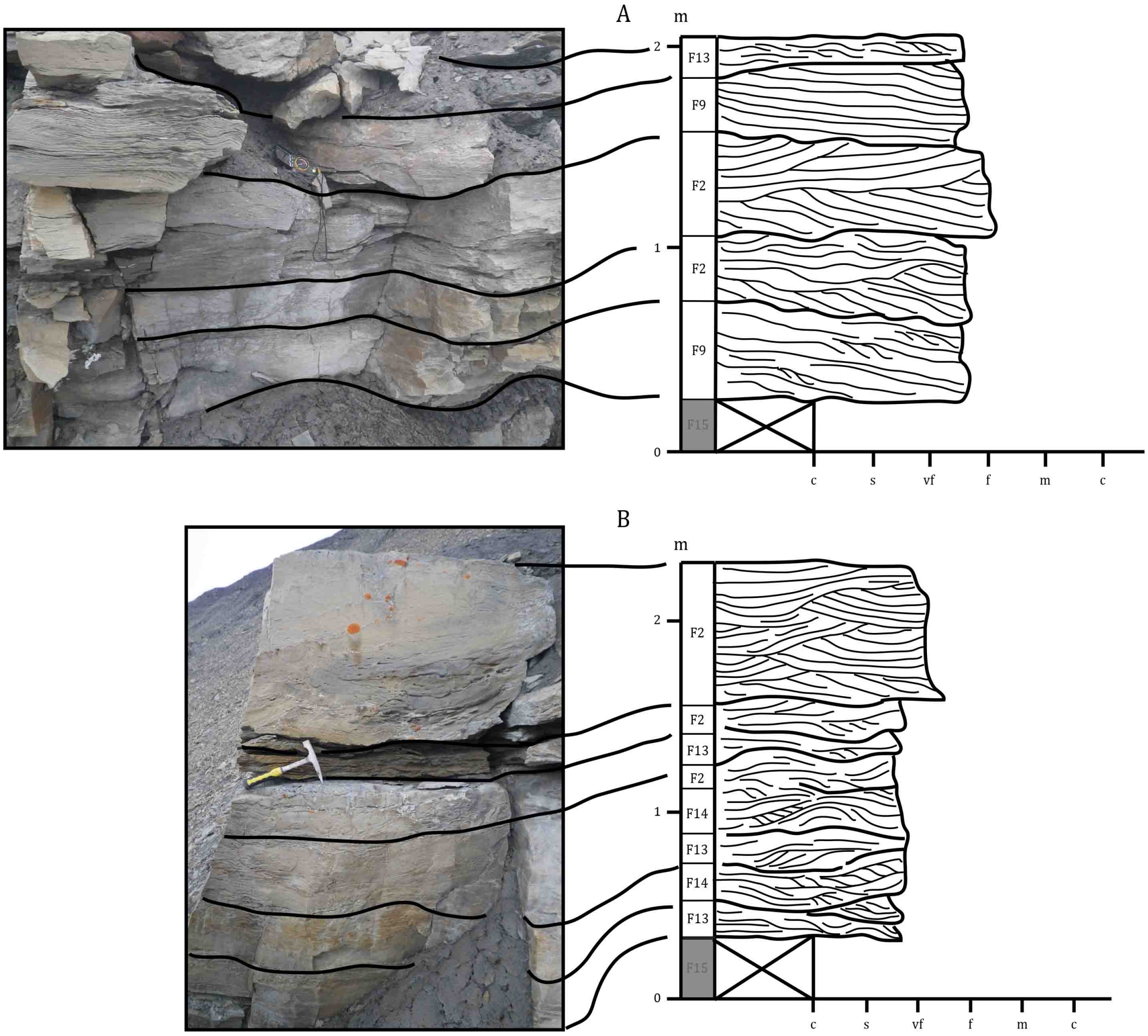

Figure 4.9: Coarsening and thickening upward lacustrine sandstone deposits. A) Up to 50 cm thick cross-stratified sandstone beds overlying lfloodplain shale (FA 2.1) and topped by current ripple (F13) dominated sandstones. Sandstone units shows a weak coarsening and thickening upwards trend indicating the lacustrine origin (FA2.5). B) Coarsening and thickening unit consisting of shale overlain by current (F13) and climbing (F14) ripple dominated very fine sandstone beds up to 25 cm thick capped by dune-scale cross-stratified beds. Beds show a prominent coarsening upwards trend.

4.2.3 Facies association 3: Shallow marine to marginal deposits:

The uppermost parts of the Battfjellet Formations contain upwards-coarsening units of tabular to tangential cross-bedded sandstones interbedded with wave rippled very fine grained sandstone beds of shallow marine origin (Grundvåg et al., 2014a; Helland-Hansen, 2010). Coal beds indicate the transition between the Battfjellet and Aspelintoppen formations. A tidal influenced interval occur in the lower 25 m of the

Aspelintiooen Formation, and above this zone (where the first fluvial channel bodies are recognized) no tidal facieses are identified (see log in appendix).

FA3.1: Tidal influenced delta front deposits.

Observations:

This facies association consists of fine to medium-grained light grey to blue-grey sandstones dominated by tangential cross-stratification (F7). The bed thickness varies from 15 to 50 cm and beds stack to generate coarsening- and thickening upwards units ranging from 1.5 to 2.0 m in thickness (fig. 4.10, A). The beds are wedge shape to tabular with sharp straight to concave upwards lower and upper boundaries. Internal structures include planar (F8) and tangential (F7) cross-stratified, and subordinately sigmoidal (F6), large trough shaped (F2) and low angular (F9) cross-stratified structures of fine to medium grained sandstones. The tangential and planar cross sets are often observed with opposing foresets paleocurrent directions developing bi-directional cross-stratafication structures. Wave rippled (F11) and planar-parallel (F5) stratified very fine to medium sandstone beds are often observed in the first sandy beds of the unit. Additionally the wave rippled sandstone (F11) layers are also observed in the upper part of units and on the top surface surface of tangential (F7), planar (F8), sigmoidal (F6) or trough cross-stratified (F2) beds. Rare folded or soft-sediment deformed intervals (F4) ranging in thickness from 10-20 cm thick occur in places.

The sediments contain a low to moderate degree of bioturbation, which includes *Siphonichnus*, *Catenarichnus* and *Ophiomorpha* trace fossils in the coarser grained cross-stratified sandstones and *Archeonossa*, *Kouphicnium*, *Lockeia*, *Macaronichnus*, *Protovirgularia* and *Skolithos* in the finer wave rippled and planar-parallel laminated sandstones of the lower parts and on top of coarser sandstone beds. Also *Asterophycus* structures are observed on the surface of wave-rippled sandstones (further described in chapter 6).

Interpretation:

The occurrence of bi-directional cross-stratified, wave ripple cross-laminated sandstone beds, and trace fossils assemblage of the *Skolithos* ichnofacies in this facies association suggests deposition in a high-energy upper shoreface environment.

The tangential (F7), planar (F8) and sigmoidal (F6) cross-stratified fine- to medium-grained sandstones represent migration of longshore bars in a shoreface or proximal delta front setting. The sigmoidal cross-stratified sandstones (F6) indicate the transition from dunes to upper plane bed stability conditions (Saunderson and Lockett, 1983). The very fine- to fine-grained planar-parallel stratified sandstones (F5) located in the lower parts of the coarsening upward units are interpreted as upper flow regime (UFR) tidal bars, deposited by low-amplitude bed waves across a flat surface (Best and Bridge, 1992), or by wave reworking. The varieties of paleocurrent directions (figure 4.10, B-D) indicated by the bi-directional cross-stratafication structures of opposing foresets of individual dunes are interpreted as tidal deposits during ebb and flood. These structures have earlier been documented by numerous of other studies including; Uroza and Steel (2008), Grundvåg et al. (2014a) and Helland-Hansen (2010), which suggested that the dunes formed as a result of breaking waves, or longshore- and possibly rip- currents in a wave dominated upper shoreface depositional environment.

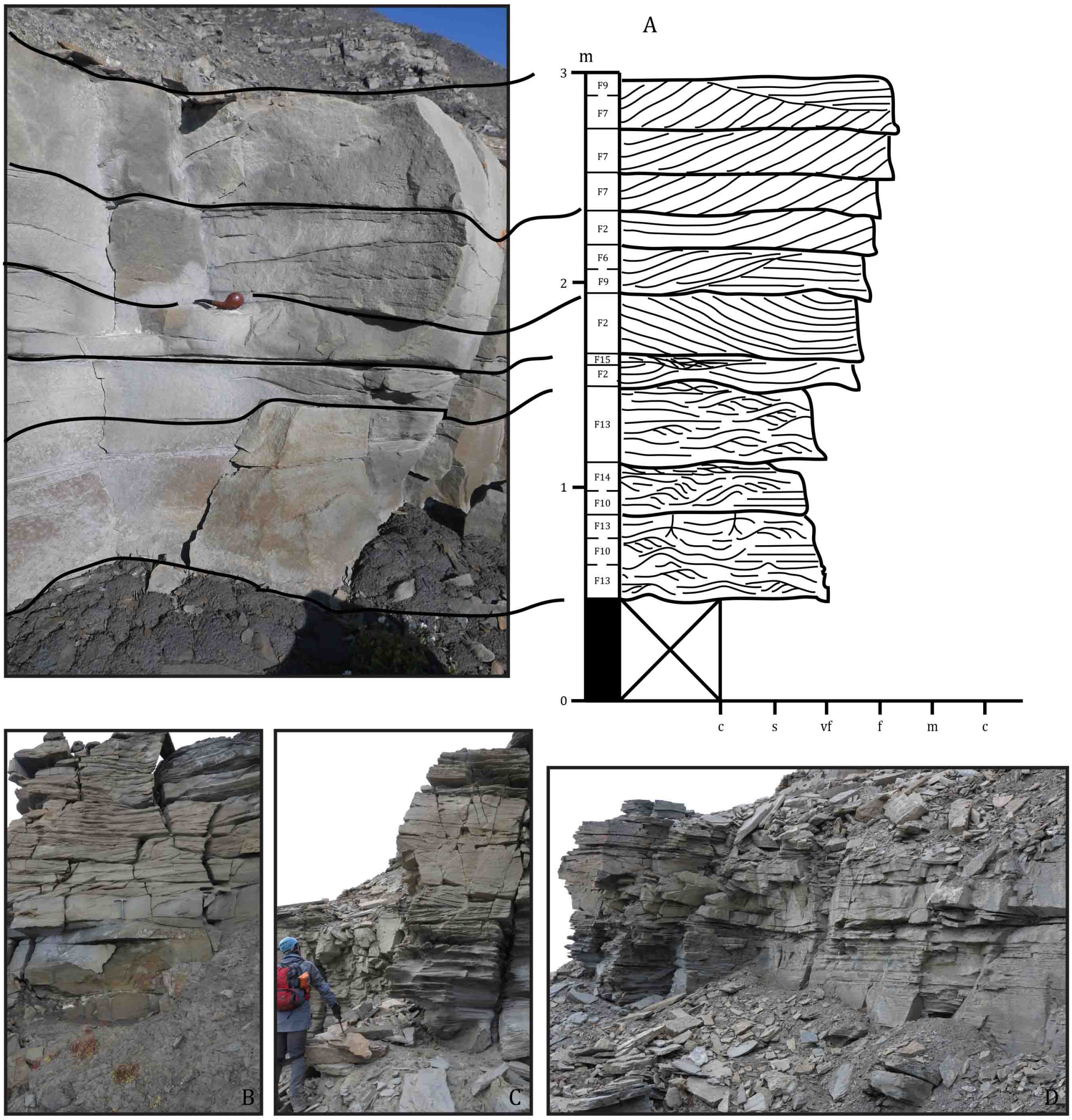

Figure 4.10: Tidal influenced delta front deposits. A) Upper Battfjellet Formation coarsening upward units is indicated by shale to very fine grained lower beds, dominated by current (F13), climbing (F14) and planar parallel (F10) stratified sandstones passing into through (F2), sigmoidal (F6), tangential (F7) and low angular (F9) cross stratified sandstones showing an overall coarsening upward trend. B-D) planar parallel wave rippled (F12) lower beds overlain by bidirectional ebb and flood generated herringbone structures and heterolitic tidal deposits (FA2.3) on top

FA3.2: Heterolithic tidal influenced deposits.

Observations:

Facies association 3.2 consists of heterolithic very fine to fine grained sandstones interbedded in a siltstones and shale. The heterolithic units range from 0.3 to 0.5 m in thickness, with rippled sandstones generating lenses and/ or sheet-like units ranging from 2.0 to 5.0 cm in thickness.

The sandstones are commonly lenticular and are dominated by wave ripple cross-lamination (F12) current ripple cross-lamination with opposing migration directions (F13), and wavy lamination (F14) (fig. 4.10, B-C). Sandstone beds are draped by up to 1.0 cm thick silty mudstones, which mostly pinch out. Only a couple of the heterolithic units are identified at one location (see log interval from 345 to 355 meters above sea-level in appendix). The current ripple cross-laminated sandstones show a wide range in paleocurrent directions and ripples foresets (F13) are typically separated by wavy lamina (F14) and topped by wave ripples (F12). The shale-dominated units (F15) consist of flaky silt, mudstones, and occasionally occurring very fine sandstone lenses (F14). Four, possibly five, coal horizons and/ or lenses (F16) have been observed typically located directly above the heterolithic sandstone beds.

Bioturbation of sandstone beds is estimated to be of low to moderate degree. The observed trace fossils include; *Arenicolites*, *Diplichnites*, *Ophiomorpha*, *Planolites* and *Skolithos* (further described in chapter 6).

Interpretation:

The very fine- to fine-grained sandstones and interbedded siltstone and shale units generating heterolithic deposits resembles tidally induced flaser bedding (Reineck, 1960). The environmental interpretation of these deposits is based on the heterolitic geometry of the deposits, typical for intertidal zones, and locally the observation of high-energy tidal zone trace fossils (further discussed in chapter 6). The reason for this is that flaser, wavy and lenticular bedding (typical for near shore tidal deposits) do not only occur in tidal zones but is also described in overbank areas of episodic flooding, or by weak storm-wave action in deeper water (Reineck and Singh, 1980).

The shale-dominated units are suggested to be of the same tidal environment only of more distal sub-tidal origin based on the larger quantity of suspended material deposited. The tidal environmental interpretation here is also based on the occurrence of high-energy trace fossils typical for tidally-influenced stressed environments. The abundance of coal lenses and/or horizons are suggested to represent periods where the tidal zone is fully terrestrially exposed, for periods of time long enough for coal to generate. The abundance and frequency of the coal layers indicates rapid fluctuations in sea level and/ or in sediment supply.

5 ICHNOLOGY

The trace fossil assemblage indicates a clear and sudden change going from the upper Battfjellet to the lower Aspelintoppen formations. The sandy Battfjellet Formation consist of coarsening-upwards parasequences, with marine ichnotaxa associated with the *Mermia* ichnofacies. The lowermost beds of the Aspelintoppen Formation consist of tidal influenced facies showing a mix of continental and shallow marine ichnotaxa associated with the *Skolithos* ichonfacies. The transition between the sandy coarsening upwards parasequences of the Battfjellet Formation and continental Aspelintoppen Formation is defined by the occurrence of the first coal bed (Dallmann, 1999). In the main log this transition was observed just above the last coarsening-upwards parasequence of the Battfjellet Formation, at 345 m.a.sl., to the first appearance of fluvial channels in the Aspelintoppen at 355 m.a.sl.. The transitional package between the Battfjellet and Aspelintoppen formation is thin (approximantely 10 m thick) and is mostly dominated by coal horizons and thin fine-grained, sandstone sheets with ripples, with a trace-fossil assemblages associated with the *Skolithos* and *Scoyenia* ichnofacies, indicating brackish-water conditions. Adjacent ridges apart from the main profile were also studied. These outcrops showed no clear brackish-water or tidally influenced trace-fossil assemblages, indicating a relative rapid transition between both formations, or absence of marine influenced strata.

5.1 Trace fossils

The trace fossil inventory was analyzed and identified in the field with the assistance of Dirk Knaust (Statoil ASA), and later on by the basis of photographs. Approximately 18 ichnotaxa were identified from the top of the Battfjellet Formation to the middle part of the Aspelintoppen Formation, on the west side of Brogniartfjella, the area where the main section was logged. The trace fossils identified were later compared with the ones identified by Alfred Uchman in his unpublished study of the Storvola and Brogniartfjella outcrops of the Battfjellet and partly Aspelintoppen formation (Uchman, 2004). Below follows a systematic description of the various ichnotaxa recognized in the present study.

5.1.1 Battfjellet Formation Ichnotaxa:

Archaenossa, Fenton and Fenton (1937)

Description: up to one cm thick groove with levees. The levees are only one-two mm thick each and the central groove up to eight mm thick. The grooved centre shows small bow shape structures.
Occurrence: Battfjellet Formation, tidal-flat sandstones (FA 3.2).
Interpretation: *Archaenossa* is interpreted as burrows made by gastropods.

Figure 5.1: Pairs of elevated parallel ridges resembling levees and a slightly grooved centre indicates *Archaenossa* (An) traces.

Aristophycus, Lesquereux (1876)

Description: Longitudinal horizontal traces propagate transverse to ripple crest. Traces range from two-five mm in width and are generally around 50 mm long. Branching and crossing are normal and the traces typically reach from the crest to the middle of the depression between the ripple crests. The burrow fill seems to be the same as the host rock (no clear change in color or grain-size) and occurs in clusters.

Occurrence: Battfjellet Formation, fine-grained wave rippled surfaces (FA 3.1).

Interpretation: *Arestophycus* is interpreted as dewatering structures associated with salt and freshwater interaction.

Fig 5.2: *Aristophycus* (As) indicated by black arrows (A-C). Arrows points to elevated ridges stretching perpendicular from wave ripple crests (A-C).

Catenarichnus, Bradshaw (2002)

Description: Wide U-shaped, partly vertical and sub-horizontal, observed cemented with siderite and host rock sand. Burrow diameter is 10-15 mm in width and length ranges from 50 – 300 mm.

Occurrence: Battfjellet Formation. Observed both in storm influenced shallow marine sediments and in floodplain sediments (FA 3.1). It seems to be limited to moderate and high energy shallow marine environments.

Interpretation: *Catenarichnus* is interpreted as a dwelling burrow of a suspension-feeding animal, perhaps a shrimp or worm.

Figure 5.4: *Catenarichnus* indicated by sideritized concave tubes on the surface and plane view of blocks associated with the upper Battfjellet Formation deltaic deposits (A-E).

Kouphichnium, Nopsca (1923)

Description: Epichnial sinuous sand filled ridges with small footprints running parallel to the ridge. The ridges are two-five mm wide and extends over the entire length of the block. The small footprints pairs are from five-10 mm long elliptical traces, 80-100 mm apart, separated by the sand filled ridge.

Occurrence: Battfjellet Formation, marginal marine heterolithic tidal flat sediments (FA 3.2). Normally found in marine and freshwater environments.

Interpretation: *Kouphichnium* is interpreted as walking trace from arthropods similar to the present day horseshoe crab.

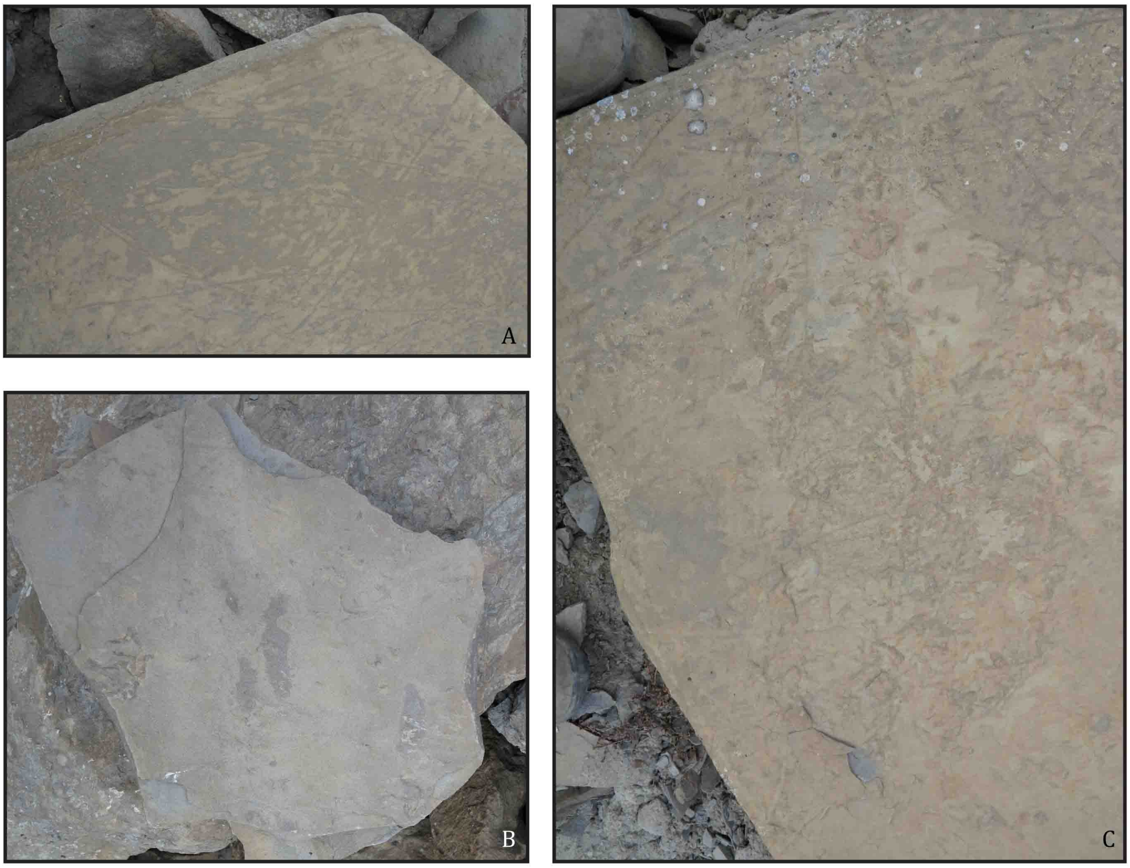

Figure 5.5: *Kauphichnium* is indicated by chaotic elongated equally spaced parallel feet trace (A-C). Straight to slightly curved ridges indicate trace of the tail being dragged between its legs (A, C). B shows faint scattered foot prints without any indication of tail trace. Traces are probably *L. siliquaria*, identified on blocks associated with the upper Battfjellet Formation.

Lockeia, James (1879)

Description: Small round to slightly elongated bodies with slightly elevated couples at each end of the body. The bodies longest axis range from five-10 mm (figure 5.10 A) and 20-30 mm (figure 5.10 B) in length.
Occurrence: Battfjellet Formation. Observed in the sandy mouth bar and prodelta deposits of the Battfjellet Formation and possibly in tidally influenced fine-grained sandstones of the Aspelintoppen Formation (FA 3.1 and 3.2). Occurs in marine to brackish to freshwater fluvial and lacustrine deposits (Mángano, 2002).
Interpretation: *Lockeia* is interpreted as resting traces of bivalves.

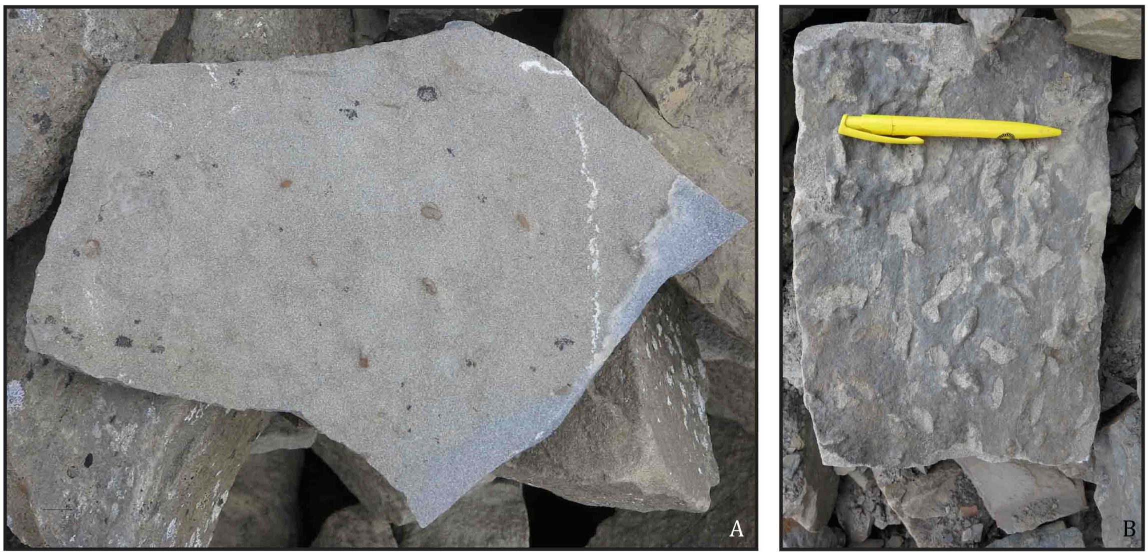

Figure 5.6: *Lockaia* is indicated by small, up to 10 mm (A) and up to 30 mm (B) long elongated resting traces from bivalves. Traces are identified on blocks associated with the upper Battfjellet Formation.

Macaronichnes, Clifton and Thompson (1978)

Description: Horizontal cylindrical ridges filled with quartz sand in the core and darker grains in the surrounding mantel. Develops concentrated patches of sinuous traces. The trace ridges are from 10-20 mm wide and from 20-50 mm long.

Occurrence: Battfjellet Formation. Observed in fine-grained heterolithic sandstone sheets (FA 3.2). Found in shallow marine near shore high energy sandy environments, associated with intertidal and shallow subtidal deposits.

Interpretation: *Macaronichnes* is interpreted as feeding traces of organisms feeding on bacteria and/or organic matter on the sand grains. They process the quartz grains through their gut and select other grains (e.g. heavy minerals) with their bristles to transport them outside of their body backwards.

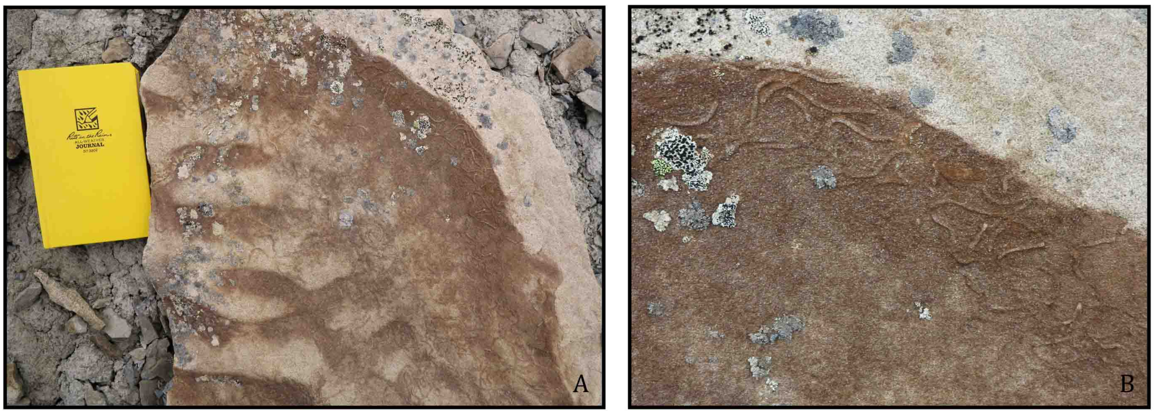

Figure 5.7: Macaronichnus is indicated by sinouse curving to looping mm thick ridges (A-B). B shows close-up of the top right corner of A.

Ophiomorpher, Lundgren (1891)

Description: eight-25 mm thick cylindrical shafts mostly filled with the same sediments as the host rock. The filled cylindrical tunnels and shafts often cross each other, and some branching is observed. Pellets filled with clay to silt are often observed on the walls of the tunnels.

Occurrence: Battfjellet/Aspelintoppen formations. Trace fossils are observed in laminated and rippled sandstone blocks of the Battfjellet and Aspelintoppen formations respectively (FA 3.2).

Interpretation: *Ophiomorpher* (Op) is interpreted as traces possibly from callianassid shrimps (Uchman, 2004). The *Ophiomorpha* (Op) trace fossil is typical for shallow marine sandstones but is also observed in brackish waters, estuaries, tidal deposits and deep sea turbidites (Uchman, 1991), (Uchman and Krenmayr, 1995).

Figure 5.8: Straight up to 25 mm thick ridges and knobs indicates *Ophiomorpha* traces (A-F). *Ophiomorpha* with active fill (F). Traces are located on blocks associated with upper Battfjellet formation deposits.

Protovirgolaria, M'Coy (1850)

Description: Slightly elevated sinuous V-shaped ridges with chevron structures propagating from the crest and outwards. The sinuous ridges are approximately six mm thick and vary from 15-20 mm in length.
Occurrence: Battfjellet Formation. Observed in fine-grained grey and red-brown sandstone associated with shallow marine deposits (FA 3.2). Trace fossil is typical for fully marine environments.
Interpretation: *Protovirgularia* is interpreted as feeding traces from the foot of a clam (molluscs such as bivalves).

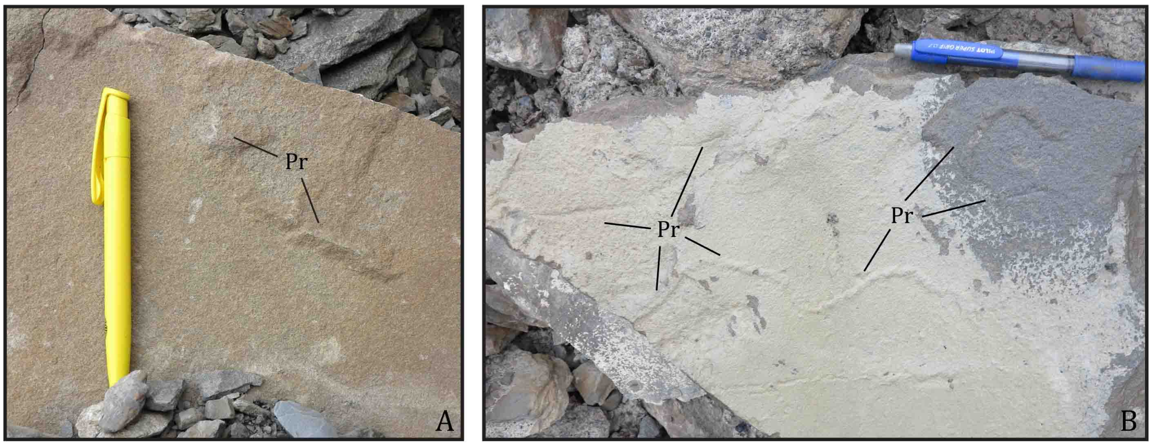

Figure 5.9: Elevated straight to slightly sinuous V-shaped ridges of *Protovirgolaria* (Pr) indicated by black lines (A). Sinuous, V-shaped ridges of *Protovirgolaria* (Pr) on the upper surface of sandstone block (B). Both blocks are from the upper Battfjellet Formation deposits.

Siphonichnus, Stanistreet et al. (1980)

Description: Patches of straight to slightly sinuous vertical tubes filled with sand. Tubes are approximately 10-15 mm wide around the outer probe and vary from three-seven mm within the inner filled tube (figure 5.4, A-C). Some traces penetrate the entire block (~5 cm thick block) whilst others only reach lengths of a few tens of mm.
Occurrence: Battfjellet formation, fine-grained sandstone block, typical shallow marine stressed environment (FA 3.2).

Interpretation: *Siphonichnus* is interpreted as vertical moving or feeding traces from clams.

Figure 5.11: Round tubes with a filled core identify *Siphonichnus* (Si) traces on the surface of sandstone blocks (A-C) associated with Battfjellet Formation deltaic deposits. Black lines indicate traces.

Skolithos, Haldeman (1840)

Description: 10 mm wide and 80 mm long vertical burrow with structure-less fill similar to the overlying sediments it propagates from.
Occurrence: Upper Battfjellet/lower Aspelintoppen formations. Most abundant in the lower Aspelintoppen Formation's heterolithic tidal influenced deposits (FA 3.2), but are also observed in the upper Battfjellet Formation's tidal influenced delta front deposits (FA 3.1). Occur in most sedimentary environment from marine to terrestrial.
Interpretation: *Skolithos* is generated by vertical to sub-vertical borrowing predominantly from roots (figure 5.18 A-D), but also worms, phoronids, insect larvae, arthropods and small vertebrates (figure 5.18 E).

Figure 5.12: *Skolithos* (Sk) trace fossils are indicated by vertical shafts seen in plane view (A-D), probably generated by roots, and knobs on top of bedding surface (E). Trace fossil located both in lower Aspelintoppen and upper Battfjellet Formation deposits.

5.1.2 *Aspelintoppen Formation Ichnotaxa:*

Arenicolites, Salter (1857)

Description: Vertical cylindrical shafts normally just observed as J-shaped or pairs of shafts preserved in positive hyporelief, e.g. along the lower bedding plane. Rare cases where the whole U-shape is exposed are also observed. The cylindrical shafts vary from five-20 mm in diameter with shafts filled with the same sediments as the host rock (figure 5.3, A-D). The smallest tubes (figure 5.3, A-B) are observed to be concentrated in the Aspelintoppen Formation while the larger ones (figure 5.3, A-B) are mostly located in the Battfjellet Formation.

Occurrence: Battfjellet/ Aspelintoppen formations. Observed in the sandy beds of the top Battfjellet Formation (FA 3.1) and in fine-grained heterolithic tidal influenced beds (FA

3.2), distal floodplain deposits (FA 2.1), Distal crevasse splay sheet deposits (FA 2.2), heterolithic levee deposits (FA 2.3) and proximal crevasse splay sheet deposits (FA 2.5) of the Aspelintoppen Formation. Occurs in aeolian (Ekdale et al., 2007), marine, freshwater lacustrine and fluvial (Eagar, 1985).

Interpretation: *Arenicolites* are interpreted as suspension-feeding burrows from polychaete worms, crustaceans, wasps, mayfly larvae, or beetles.

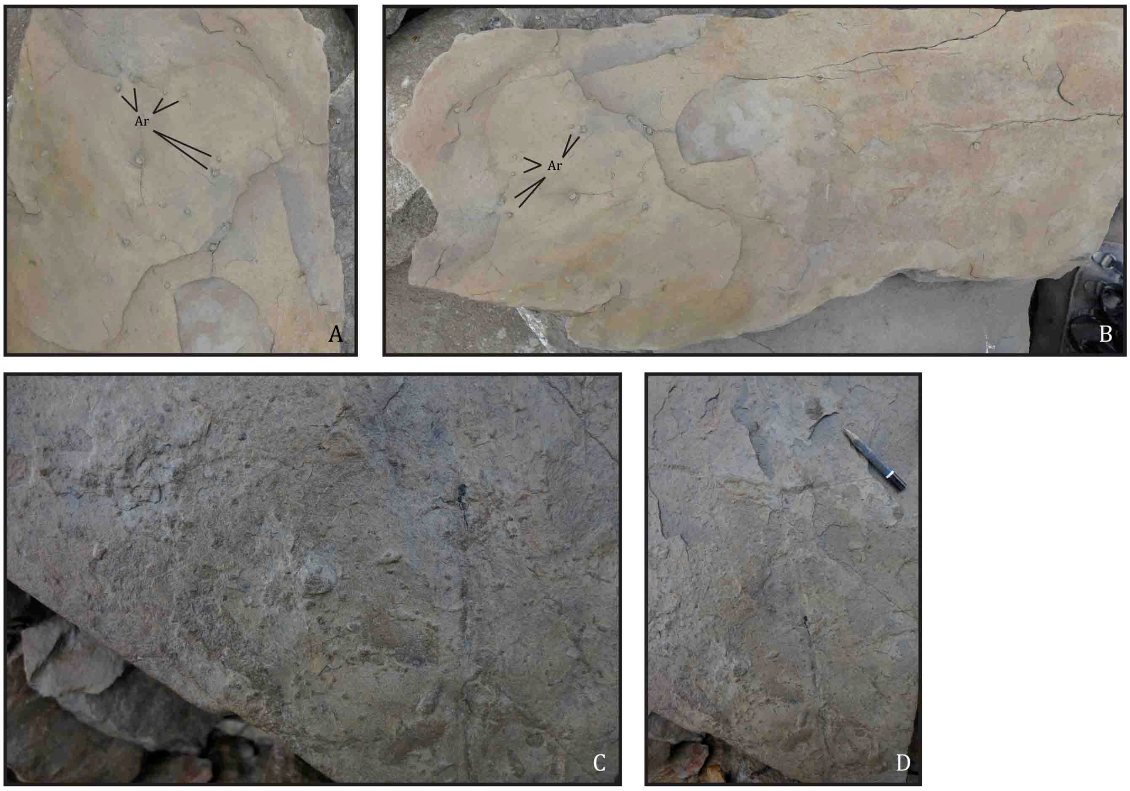

Figure 5.14: *Arenicolites* (Ar) are identified as pairs of tubes with variable diameter and spacing on the surface of heterolitic floodplain beds of the Aspelintoppen Formation (A-B) and marine deltaic beds of the Battfjellet Formation (C-D).

Cylindricum, Linck (1949)

Description: Thick, short tubes without branching but slightly bent. The cylindrical structures are thickening towards the surface of the block ranging from five-15 mm in width and up to 30 mm in length.

Occurrence: Aspelintoppen Formation. Observed in very fine to silty sandstones, related to episodically or periodically flooded floodplain deposits. Occurs in continental floodplain or lacustrine environments (FA 2.1, 2.2, and 2.6).

Interpretation: *Cylindricum* is interpreted as feeding or dwelling traces from crustacean (e.g. crayfish).

Figure 5.15: Elongated to spherical ridges of a darker color than the host rock indicated the *Cylindricum* (Cy) trace fossil. Some *Arenicolites* (Ar) traces are also identified on the same block. Trace fossil is located on a block associated with fine-grained lacustrine or floodplain shale to siltstones of the Aspelintoppen Formation.

Diplichnites, Dawson (1862)

Description: Up to four mm thick moving traces as well as up to two mm thick slightly sinuous ridges, with internal parallel ridges (figure 5.5 A), were observed in brown-red sandstones associated with the Aspelintoppen Formation.

Occurrence: Aspelintoppen Formation. Observed in lower Aspelintoppen Formation brackish water or tidal influenced very fine-grained sandstone sheet (FA 3.2) and floodplain shale (FA 2.1) deposits. Trace fossil occur both in marine and alluvial and lacustrine continental settings.

Interpretation: The *Diplichnites* (Di) traces are suggested to be developed by continental arthropods such as centipedes or millipedes.

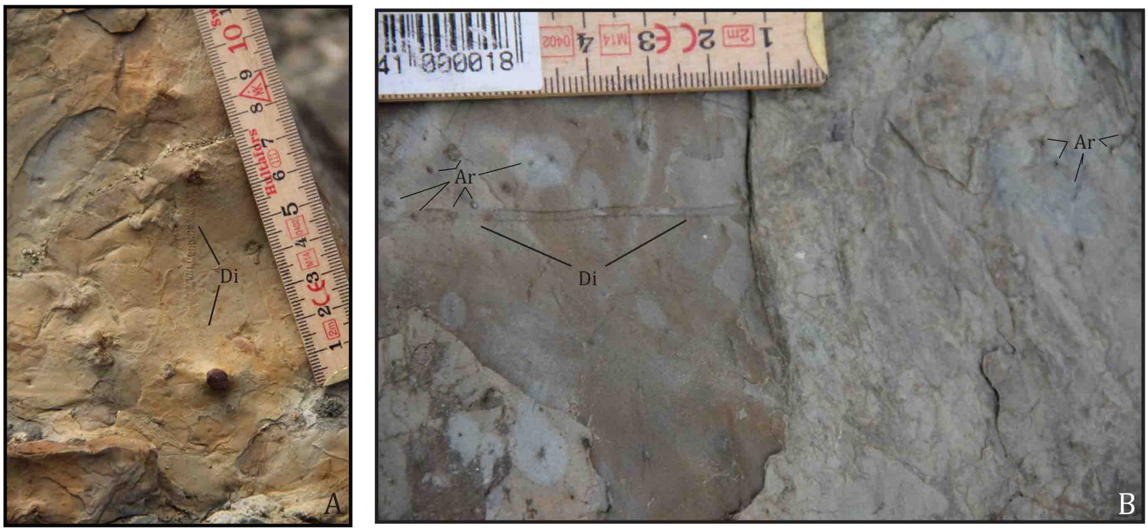

Figure 5.16: *Diplichnites* (Di) moving trace from *Arthropod* in lower Aspelintoppen formation tidal facies (A-B)

Helminthoidichnites, Fitch (1850)

Description: Thin grooves with branching and/or sand filled simple ridges, straight to slightly sinuous. The grooves or ridges are from 1 to 2 mm thick and from 30-60 mm long.

Occurrence: Aspelintoppen Formation fine-grained floodplain sediments (FA 2.1) and Battfjellet Formation heterolithic tidal sediments (FA 3.2). Observed in fine-grained rippled sandstones in the last beds of the Battfjellet Formation and the first beds of the Aspelintoppen Formation.

Interpretation: *Helminthoidichnites* is interpreted as traces generated by insect larvae.

Figure 5.17: *Helminthoidichnites* (He) indicated by black lines as slightly sinuous branching ridges ranging from 2-3 mm in thickness and from1-3 cm in length. Picture of trace fossil is located on the surface of a block associated with the lower Aspelintoppen Formation.

Planolites, Nicholson (1872)

Descriptions: 15 mm wide and 50 mm long horizontal straight to slightly sinuous burrow with a passive fill. The burrow fill is of the same sediments as the host rock. Some vertical shafts are also observed on the surface of the block, these are interpreted as *Siphonichnus* trace fossils (described above).

Occurrence: Upper Battfjellet/ lower Aspelintoppen formations. Observed in fine-grained shallow marine sediments of the upper Battfjellet Formation and in fine-grained tidal influences thin sand sheets of the lower Aspelintoppen Formation (FA 3.2). Occurs from continental to shallow marine to deep marine depositional environments.

Interpretation: *Planolites* are generated by burrowing organisms (e.g. worms) producing active fill by deposit feeding (Uchman, 2004).

Figure 5.18: Planolites ichnotaxa. A) Vertical knobs of *Siphonichnus* (Si) and horozontal trace. B) Sideritized sub-horizontal *Planolites* (Pl) traces. C) Horizontal slightly curved *Planolites* (Pl) traces. Traces are located on blocks associated with the lower Aspelintoppen formation inter-channel sandstone beds.

Scoyenia, White (1929)

Description: Thick horizontal and partly horizontal, branching trace fossils ranging from 10-20 mm in width and over 60 mm in length (extending the entire length of the block). The internal structure is wrinkle with transverse lamina crossing the traces width and sediment fill similar to the host rock.

Occurrence: Aspelintoppen formation. Observed in distal floodplain (FA 2.1), distal crevasse splay sheet deposits (FA 2.2), heterolithic levee deposits (FA 2.3), proximal crevasse splay sheet deposits (FA 2.5) and interdistributary bay fill deposits (FA 2.6) of the Aspelintoppen Formation. The trace fossils are observed at multiple locations over the entire vertical profile of the Aspelintoppen formation. Occurs in low energy continental environments such as floodplains.

Interpretation: *Scoyenia* is interpreted as deposit feeding or dwelling trace from beetles, larvae or cicades.

Figure 5.19: Straight (A-B,F) to curved (C-E) horizontal ridges (A-B, F) and grooves (C-E) with internal structures and sediment infill similar as the host rock indicates the *Scoyenia* (Sc) trace fossils. Trace fossils are located on blocks and surfaces of interchannel sandstones of the Aspelintoppen Formation.

Leaf Prints and Underminings

Description: two-four mm thick concave ridges curving to looping over the surface of the leaf print. Leaf prints are observed as carbonaceous or sideritized layers with leaves on the lower surface of interchannel sandstones with well defined structures indicating the leaf. Other plant debris includes carbonaceous cones found in the same sediments.

Occurrence: Aspelintoppen Formation. Observed on the surface of leaf prints in interchannel very fine to fine-grained sandstone sheets.

Interpretation: *Leaf Underminigs* are feeding or resting traces by insect larvae on leaves, because of the protection and nutrients provide (Uchman, 2004). Leaf imprints and cones are deposited by seasonal leaf fall at the floodplain resulting in large areas covered by leaves.

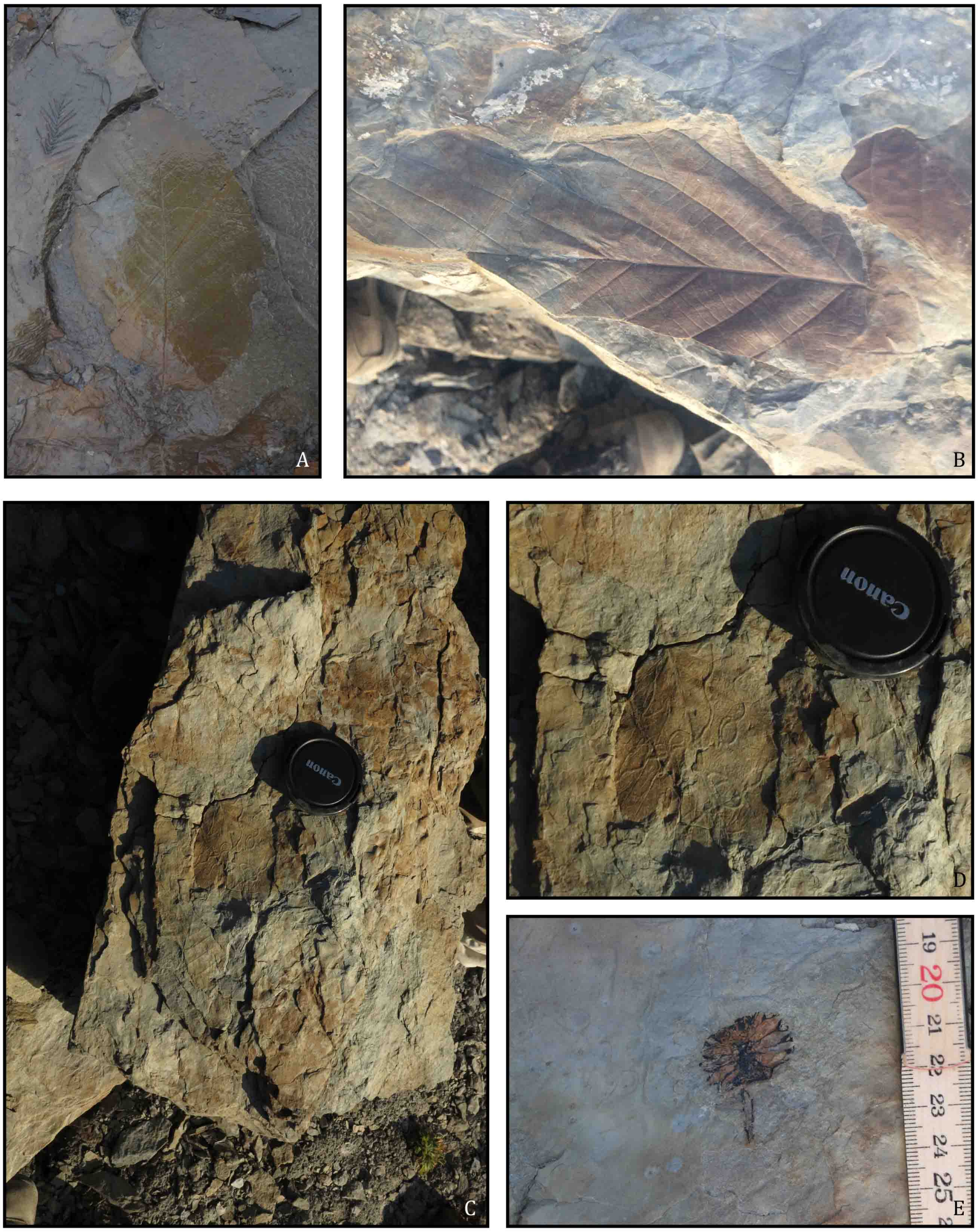

Figure 5.20: Leaf print up to 20 cm long and 10 cm wide, with a brown-red sharp color and well-defined internal structures (A-B). sinuous and looping up to two mm thick ridges indicates Leaf Underminings (C-D). Star-shaped carbonaceous knobs approximately two cm in diameter indicates fossil cone (E).

Root traces, horstail plants and stems and strains:

Description: A wide variety of roots and different plant fragments are observed in the Aspelintoppen formation. Root traces are observed in the form of; one mm wide carbonaceous veins reaching from the top of beds and down, five mm wide siderite concreted horsetail plants generating star-shaped structures on the surfaces and fractured stems and strains often observed near fluvial channel bases.
Occurrence: Mostly observed in-situ in interchannel sandstones (FA 2.2, 2.3, 2.5 and 2.6) and fractured in the base of channelized sandstone bodies (FA 1.1, 1.2 and 2.4).
Interpretation: *Root traces* are generated as different kinds of roots penetrates the subsurface soft sediments.

Figure 5.21: Carbonaceous root traces up to two mm thick are observed in the top surfaces of bedding planes (A). Stem print and carbonaceous stems are observed orientated vertically to horizontal in the base of coarsening-upwards sandstones (B-C). Mostly vertically but also horizontally orientated horsetail plants with internal structure, distinguishable joints and siderite infill (D-G). All root traces are located on blocks or in-situ in the Aspelintoppen Formation.

5.2 Ichnofacies and environmental setting

5.2.1 Battfjellet Formation deposits:

The study area is largely dominated by typical thickening upwards parasequences. The lower part of the deposits contains mudstones passing into sandier mouth bars and prodelta deposits. Most of the deposits are typically associated with the moderate to high-energy conditions above normal wave base.

In the coarser mouth-bar dominated sandstones above normal wave base *Siphonichnus* and *Catenarichnus* are observed in large numbers. The abundance of these traces fossils indicates that the organisms generating them rapidly colonized these areas. The occurrence of *Catenarichnus t*race fossils is suggested to indicate shallow marine storm influenced conditions (previously referred by Uchman 2004 as Glyphicnus). Less frequently observed are *Ophimorpha* trace fossils. The *Ophimorpha* traces is observed in the upper parts of the Battfjellet formation together with more locally observed *Archeonossa*, *Kouphichnium*, *Lockeia*, *Macaronichnus*, *Protovirgularia*, and *Skolithos*. These trace fossils are apparently related to foreshore areas, probably with relatively hard near brackish-water conditions. The occurrence of *Asterophycus* dewatering structures, generated by fresh and saltwater interactions further emphasises this assumption.

5.2.2 Aspelintoppen Formation deposits:

The zone from the last coarsening upward parasequece of the Battfjellet Formation and the first fluvial channel of the Aspelintoppen Formation contained a low degree of bioturbation. This zone is marked by the first appearance of *Planolites* and the last observation of *Ophiomorpha* traces. The sedimentological facies also change from fine to medium-grained tabular cross-stratified sandstone to shales and very fine-grained both directional current rippled heterolithic sandstone sheets. *Planolites*, *Arenicolites* and *Skolithos* are the most common traces in the lower beds close to the Battfjellet formation. *Planolites* and *Skolithos* are mostly recognized in the marginal marine to continental zones, while *Arenicolithos* is observed in most intervals both in the

Battfjellet and Aspelintoppen formations, with the distinction that the ones observed in the Battfjellet Formation are larger than those in the Aspelintoppen Formation. The size of the traces reflects the environmental conditions, which it settles in. Hard conditions (high-energy or competitive) should develop smaller specimens easier.

Less frequently observed are *Diplichnites*, which is suggested to be related with partly flooded very fine-grained tidal flats or lacustrine environments.

Sandy sheet and floodplain fines dominate the non-marine continental to lacustrin facies of the Aspelintoppen Formation, with abundant interbedded coal horizons and crevasse splay channels. The fluvial channel sandstones only contain some carbonaceous stems and stains, and therefore are of relatively low interest because of the low in diversity ichnoassemblage. Most trace fossils are observed in the interchannel sandstones sheet, siltstones and mudstones. *Arenicolites*, *Scoyenia*, *Arthropod* trackways are the most abundant trace fossils found. Most of these traces are limited to the *Scoyenia* ichnofacies indicating that the floodplains were covered by water for longer periods, and that the predominant *Scoyenia* trace fossil rapidly colonized the floodplain sediments. Other trace fossils recorded more locally such as; *Helminthoidichnites,* leaf underminings and *Cylindricum* fit within the *Mermia* ichnofacies (Buatois and Mángano, 1998). This also could explain the low intensity and diversity of bird footprints and other larger mammals found in the continental deposits of the Aspelintoppen Formation (Uchman, 2004). Besides trace fossils the occurrence of abundant horsetail plants, root traces and leaf prints from the first crevasse splay sheet, about five-10 m above the first coal bed (see log interval 345 to 355 m.a.sl. in appendix), further indicates that most of the Aspelintoppen Formation is of a fully continental origin.

6 SANDSTONE BODIES ARCHITECTURE, VERTICAL VARIATIONS AND SAND VOLUMES:

6.1 Introduction: Architectural elements

Sandstone deposits of the Aspelintoppen Formation at western Brogniartfjella, comprise a large variety of geometrical features, which are distributed along the whole vertical length of the logged profile (appendix). The most prominent features are four large channelized sandstone bodies (see intervals, 380-388 m.a.sl., 506-516 m.a.sl., 593-600 m.a.sl. and 741-748 m.a.sl. in appendix), which are distributed with approximately equal spacing along the logged profile (see appendix). In between these larger fluvial channels, smaller distibutary (FA 1.2) and crevasse channel (FA 2.4) occur along with sheet-like sandstones representing crevasse splays and levees (FA 2.2 and 2.3). Most of the sandstones preserved in the formation are situated in interchannel sheets. Fluvial channel facies only comprise roughly one fourth of the sandstone in the logged section. Thus, the sandstone-dominated units in the Aspelintoppen Formation can be classified according to the geometries of the deposits either as: 1) channels, or 2) sheets. The channel fill is characterized according to the terminology by Vail et al. (1977) and later Miall and Postma (1997) and is divided into packages separated by 1-5th order surfaces, which range from structural conformable discontinuities reflecting climate or eustatic processes, to regional angular unconformities generated by tectonism. In this study 3, 4 and 5th order surfaces are used to explain the different depositional units occurring in channel bodies. The 3th order surfaces represent macroform growth elements, possibly reflecting seasonal events. The 4th order surfaces represent convex upward macroforms, possibly developed as minor channel scours by larger flooding events. The 5th order surfaces represents flat to concave upward major channel bases developed long-term geomorphic processes like channel avulsion. The architectural elements will be described in more detail below.

6.2 Channels:

A total of 54 channelized sandstone body segments were identified in the main logged section at Brogniartfjella west. These bodies range from approximately 0.6 to 10.0 m in thickness. This size range will represent channel bodies from very thin (<1 m) to medium (>5 m) according to the classification of Gibling (2006). At Brogniartfjella, channel widths are only possible to measure on smaller sandstone bodies. Larger channel body widths are difficult to measure due to outcrop limitations generated by scree cover. Some attempts to measure larger channels where attempted, but these measurements must be considered to have minimum value and will therefore be inconclusive.

Based on the sandstone body dimensions, architectural elements and facies assemblages three main types of channelized sandstone bodies were distinguished; 1) crevasse splay channels (type one), 2) distributary channels (type two), and 3) trunk channels (type three). Between type one and two some overlap is assumed to occur as some of the larger crevasse channels of type one are interpreted as terminal distibutary channels (see chapter five). In addition some major distributary channels may be similar to smaller trunk channels and visa versa.

Based on the thickness of channel bodies, bodies are divided into; 0.5-2.25 m (type one), 2.4-5.35 m (type two) and > 6.7 m (type three) in thickness. This subdivision of channel bodies, is modified from Gibling (2006)'s characterization of fluvial channel bodies, which is based on dimensions, sedimentary features and geomorphic settings.

Note however, that modification of the characterization given by Gibling (2006) is implemented due to difficulties in seperating channel types based on dimensions alone, as the evolution of channels are dynamic. In the present study, there is a lack of lateral controle of channel width, and there is no clear definition given on how to separate them from each other based on thickness estimated alone.

6.2.1 Type 1:

Type one channels, represented by blue bars in fig. 7.3, comprise bodies ranging from 0.5-2.25 m in thickness. Channels are characterized by massive (F3) and soft-sediment deformed (F4) basal lag deposits, including abundant mud-clasts and plant detritus. Various cross-stratified sandstones and current ripple cross-laminated sandstones often overlay the basal parts. Thicknesses of these channel bodies are based on field measurements, and it is important to emphasize that smaller bodies are assumed to occur but are hard to recognized because of their similarities to sheet-like sandstones, with limited lateral extent. In total 41 sandstone bodies of this type were identified in the main log (appendix), with a mean thickness of 1.23 m and a standard deviation of 0.46 m (fig. 7.3).

Channel fills comprise a U-shaped geometry and include adjacent laterally extensive levees (FA 02.5) generating an overall ribbon shaped geometry (fig. 4.7). Boundaries comprise of high relief 4th order erosional scoured lower surfaces and sharp non-erosive upper surfaces. Most channels of this unit are interpreted as single-story crevasse channels (see FA 2.4, chapter 5), on the basis of facies assemblage, stacking patterns, dimensions, and sandstone body geometry (minor channel fig. 7.2, C). Some bodies close to the Battfjellet Formation deltaic deposits and are interpreted as terminal distributary channels, but are here included in type one because of their similar dimensions to crevasse channels. Channel bodies are observed eroding into both crevasse splay sheets (FA 2.5) of earlier flooding episodes, and into floodplain fines (FA 2.1). Channel widths are estimated to range from five to 33 m, reflecting large differences in channel dimensions, probably related to proximal or distal orientation to main (trunk) channels (Bridge, 2009). Some channel bodies are orientated oblique to the paleocurrent direction, giving a too large width estimate. Stacking of crevasse channel units are common, generating packages of several ribbon shaped units on top of each other developing larger crevasse channel complexes. Some outcrops display several crevasse channels adjacent to one another (illustrated in fig. 7.1, B-C). These thicker and laterally more complex crevasse splay systems reflect systems similar to the ones described by (Smith et al., 1989). Smith et al. (1989) displayed a three-stage model for the development of crevasse splay systems, illustrating the progradational and retrogradational trends of the crevasse splay evolution (fig. 7.1).

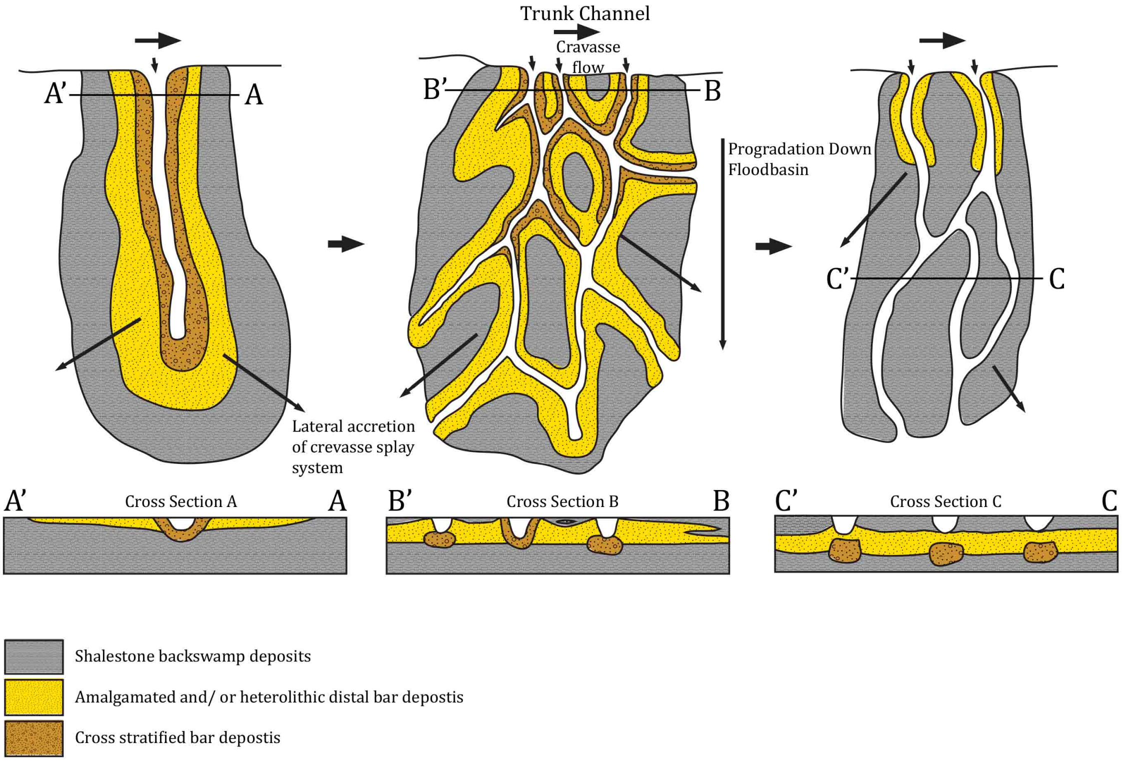

Figure 7.1: Crevasse splay system evolution. Initial crevasse of channel banks with associated splay sheet (A). Progradation of crevasse splay system, multiple active channel elements depositing sediments father out on the floodplain basin (B). Retrogradation of crevasse system, less active channel elements and more deposition of finer-grained sediments (C). Figure modified from Farrell (2001) and of Smith et al. (1989).

6.2.2 Type 2:

Type two channels (fig. 7.2, C-E), represented by green bars in figure 7.3, comprise bodies ranging from 2.4-5.35 m thick, with a mean thickness of 3.7 m and a standard deviation of 1.0 m (fig. 7.2). Bodies constitute both single- and multi-storey type channels. In total 10 bodies were identified over the whole length of the logged profile. Type two channel bodies are typically dominated by trough cross-stratified sandstones, which locally contain pebble lags in the lower parts of each unit. Locally soft-sediment deformed (F4) planar-parallel cross-stratified (F5), tabular cross-stratified (F8) and low angular cross-stratified (F9) occur in the uppermost parts of the channel bodies.

These channel bodies are interpreted as distributary channels based on channel dimension and facies assemblage (further described in FA1.2). When applying these channels to Gibling (2006)'s characterization, most channel will fit within the thin to medium thick channel bodies.

Geometries include 5th order lower boundaries, which often consist of U-shaped incision pinches out into adjacent levee or crevasse splay deposits. Together with upper straight non-erosive boundaries these bodies generate an overall ribbon shaped channel body geometry (fig. 7.2, C-E). In multi-story channels internal 4th order bounding surfaces are characterized by multiple lenticular to sheet shaped bodies, with pronounced undulating to convex upward shaped lower surfaces, which erode into underlying channel bar systems. Most internal channel bar systems range from 0.5-3.0 m in thickness and are limited by the initial scouring of the main channel body. Some exceptions are observed were distinct wings of the internal body pinch out into adjacent heterolithic levee deposits of FA 2.3 (fig. 7.2, E). Sandy bedforms are abundant within the channel bodies, the only deviation is thin basal conglomerates.

Some few channel body thickness measurements conducted suggests that most channels did not extent laterally for more than a few couple of hundred meters, placing them within the distributary systems of Gibling (2006) characterization.

Similarities between thicker type two and three channels makes it difficult to separate them, meaning that some of the larger type two bodies could be interpreted as type three trunk channels.

6.2.3 Type 3:

Type three channels, represented by red bars in figure 7.3, comprise channels that range from 6.7 to 10.0 m thick, with a mean thickness of 8.0 m and standard deviation of 1.27 m. The type three channels are characterized by multi-story channel geometries (fig. 7.2, A-B). Type three channel bodies are typically characterized by abundant trough cross-stratified sandstones (F2), which locally include pebble lags, mud clasts and organic detritus (F1) and soft-sediment deformed sandstone beds (F4).

Based on the dimensions and facies distribution these large-scale channel features are interpreted as central trunk channels. These channels are the main agents for transporting sediments from the hinterland out onto the floodplain.

Differentiation from type 3 to channels and the other two types is apparent from the channel bodies thickness and bounding surface geometries. These major channel bodies represent a higher order of incision than the lower types, but are not thought to be of the dimensions incised valleys generated during forced regression described by Plink-Bjørklund (2005). Incisions are rather suggested to be avulsions triggered by base-level changes in the fluvial systems profile (further described in chapter 8).

Lower bounding surfaces are typically defined by sharp concave to undulating boundaries, eroding into floodplain fines or sands. Concave scours promote wide U-shaped geometries tinning laterally to one or both sides (depending on the outcrops exposure) generating an overall ribbon shaped sandstone body (fig. 7.2, A-B). The first trunk channel body observed in the logged section comprises a straight undulating lower boundary with a less pronounced concave scoured lower surfaces (fig. 7.2, B), and with no apparent relief changes over the outcrops length. This body is interpreted based on its geometrical features as a narrow sheet sandstone body from Gibling (2006)'s characterization. The location of this channel body close to the delta front and the sheet geometry suggests that some lateral accretion could have occurred (Makaske, 2001).

The absence of lateral accretion packages is assumed to be because of secondary soft-sediment deformation or because of difficulties in recognizing lateral accretion packages when outcrops do not promote a perfect cut through the channels (see log in appendix). All trunk channel bodies promote straight non-erosive upper boundaries, mostly passing into overlying coals and floodplain shale (FA 2.1), and occasionally into heterolithic levee deposits and proximal crevasse splay deposits (FA 2.3 and 2.5 respectively).

Internal structures of channel bodies comprises lenticular (fig. 7.2, A) to sheet (fig. 7.2, B) shaped bar complexes, generally thicker than the ones observed in distributary channels. Most bar complexes observed range from two-five m in thickness and are bounded by 4th order concave-upwards erosional surfaces, which partly erodes into underlying bar complexes. Internal 3rd order erosional surfaces are also observed.

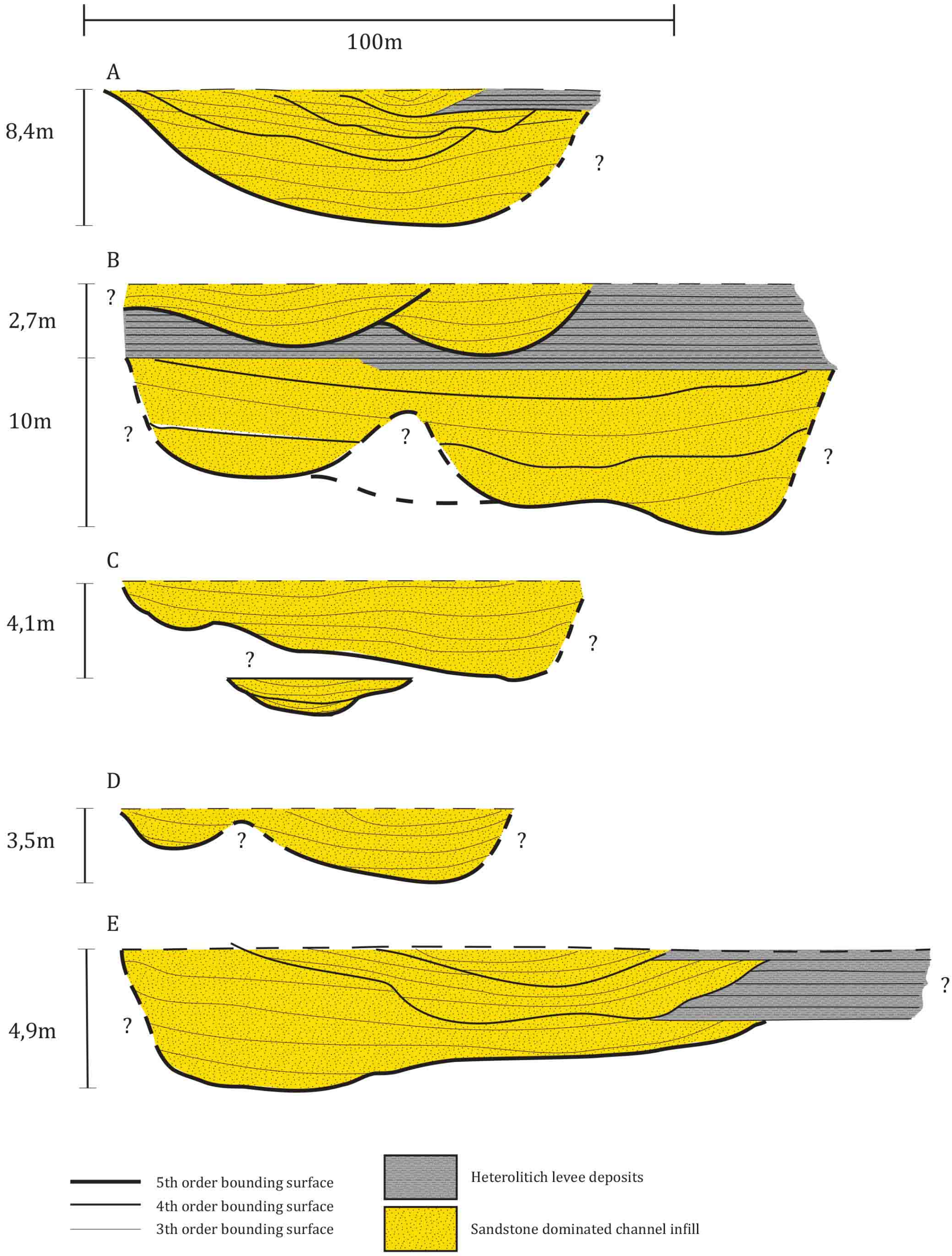

Figure 7.2: Channelized sandstone bodies, Aspelintoppen Formation. The two uppermost sandstone bodies (A-B) represents ribbon shaped trunk channels (type 3), with associated internal structures. Next two bodies (C-D) represents ribbon shaped single-story distributary channels (type 2), channel C) with an associated type 1 channel located underneath. The lowermost sandstone body (E) represents multistory distributary channel (type 2) with wings pinching into adjacent levee deposits.

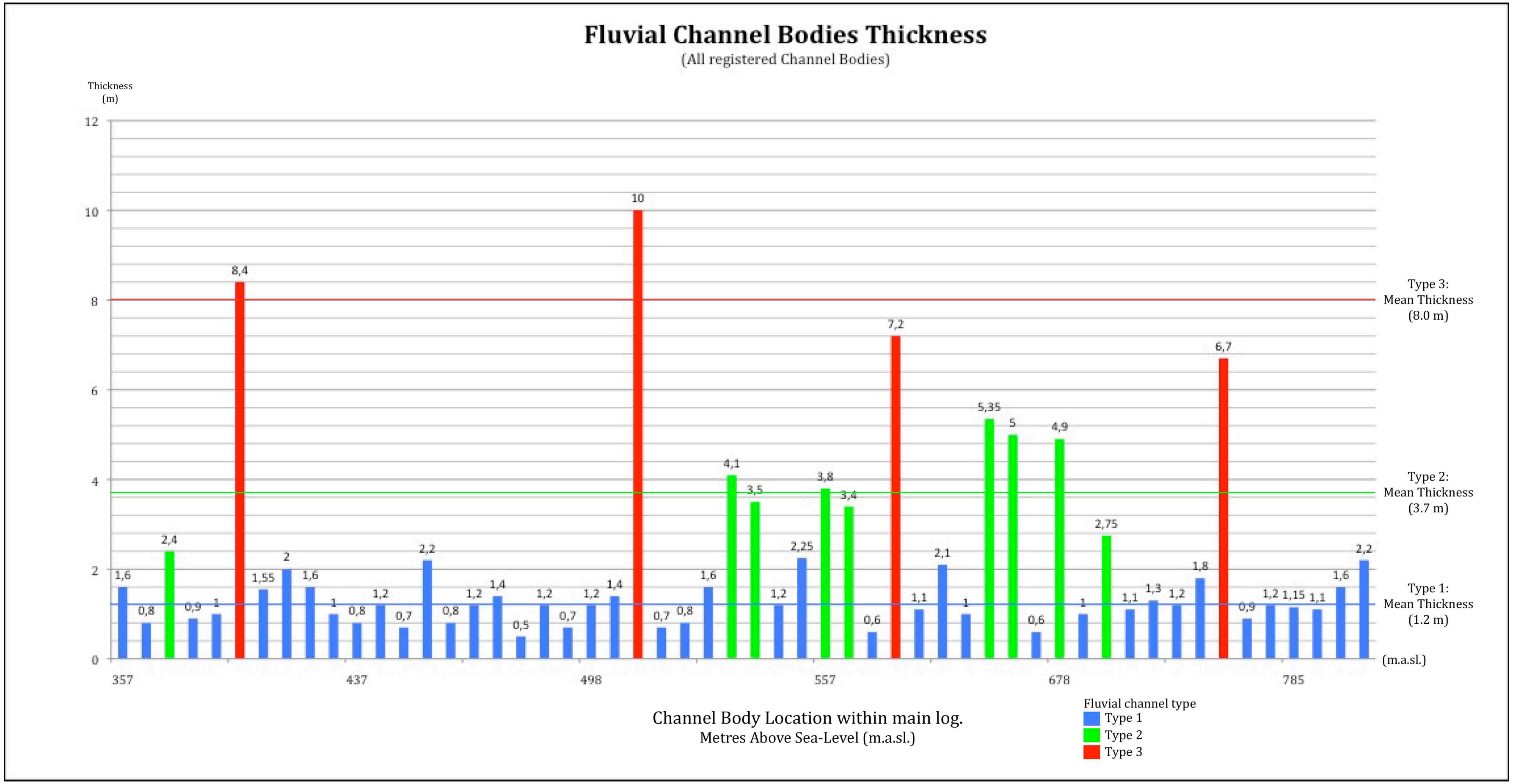

Figure 7.3: Bar diagram of all fluvial channel bodies registered in the main log. The colored bars represent the respective units which channelized sandstone bodies are divided into. Colored lines represent mean thickness of associated units.

6.3 Sheets

Interchannel sandstone sheets volumetrically represents most of the sandstone deposited in the Aspelintoppen Formation. Although these deposits are described as sheet-like some also show lateral thinning and are more like wedge, locally comprising lenticular shaped units (fig. 7.4). Dimension of interchannel sheets typically range from a few decimeters up to some few meters in thickness and widths exceeds outcrop exposure in almost all recognized bodies. The exception is some lenticular shaped units only extending for a few meters laterally. Sheet-like units typically consist of massive (F3) to soft-sediment deformed (F4) lower beds and current rippled (F13+F14) upper beds. Locally planar-parallel cross-stratified (F10) and low angular cross-stratified (F9) very-fine to fine grained sandstone beds occur.

Sheets (fig. 7.4) are mostly associated with crevasse splays and exhibits mostly ripple cross-stratified sandstones and minor dunes (described in FA 2, chapter 5). These deposits are laterally limited by scree cover and could therefore potentially also represent wings or wedges attached to channel sandstone bodies, if the exposure were better. Other deposits with similar geometries include paleosols or coal horizons and laminated interchannel fines.

Sandstone wedges are mostly observed close to type one and two channels generate sheet-like units, locally with distinct thinning from the channels and outward (fig. 7.4). Close to the assosiated channel sandstone bodies, these wedges range in thickness from 1.0 to 5.0 m, and are assumed to extend laterally in order of 10 to 100 of meters.

Lenticular shaped bodies are indicated by straight lower and convex upper surfaces, with bodies varying from decimeter up to one m in thickness (fig. 7.4). Laterally these bodies stretch for a few meters before terminating into adjacent floodplain fines. These bodies are interpreted as bar forms resting in-between crevasse splay channels.

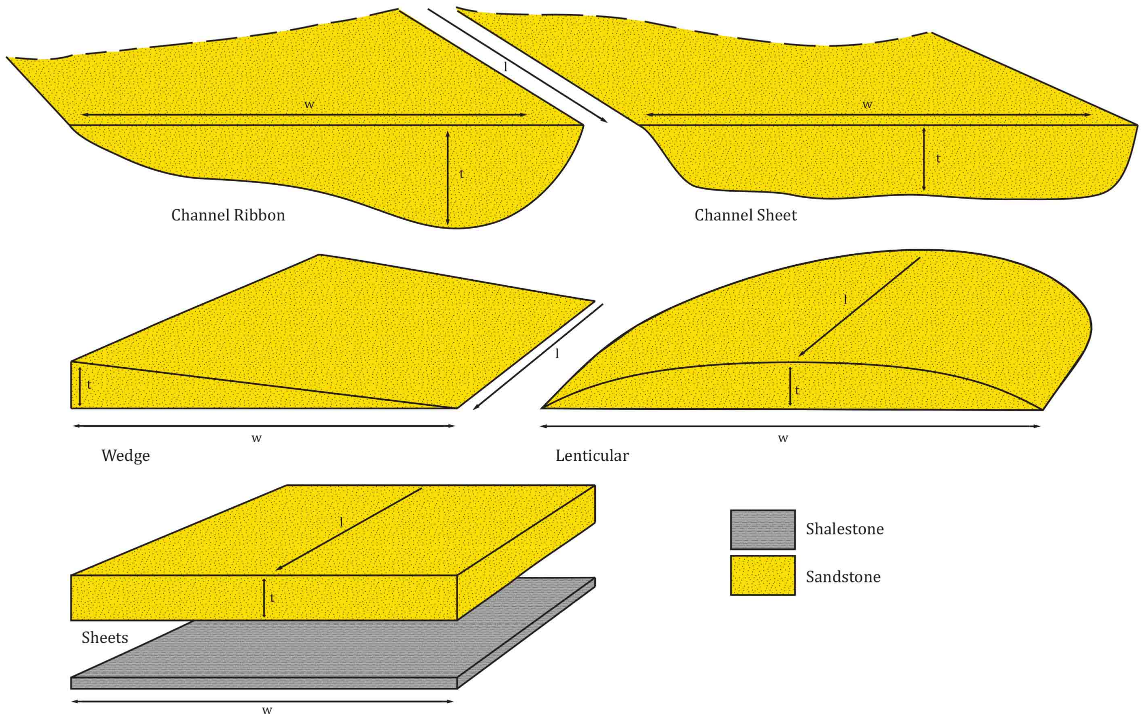

Figure 7.4: Sandstone body geometries, modified from Bridge (1993).

6.4 Vertical variations and sandstone distribution

In total 64.9% of the investigated parts of the Aspelintoppen Formation comprises sandstone-dominated deposits. The remaining 35.1% are fine-grained shale, siltstone and coal accumulated on the distal floodplain. It is important to emphasize that the thickness of interchannel shale intervals are hard to calculate in the field because they are estimated from intervals dominated by debris cover. Calculations of sand to mud ratios can therefore both be over and underestimated, based on the fact that intervals containing sandstone deposits can be overlooked and thickness calculations conducted in the field can therefore give thicker or thinner estimates than the true thicknesses. Of the 64.9% sandstone deposited in the studied section, only 10.1% are situated within major trunk channels, 10.9% within distributary channels and 15.7% in crevasse channels. The remaining 63.3% of the sandstone deposited in the studied section is located within interchannel sheet sandstone deposits. This distribution emphasizes the dominance of interchannel deposits within the Aspelintoppen Formation.

Type one, crevasse channels and possibly terminal distributary channels constitute only 15.7% of the total sand deposited within the logged. These channel bodies are distributed along the whole vertical length of the logged profile and are often observed to occur in clusters of multiple stacked crevasse channel complexes. Complexes or clusters are suggested to be related to the progressive progradation and/or retrogradation of a crevasse systems within a specific area of the floodplain, and are bounded by coal horizons. Once the floodplain area is filled or the main channel segment changes path, sandstone deposition will shift to a more preferred locations.

Most distributary channels of type 2 are grouped within two thickness intervals of approximately 100 m (green aras fig. 8.2), each in the central part of the main log (between approximately 500-700 m.a.s.l. in fig. 7.3). These packages are suggested to indicate locations of intense bifurcation, possibly from trunk channels close to the delta systems apex. This bifurcation of larger channel segments (type three) occur where gradient variation normal to the stream direction is similar to the downstream gradient (Olariu and Bhattacharya, 2006).

Type three channels are evenly distributed over the vertical length of the logged profiles (red bars fig. 7.3, and red areas fig. 8.2). This type of channel body only makes out 10.1% of the sandstone deposits at the logged section; further emphasizing the dominating depositional volume of interchannel sediments. The scarcity of fluvial trunk channels reflects the lack of sediment preservation within the trunk channels themselves. This is probably promoted by bypassing of sediments under normal flow condition for longer periods, resulting in deposition in the basins and floodplains rather than in the channels themselves.

Interchannel sheets, lenses and wedges represent the largest volumes of sandstone, comprising 66.4% of the sandstone deposits of the Aspelintoppen Formation. No clear vertical changes are noticed from the logged section, but a rather subtle trend of more frequent crevasse splay deposits in the upper part of the formation can be inferred. This is possibly due to the better exposure in the upper half of the formation, but as accommodation generally is larger at the more distal parts of the delta plain, it is reasonable to assume that thicker packages of interchannel fines would accumulate here.

A small increase in grain-size of interchannel sandstone beds, generally thinner shale intervals and more pebble dominated conglomeratic channel fill observed in the upper parts of the formation suggest an minor overall regressive trend, indicating progradation of the fluvial system and gradually more proximal facies moving upward in the formation.

7 DEPOSITIONAL ENVIRONMENT AND PALEOGEOGRAPHY

7.1 Application of an Anastomosing Fluvial System Model

Evidence of vegetation, multiple coal horizons, abundance of crevasse splays, and distribution of infrequent major channel elements suggests that the Aspelintoppen Formation partly was an anastomosing river system. Sedimentary environments and depositional architecture of deposits are illustrated in fig. 7.1.

Sandstone dominated ribbon shaped channel bodies with abundant organic detritus, coal and mud fragments near channel bases and adjacent attached heterolithic deposits similar to the deposits encountered in the Aspelintoppen Formation has been described by Makaske (2001) attributing them to have been deposited in anastomosing rivers. Additional characteristics according to Makaske (2001) are; dominance of mudrock facies; thin coal horizons representing accumulation of peat; intervening lacustrine deposits; high aggradation rates; and high proportions of overbank deposits.

In contrast to the incised valley model proposed by Plink-Bjørklund (2005) comprising sequences of lowstand fluvial deposits, transgressive estuarine deposits and highstand estuarine deposits, this study suggests high aggradation rates of floodplain deposits during frequent flooding of channel banks, and subsequent progradation of crevasse splay systems filling up floodplain basins. This could of course only be achieved through a continuously growing amount of accomondation space in the coastal plain area that backed-up the delta front.

Uplift of the West-Spitsbergen orogeny causing proximal uplift and subsequently extensive foreland-basin subsidence in combination with a high eustatic sea-level is suggested to have promoted suitable conditions for high floodplain aggradation. Thickness estimates of the Aspelintoppen Formation based on vitrnite reflectance studies have indicated that the formation originally reexceeded 2500 m in thickness (Manum and Throndsen, 1978). The thickness of the formation also suggests that floodplain aggradation would reflect some type of normal condition while channel avulsion would rather be considered as a state of disequilibrium (Makaske, 1998). Evolution of the fluvial system would therefore include repeated states of disequilibrium.

These states of disequilibrium will typically be promoted by low floodplain gradients possibly generated by high floodplain aggradation, which could be triggered by climatic events (abnormally high precipitation) (Makaske, 1998), sea-level rise as a downstream control for upstream avulsion (Smith and Smith, 1980) or rapid subsidising foreland basin (Smith, 1986; Smith and Putnam, 1980). Less likely is it that tectonic uplift of riverbed (Burnett and Schumm, 1983; Ouchi, 1985) caused low floodplain gradients, this because of the prominent uplift of the hinterland during deposition. Avulsion triggering mechanisms not dependent on a low floodplain gradient would include channels changing paths to a more preferred area of lower flow resistance, probably situated in a low lying floodplain. For this type of avulsion to occur a breach of the river bank, generated by violent floods, is needed to redirect the flow to an area of lower resistance.

The tectonic setting of the Aspelintoppen Formation (see chapter 3) implies that most of the avulsion triggering scenarios mentioned above could have occurred. The amount of soft-sediment deformation structures located in the deposits of the Aspelintoppen Formation suggests that earthquakes probably were of great importance. Tectonics and frequent flooding of channel banks induced by climatic changes suggest a strong control by allogenic processes (Miall and Postma, 1997) leading to channel avulsion. Autogenic processes influencing the fluvial system is suggested to include delta lobe switching (Grundvåg et al., 2014a).

High bank resistance here is argued to be the main factor for high lateral stability of individual channels, promoting the development of anastomosing rivers. Generally when thick cohesive sediments (including peat and vegetation) accumulate anastomosing river systems will develop (Tornqvist, 1993). As lower floodplain gradients are reached, avulsion can occur in several possible ways. Grundvåg (2014) argued that a decreasing hydraulic gradient followed by storm induced river floods could result in deposition and filling of channel segments promoting channel avulsion.

The multistory channels observed in the Aspelintoppen Formation suggests that this process could occur in several steps before filling the entire channel body, which subsequently lead to avulsion. Homogeneity of channel fill suggests that this filling of channel bodies would occur relatively rapidly, refusing development of distinct fining upward channel fill sequences. Other avulsion triggering mechanisms related to the Aspelintoppen Formation channels may involve bank collapse triggered by earthquakes blocking discharge in main channels leading to avulsion.

The formation thickness, abundance of crevasse splays and fluvial channel frequency suggests that the genesis and lifespan of this system was of a "*rapid aggrading anastomosing rivers in a humid setting"* (Makaske, 2001). The humid climate is reflected in the abundant detritus fragments and leaf prints prominent in the formation (further described below).

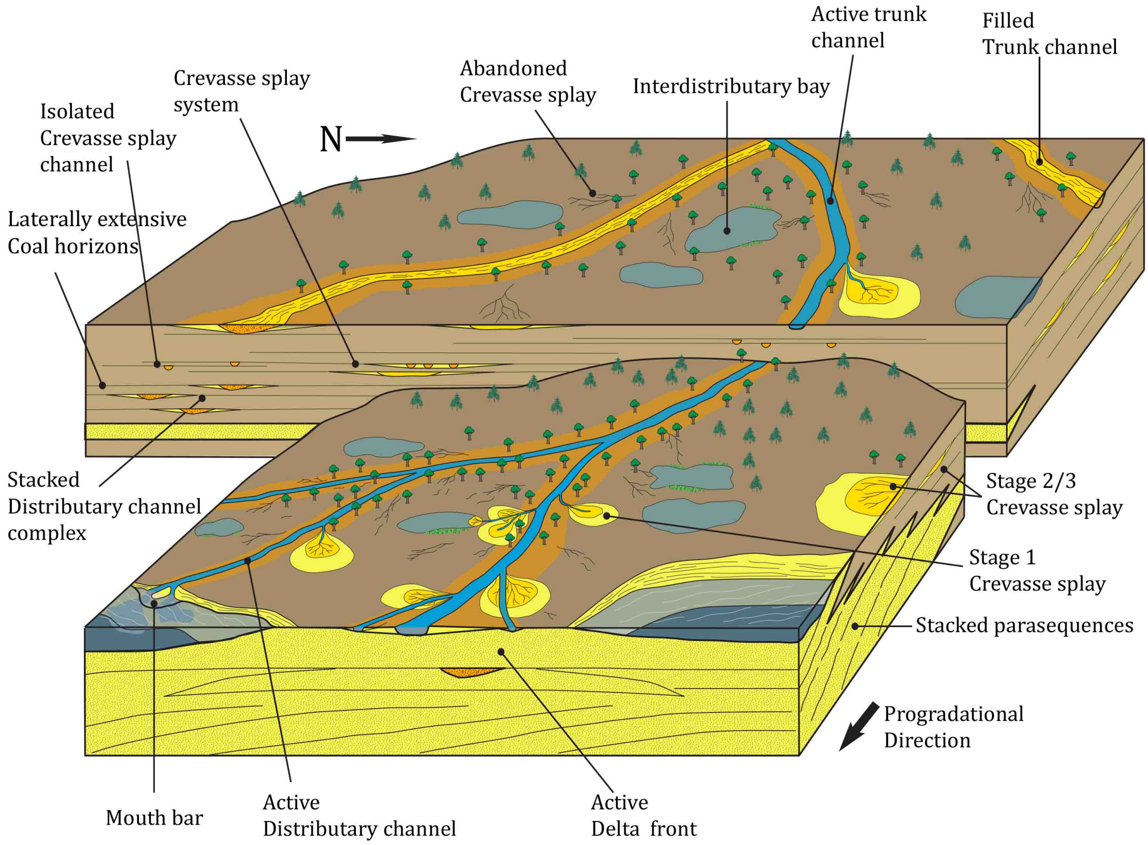

Figure 7.1: Schematic block diagram illustrating depositional environments and architectural elements of the studied deposits. Facies analysis of the Aspelintoppen Formation indicates a change from a fluvial, wave or locally tidal dominated delta front environment to coastal plain, floodplain and fluvial channel environment.

7.2 Modern analogues

Anastomosing rivers of the Lower Saskatchewan River in western Canada is suggested as a modern analogue to the Aspelintoppen Formation. Important features in the lower Saskatchewan River include: repeated avulsions driven by continuous rapid floodplain aggradation and abundant vegetation and peat layers promoting lateral channel stability (Makaske, 2001; Smith et al., 1989). Other similarities are channel thickness and percentage of deposition within floodplain environments. The lower Saskatchewan Rivers channel elements range from five-12 m in thickness, whereas the Aspelintoppen Formation channels range from three-10 m in thickness. Floodplain environments in the lower Saskatchewan River comprises about 60-90% of the anastomosing river deposits, whereas the studied location of the Aspelintoppen Formation, floodplain environments are estimated to comprise 78% of the deposits. The degree of meandering channel segments in the lower parts of the Saskatchewan River is believed to represent one of the significant differences from the Aspelintoppen Formation, where no lateral accretion is prominent. Although some meandering is suggested for channels in the lower parts of the Aspelintoppen Formation (see chapter 7.2.3), this only reflects minor parts of channel deposition. The Rhine-Meuse delta river system also shows similar characteristics as the Aspelintoppen Formation fluvial system. As with the lower Saskatchewan River the Rhine-Meuse delta river system comprises a higher degree of meandering rivers than what is assumed for the Aspelintoppen Formation.

The limited amount to absence of meandering channel in the lower parts of the Aspelintoppen Formation could indicate that the fluvial system has a steeper gradient and/ or a shorter distance to the source area than the above-mentioned modern analogues. This would subsequently promote rapid channel infill and not give the sufficient time needed for meandering to occur.

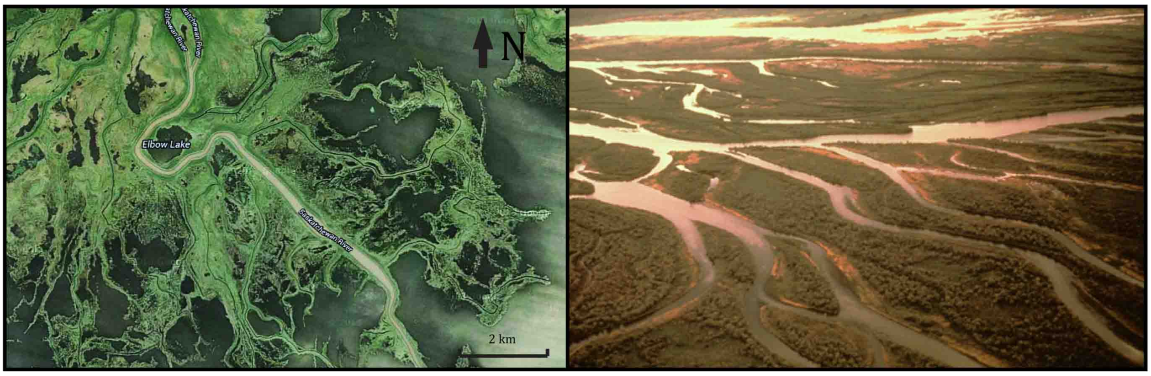

Figure 8.2: Map and picture of the Saskatchenwan River showing typical morphology of an anastomosing river system (map retrieved from google maps, and picture retrieved from www.geo.uu.nl).

7.3 Paleogeography and Environment

The vertical relationship of the facies assemblages and their respective sub-groups (described and interpreted in chapter 4), suggests that the investigated parts of the Aspelintoppen Formation was deposited within a delta plain to alluvial setting.

Paleocurrent data in trunk channels (chapter 4) indicate a general flow direction towards the southeast (fig. 7.1). Distributary channel paleocurrent data shows a more radial shape with flow directions towards the northeast and south, mainly perpendicular to the trunk channels. Crevasse splay and heterolithic levee deposits have even more radial paleocurrent directions, which are slightly skewed towards the east-southeast. Earlier documented sediment dispersal directions conducted in the Battfjellet Formation point to an east-, southeast- and southwards direction (Helland-Hansen, 1990; Plink-Bjørklund, 2005; Uroza and Steel, 2008). This coincides well with the paleocurrent directions documented in this study, suggesting that the transport direction possibly shifted from southeast to east.

Grundvåg (2014) argued that the deltas were mainly flood- and wave-dominated, but with some tidal influence at location protected by waves. In contrast Plink-Bjørklund (2005) argued that the main deposition occurred in tidal-influenced deltas. Based on the aggradational flood-dominated anastomosing fluvial system suggested for this study, delta settings similar to the ones presented in Grundvåg (2014) study is thought to occur.

Fluvial channels are as mentioned earlier moderately thick (three-10 m) and straight, and assumed to be of limited lateral extent due to cohesive banks (fig. 7.1). Based on facies assemblages of interchannel deposits, including leaf imprints in finer sediments and accumulation of peat, floodplain environments are assumed to comprise frequent flooded wetlands covered by abundant vegetation. These wetlands often include ephemeral lakes documented by distinct coarsening upwards sequences (see chapther 4.2) generated by crevasse systems transporting sediments into lakes located on the floodplain. Crevasse splay systems are also an important feature on the floodplain, and these are responsible for most of the sandy deposits in the formation. These deposits are expressed as three-10 m thick splay sheet systems, probably extending laterally 10-100 m out from associated channels.

Clifton (2012) stated in her research on the Aspelintoppen Formation flora and temperature estimates conducted on samples shows a close resemblance to today's arctic climate in Canada. Vegetation was characterized as lowland vegetation containing extensive swamps and ephemeral lakes. Climatic proxies indicate a wet region, subjected to heavy rainfall with seasonable shifts in temperatures from warm summer with average temperatures of approximately 18.7 degrees (±3.5) and relatively cold winters with average temperatures of 4.5 degrees (±4) (Clifton, 2012).

7.4 Sequence Stratigraphy

To link the sequence stratigraphy concepts to the fluvial system and relate these to the shallow marine parasequences of the Battfjellet Formation are difficult, as fluvial processes dominate deposition over marine processes that are only prominent close to the delta front. Internal sequence stratigraphy of the fluvial deposits is possible to apply for the individual aggradational events of the floodplain deposits. Each aggradational sequence is bounded by immature paleosols and/or coal horizons, representing periods of low floodplain aggradation. Generally these sequences range from three-10 m, reflecting differences in duration and intensity of flood events. Because each aggradational sequence is followed by distal floodplain fines it is also believed that each aggradational sequence is followed by channel avulsion, and subsequently change of sedimentation to a more preferred area. This would include all channel elements, from minor crevasse channels to larger trunk channels, and would subsequently reflect the magnitude of the avulsion triggering mechanism (fig. 8.3 and 8.4).

At present there is little literature discussing application of sequence stratigraphy to anastomosing fluvial environments and the interaction between the fluvial and fluviodeltaic environments (Makaske, 2001). Tornqvist (1993) argued that alternating meandering and anastomosing river systems reflected changes in river system gradients induced by sea-level rise. Under rapid sea-level rise aggradation rate and avulsion frequency increased in marginal parts resulting in the development of multiple coexisting anastomosing channels. As aggradation rates decreased development of meandering channels could occured due to deposition of relatively thin non-cohesive sands. In sequence stratigraphic terms the coexisting anastomosing distributary channel may characterize transgressive system tracts (TST) (Makaske, 2001). However Makaske (2001), stated that some authors (Shanley and McCabe, 1994) argue that initially rapid sea-level rise creates limited accommodation space in upper non-marine parts of deltas, and that sea-level rise is only felt when the coastline has shifted far inlands, meaning that multiple coexisting channel can be expected under highstand system tract (HST) rather than TST.

Applying this concept to the fluvial channels of the Aspelintoppen Formation is difficult, but two distinct intervals between 520-570 m.a.sl. and 640-700 m.a.sl. in the logged section (green areas fig. 8.3 and 8.4) are identified as stacked distributary system similar to the ones described by Tornqvist (1993).

In broader sense intervals dominated by multiple channel bodies and related crevasse splay complexes are suggested to reflect rapid fluvial aggradation, whereas intervals with major channel fill reflects low fluvial system gradients and low aggradation. In addition to this, intervals dominated by interchannel crevasse spalys and fines could reflect periods of steady aggradation and minor channel avulsion (fig. 8.3 and 8.4). Change in fluvial characteristics by avulsion could also indicate delta lobe switching, where channel complexes are overlain by thick units of interchannel fines (Grundvåg et al., 2014a).

As mentioned above aggradation of the fluvial system is considered to have lasted for longer periods, whilst low aggradation and low fluvial system gradients lasted only for shorter periods of the fluvial systems evolution. Helland-Hansen (2010) and Grundvåg et al. (2014a) suggested that the clay dominated poorly sorted shoreface sandstones and the delta front architecture point to steady shoreline progradation into the basin due to high and sustained fluvial sediment supply from the fluvial system (Grundvåg, 2014). This corresponds well with the aggradational nature suggested for the Aspelintoppen Formation.

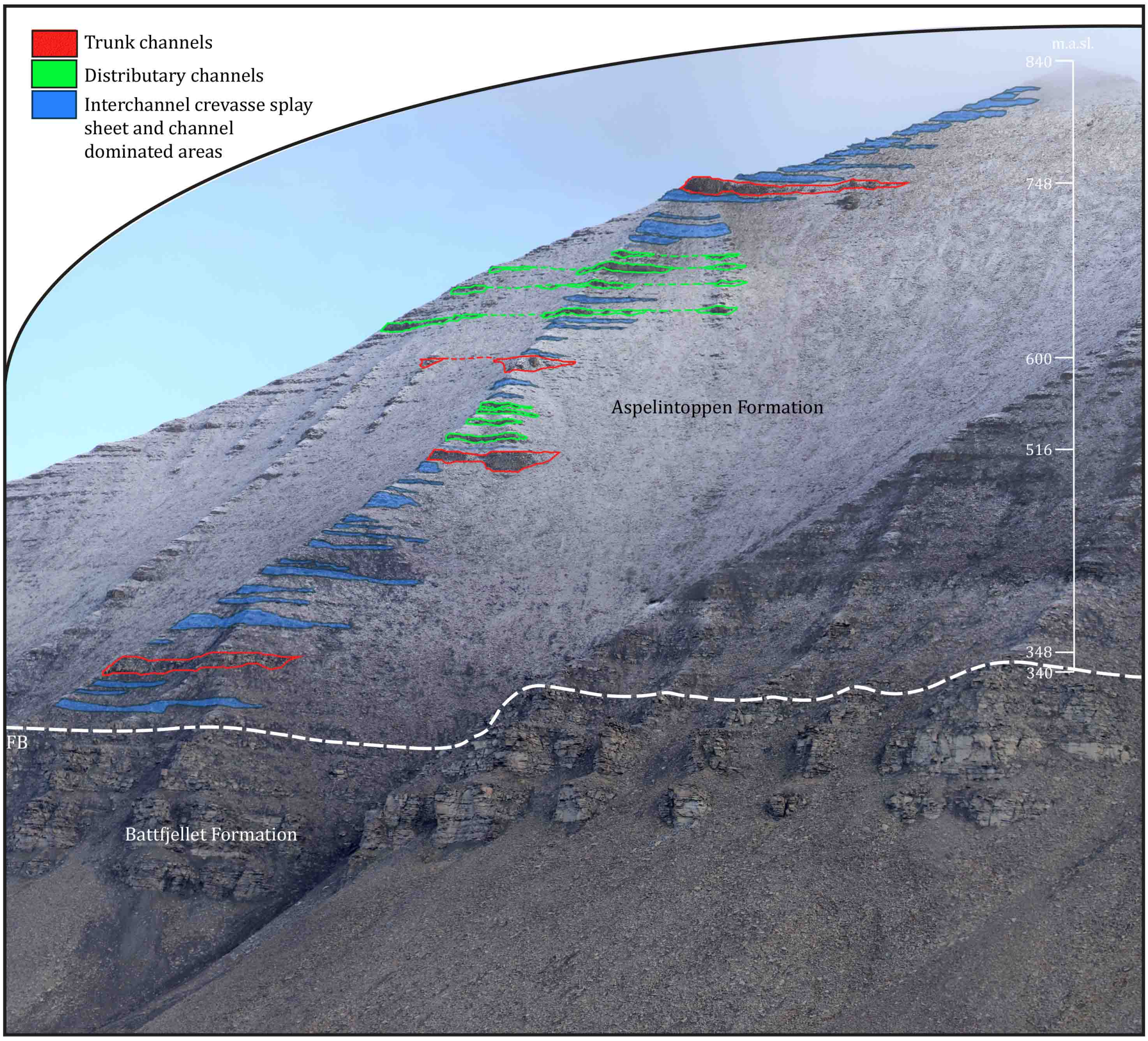

Figure 8.3: Distribution of depositional units within the Aspelintoppen Formation., Brogniartfjella west.

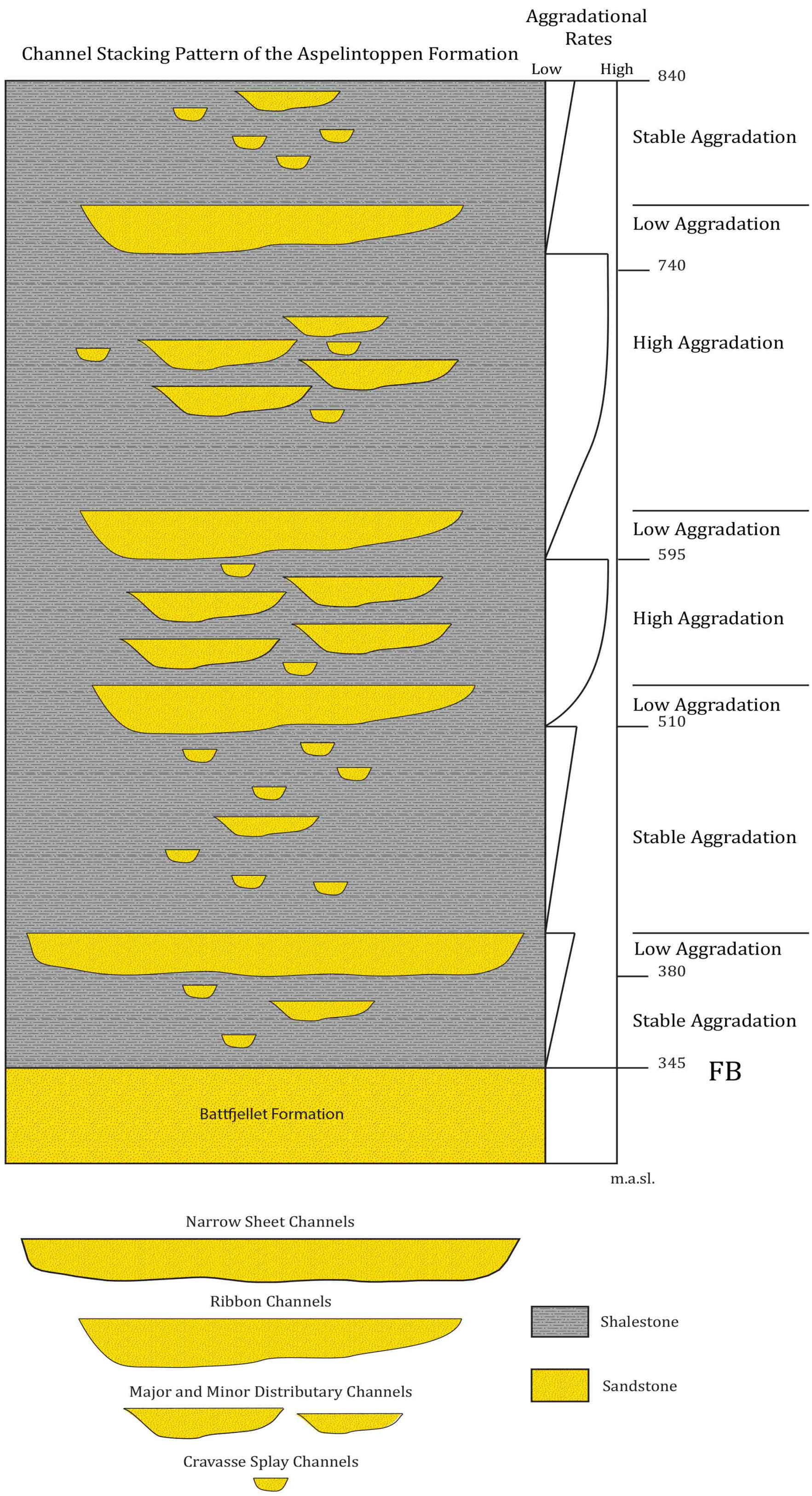

Figure 8.4: Illustration of channel stacking pattern in the Aspelintoppen Formation channel. FB: formation boundary, m.a.sl.: meters above sea-level, LST: lowstand system tract, TST: transgressive system tract, HST: highstand system tract, MFS: maximum flooding surface. Figure is compressed, meaning that channel bodies are vertically stacked even if they appear to be laterally separated.

8 SUMMARY AND CONCLUSIONS

The sedimentological development of channel and interchannel deposits in the Aspelintoppen Formation at the western parts of Brogniartfjella has been the main focus of the present study. Previous work have been concentrated around the lower parts (Grundvåg et al., 2014a; Plink-Bjørklund, 2005) of the Aspelintoppen Formation whereas this study comprises the whole vertical exposure of the Aspelintoppen on the western parts of Brogniartfjella. In total four major fluvial channel bodies were identified over the vertical length of the main log, extending from the top Battfjellet Formation at 340 m.a.sl. to the top of the mountain at approximately 840 m.a.sl.. Between the, close to equally spaced trunk channels, aggradational interchannel fines and sandstone-dominated sheets, as well as intersecting distributary channels occur.

The Aspelintoppen Formation consists of a south to eastwards draining aggrading fluvial system, with sediments derived from the West Spitsbergen fold-and-thrust belt and with sediments taking place in the adjacent foreland basin shallow marine deltas and associated clinothms were deposited. The channels in the lower part of the formation is directly linked to delta front and slope wedges in the underlying Battfjellet Formation.

Documentation of the depositional architecture of channel and interchannel deposits through facies analysis and correlation of logged section, combined with paleoflow and ichnological data demonstrate the following main conclutions:

1. The studied succession is subdivided into facies association base on its constituent fluvial to deltaic depositional environments. Lateral compilations of these facies assosiations typically show gradual transitions from main channel segments (FA 1.1/1.2) to heterolithic levee deposits (FA 2.3), crevasse channels and proximal crevasse splay sheet deposits (FA 2.4 and 2.5), distal crevasse splay sheets and interdistributary bay fill deposits (FA 2.2 and 2.6), and to distal floodplain shale deposits (FA 2.1). More distal settings close to the delta front comprise coarsening upward tidal influenced delta front deposits (FA 3.1) transitioning relatively sharply into either heterolitic tidally influenced deposits

(FA 3.2), distal crevasse splay sheet deposits (FA 2.2), distal floodplain shale deposits (FA 2.1), or to crevasse channel deposits (FA 2.4). Vertically the succession comprises thick interchannel dominated units separated either by trunk channels (FA 1.1) or stacked distributary complexes (FA 1.2) and related heterolitic levees (FA 2.3). Interchannel units comprise crevasse splay deposits (FA 2.5) or distal crevasse splay sheet deposits (FA 2.2) separated by distal floodplain shale dominated units (FA 2.1).

2. Trace fossils studies conducted from the top Battfjellet Formation to the mid Aspelintoppen Formation is subdivided into ichnofacies on the basis of depositional environments. The complete vertical compilation of these ichnofacies represents a transition from upper shoreface and foreshore (FA 3.1) *Cruziana* ichnofacies (chapter 5.2.1), brackish water and tidal influenced (FA3.2 and 2.1) *Skolithos* ichnofacies (chapter 5.2.2), to continental floodplain (FA 2.1, 2.3, 2.4, 2.5) and interdistributary bay fill (FA 2.6) *Scoyenia* and *Mermia* ichnofacies (chapter 5.2.3). Successively these ichnofaceis assemblages indicates a rapid change from fully marine to fully continental, with a minor brackish to tidal influenced interval no more than 10 m thick from the last CU-parasequence of the Battfjellet Formation.

3. Geometry, size and stacking patterns of fluvial channels and interchannel sandstone sheets is important for understanding the fluvial systems evolution and building mechanisms.

   Trunk channel bodies (FA 1.1), categorized as type 3 channels in chapter 6, range from 6.7-10.0 m in thickness, mostly showing ribbon shaped geometries with multiple lensoid to sheet shaped erosional scoured internal structures indicates channel filling by several phases of vertical aggradation. One single channel sandstone body in the basal parts of the Aspelintoppen Formation exhibits a narrow sheet geometry suggested to indicate some degree of lateral accretion, despite the absence of clear lateral accretion surfaces. Sedimentary deposits are typically characterized by abundant trough cross-stratified (F1+F2), soft-sediment deformed (F4) and massive sandstone beds, which includes pebble lags, mud clasts and coal fragments in basal parts of channel bodies. Vertically stacking of trunk channel bodies are approximantly equally spaced over the logged section.

Distributary channels (FA 1.2), categorized as type 2 channels in chapter 6, show similar ribbon shaped geometries as most trunk channel bodies and occur as vertically stacked complexes comprising several distributary channel segments, indicating highly aggradational conditions. Sedimentary deposits are characterized by abundant trough cross-stratified (F1+F2) and soft-sediment deformed (F4), and locally planar-parallel stratified (F5) planar cross-stratified and low angular cross-stratified (F9) sandstone beds, typically located in the upper parts of channel bodies.

Crevasse channels (FA 2.4) are categorized as channel type 1 and comprises 0.3 to 2.2 m thick ribbon- to U-shaped channel bodies extending laterally for a few meters. These channel bodies typically consist of, massive (F3) to soft-sediment deformed (F4) basal deposits, typically overlain by trough cross-stratified (F2) or low-angular cross-stratified (F9) sandstones and locally planar-parallel cross-stratified sandstones (F5). Upper parts comprise current rippled beds (F13+14).

Interchannel sheet-like sandstone bodies volumetrically represents most of the sandstone deposited in the logges section. These sheet-like bodies comprise thick wedges associated with heterolithic levee deposits (FA 2.3), vertically stacked proximal crevasse splay sheet complexes (FA 2.5) including crevasse channels, and distal lenticular shaped crevasse splay bodies (FA 2.2). Vertically these intervals increase in frequency upwards and with accompanying thinner shale units upwards in the logged section, indicating more proximal deposits upwards in the formation. Sedimantary deposits are dominated by current rippled (F13+F14) sandstone beds and locally massive (F3), soft-sediment deformed (F4) and wave ripple cross-laminated (F12) sandstone beds.

4. The channel body geometries and their distribution, the abundancy of interchannel sandstone deposits, the occurrence of multiple coal horizons, and

the abundant leaf prints supports an anastomosing fluvial model. Evolution of the fluvial system is promoted by floodplain aggradation from frequent flood events, triggered by earthquakes and climatic factors like increased precipitation, and possibly rapid sea-level rise. Subsequently channel evolution is controlled by channel avulsion. Cohesive banks, high floodplain aggradation rates lowering the fluvial gradient is considered as the most important mechanisms for generating suitable conditions for avulsion to occur. Avulsion can then occur by breaching of channel banks and bifurcation of the channel by high stream velocities during relatively high river gradient, change in stream velocity because of lowering of the fluvial gradient promoting in channel deposition, which subsequently leads to avulsion, or bank collapse generated by earthquakes blocking channel, forcing it to change path.

5. The paleogeographical setting, as supported by paleocurrent measurements, show a southeast to eastwards transport and progradational direction of the fluvial system, consistent with the eastward progradation of the underlying delta system.

6. The paleoenvironmental setting of the Aspelintoppen Formation is suggested to be similar to the modern day western Canada arctic wet temperate climate, on the basis of paleoflora and fluvial system evolution. This includes lowland vegetation with extensive swamps and ephemeral lakes. The environmental settings, high aggradational floodplains dominated by crevasse splay sheet sandstones and thin coal horizons, and the scarcity of sandstone preserved in trunk channel bodies give rise for the anastomosing river system interpretation.

7. Aggradational rates of the sediments deposited in the studied area are suggested to be indicated by the responsible facies stacking patterns prominent in each depositional unit. Intervals dominated by interchannel deposits (FA 2) are here suggested to reflect periods of stable aggradation, while distributray channel complexes indicate periods of rapid or high aggradation (FA 1.2), and major channel bodies indicate periods of low aggradational rates.

Suggestions for further work:

Little is known about the evolution of the Aspelintoppen formation and consequently the triggering mechanisms responsible for the high aggradational rates of the system. Further work should focus on the mapping of channels and their dimensions, distribution and frequency, combined with mapping of associated interchannel deposits. Additionally, linking depositional segments to tectonic events or sea-level fluctuations, and their importance for increasing floodplain aggradation and channel avulsion, is believed to be of great importance for the understanding of the fluvial systems evolution.

9 REFERENCES:

Atkinson, D. J., 1963, Tertiary Rocks of Spitbergen: AAPG Bulletin, v. 47, no. 2, p. 302-323

Bergh, S. G., Braathen, A., and Andresen, A., 1997, Interaction of basement-involved and thin-skinned tectonism in the Tertiary fold-thrust belt of central Spitsbergen, Svalbard: AAPG bulletin, v. 81, no. 4, p. 637-661

Best, J., and Bridge, J. S., 1992, The morphology and dynamics of low amplitude bedwaves upon upper stage plane beds and the preservation of planar laminae: Sedimentology, v. 39, no. 5, p. 737-752

Birkenmajer, K., 1981, The geology of Svalbard, the western part of the Barents Sea, and the continental margin of Scandinavia, The Arctic Ocean, Springer, p. 265-329

Blinova, M., Faleide, J. I., Gabrielsen, R. H., and Mjelde, R., 2012, Seafloor expression and shallow structure of a fold-and-thrust system, Isfjorden, west Spitsbergen: Polar Research, v. 31

Blinova, M., Thorsen, R., Mjelde, R., and Faleide, J. I., 2009, Structure and evolution of the Bellsund Graben between Forlandsundet and Bellsund (Spitsbergen) based on marine seismic data: Seismic study along the west Spitsbergen continental margin and adjacent area of the West Spitsbergen Fold and Thrust Belt (Isfjorden).

Blythe, A. E., and Kleinspehn, K. L., 1998, Tectonically versus climatically driven Cenozoic exhumation of the Eurasian plate margin, Svalbard: fission track analyses: Tectonics, v. 17, no. 4, p. 621-639

Bouma, A., 1964, Turbidites: Developments in sedimentology, v. 3, p. 247-256

Bradshaw, M. A., 2002, A new ichnogenus Catenarichnus from the Devonian of the Ohio Range, Antarctica: Antarctic Science, v. 14, no. 04, p. 422-424

Bridge, J. S., 1993, Description and interpretation of fluvial deposits: a critical perspective: Sedimentology, v. 40, no. 4, p. 801-810

Bridge, J. S., 2009, Rivers and floodplains: forms, processes, and sedimentary record.

Bruhn, R., and Steel, R., 2003, High-resolution sequence stratigraphy of a clastic foredeep succession (Paleocene, Spitsbergen): An example of peripheral-bulge-controlled depositional architecture: Journal of Sedimentary Research, v. 73, no. 5, p. 745-755

Braathen, A., Bergh, S. G., and Maher, H. D., 1999, Application of a critical wedge taper model to the Tertiary transpressional fold-thrust belt on Spitsbergen, Svalbard: Geological Society of America Bulletin, v. 111, no. 10, p. 1468-1485.

Buatois, L. A., and Mángano, M. G., 1998, Trace fossil analysis of lacustrine facies and basins: Palaeogeography, Palaeoclimatology, Palaeoecology, v. 140, no. 1, p. 367-382

Burnett, A. W., and Schumm, S. A., 1983, Alluvial-river response to neotectonic deformation in Louisiana and Mississippi: Science, v. 222, no. 4619, p. 49-50

Clifton, A. J., 2012, The eocene flora of Svalbard and its climatic significance: University of Leeds.

Clifton, H. E., and Thompson, J. K., 1978, Macaronichnus segregatis: a feeding structure of shallow marine polychaetes: Journal of Sedimentary Research, v. 48, no. 4.

Dalland, A., Structural geology and petroleum potential of Nordenskiold Land1979, p. 1-20.

Dallmann, W. K., 1999, Lithostratigraphic lexicon of Svalbard.

Dawson, J. W., 1862, Notice of the discovery of additional remains of land animals in the coal-measures of the South Joggins, Nova Scotia: Quarterly Journal of the Geological Society, v. 18, no. 1-2, p. 5-7.

Dietmar-Müller, R., and Spielhagen, R. F., 1990, Evolution of the Central Tertiary Basin of Spitsbergen: towards a synthesis of sediment and plate tectonic history: Palaeogeography, Palaeoclimatology, Palaeoecology, v. 80, no. 2, p. 153-172

Dreyer, T., and Helland-Hansen, W., 1986, Aspelintoppen Fm. (Paleogene), Spitsbergen: Aspects of deposition and contribution to basin developments: Report: Norsk Hydro.

Eagar, R. M. C., 1985, The stratigraphical and palaeoecological distribution of non-marine bivalves in the coalfields of northwest Spain: 10th International Carboniferous Congress, Compte Rendu, Madrid, 1983, no. 2, p. 455–476.

Ekdale, A. A., Bromley, R. G., and Loope, D. B., 2007, Ichnofacies of an ancient erg: A climatically influenced trace fossil association in the Jurassic Navajo Sandstone, southern Utah, USA: Trace Fossils: Concepts, Problems, Prospects: Elsevier, Amsterdam, p. 562-574.

Elliott, T., 1974, Interdistributary bay sequences and their genesis: Sedimentology, v. 21, no. 4, p. 611-622

Faleide, J. I., Vågnes, E., and Gudlaugsson, S. T., 1993, Late Mesozoic-Cenozoic evolution of the south-western Barents Sea in a regional rift-shear tectonic setting: Marine and Petroleum Geology, v. 10, no. 3, p. 186-214

Farrell, K. M., 2001, Geomorphology, facies architecture, and high-resolution, non-marine sequence stratigraphy in avulsion deposits, Cumberland Marshes, Saskatchewan: Sedimentary Geology, v. 139, no. 2, p. 93-150

Fenton, C. L., and Fenton, M. A., 1937, Archaeonassa: Cambrian snail trails and burrows: American Midland Naturalist, v. 18, no. 3, p. 454-456

Fitch, A., 1850, A historical, topographical and agricultural survey of the County of Washington: Transactions of the New York Agricultural Society, v. 9, no. Part 2-5, p. 753-944.

Gibling, M. R., 2006, Width and thickness of fluvial channel bodies and valley fills in the geological record: a literature compilation and classification: Journal of sedimentary Research, v. 76, no. 5, p. 731-770

Gjelberg, H. K., 2010, Facies Analysis and Sandbody Geometry of the Paleogene Battfjellet Formation, Central Western Nordenskiöld Land, Spitsbergen: Master of Science Thesis in Petroleum Geology, Department of Earth Science, University of Bergen, and Department of Arctic Geology, University Centre in Svalbard, p. 1-163.

Grundvåg, S.-A., 2014, Clinoform and parasequence variability in the Eocene Battfjellet Formation, Nathorst Land, Spitsbergen: Submitted to Sedimentology, p. 1-78.

Grundvåg, S. A., Johannessen, E. P., Helland-Hansen, W., and Plink-Björklund, P., 2014a, Depositional architecture and evolution of progradationally stacked lobe complexes in the Eocene Central Basin of Spitsbergen: Sedimentology, v. 61, no. 2, p. 535-569

Grundvåg, S. A. e. a., Helland-Hansen, W., Johannessen, E. P., Olsen, A. H., and Stene, S. A. K., 2014b, The depositional architecture and facies variability of shelf deltas in the Eocene Battfjellet Formation, Nathorst Land, Spitsbergen: Sedimentology.

Haldeman, S. S., 1840, Supplement to Number One of" A Monograph of the Limniades, Or Freshwater Univalve Shells of North America": Containing Descriptions of Apparently New Animals in Different Classes and the Names and Characters of the Subgenera in Paludina and Anculosa.

Harland, W. B., 1969, Contribution of Spitsbergen to Understanding of Tectonic Evolution of North Atlantic Region: Chapter 58: Arctic Regions.

Harland, W. B., Anderson, L. M., Manasrah, D., Butterfield, N. J., Challinor, A., Doubleday, P. A., Dowdeswell, E. K., Dowdeswell, J. A., Geddes, I., and Kelly, S. R. A., 1997, The geology of Svalbard.

Harland, W. B., and Horsfield, W. T., 1974, West Spitsbergen orogen: Geological Society, London, Special Publications, v. 4, no. 1, p. 747-755

Helland-Hansen, W., 1990, Sedimentation in Paleogene Foreland Basin, Spitsbergen (1): AAPG Bulletin, v. 74, no. 3, p. 260-272

Helland-Hansen, W., 2010, Facies and stacking patterns of shelf-deltas within the Palaeogene Battfjellet Formation, Nordenskiöld Land, Svalbard: implications for subsurface reservoir prediction: Sedimentology, v. 57, no. 1, p. 190-208

James, U. P., 1879, Description of new species of fossils and remarks on some others, from the Lower and Upper Silurian rocks of Ohio: The Paleontologist, v. 3, p. 17-34.

Kellogg, H. E., 1975, Tertiary stratigraphy and tectonism in Svalbard and continental drift: AAPG Bulletin, v. 59, no. 3, p. 465-485.

Kundu, A., Matin, A., Mukul, M., and Eriksson, P. G., 2011, Sedimentary facies and soft-sediment deformation structures in the late miocene-pliocene Middle Siwalik subgroup, eastern Himalaya, Darjiling District, India: Journal of the Geological Society of India, v. 78, no. 4, p. 321-336

Lesquereux, L., 1876, Species of fossil marine plants from the Carboniferous Measures. Linck, O., 1949, Lebens-Spuren aus dem Schilfsandstein (Mittl. Keuper, km 2) NW-W¨urttembergs und ihre Bedeutung f¨ur die Bildungsgeschichte der Stufe: Jahreshefte des Vereins f¨ur vaterl¨andische Naturkunde in W¨urttemberg, p. 97-101: 101-100.

Lundgren, B., 1891, Studier öfver fossilforande lösa block: Geologiska Föreningen i Stockholm Förhandlingar, v. 13, no. 2, p. 111-121.

M'Coy, F., 1850, On some genera and species of Silurian Radiata in the collection of the University of Cambridge: Annals and Magazine of Natural History, v. 2, p. 270-290.

Maher, H. D., Braathen, A., Bergh, S., Dallmann, W., and Harland, W. B., 1995, Tertiary or Cretaceous age for Spitsbergen's fold-thrust belt on the Barents Shelf: Tectonics, v. 14, no. 6, p. 1321-1326

Major, H., and Nagy, J., 1972, Geology of the Adventdalen map area: with a geological map, Svalbard C9G 1: 100 000.

Makaske, B., 1998, Anastomosing rivers: forms, processes and sediments: Nederlandse Geografische Studies (Netherlands)

Makaske, B., 2001, Anastomosing rivers: a review of their classification, origin and sedimentary products: Earth-Science Reviews, v. 53, no. 3, p. 149-196.

Manby, G. M., and Lyberis, N., 1996, State of stress and tectonic evolution of the West Spitsbergen Fold Belt: Tectonophysics, v. 267, no. 1, p. 1-29

Mángano, M. G., 2002, Ichnology of a Pennsylvanian equatorial tidal flat: the Stull Shale Member at Waverly, eastern Kansas, State Printing Office.

Manum, S. B., 1962, Studies in the Tertiary flora of Spitsbergen, with notes on Tertiary floras of Ellesmere Island, Greenland, and Iceland: a palynological investigation.

Manum, S. B., and Throndsen, T., 1978, Rank of coal and dispersed organic matter and its geological bearing in the Spitsbergen Tertiary: Nor. Polarinst. Arbok, v. 1977, p. 159-177.

Miall, A. D., and Postma, G., 1997, The Geology of Fluvial Deposits, Sedimentary Facies, Basin Analysis and Petroleum Geology: Sedimentary Geology, v. 110, no. 1, p. 149

Nagy, J., Kaminski, M. A., Kuhnt, W., and Bremer, M. A., 2001, Agglutinated foraminifera from neritic to bathyal facies in the Palaeogene of Spitsbergen and the Barents Sea.

Nichols, G. J., and Fisher, J. A., 2007, Processes, facies and architecture of fluvial distributary system deposits: Sedimentary Geology, v. 195, no. 1, p. 75-90

Nicholson, H. A., 1872, Contributions to the Study of the Errant Annelides of the Older Palaeozoic Rocks: Proceedings of the Royal Society of London, v. 21, no. 139-147, p. 288-290

Nopsca, F. B., 1923, Die familien der Reptilien.

Olariu, C., and Bhattacharya, J. P., 2006, Terminal distributary channels and delta front architecture of river-dominated delta systems: Journal of Sedimentary Research, v. 76, no. 2, p. 212-233

Ouchi, S., 1985, Response of alluvial rivers to slow active tectonic movement: Geological Society of America Bulletin, v. 96, no. 4, p. 504-515

Paech, H. J., 2001, The Tertiary and Cretaceous of Spitsbergen and North Greenland: its alpine signature: Polarforschung, v. 69, p. 107-115

Plink-Bjørklund, P., 2005, Stacked fluvial and tide-dominated estuarine deposits in high-frequency (fourth-order) sequences of the Eocene Central Basin, Spitsbergen: Sedimentology, v. 52, no. 2, p. 391-428.

Reineck, H.-E., 1960, Über Zeitlücken in rezenten Flachsee-Sedimenten: Geologische Rundschau, v. 49, no. 1, p. 149-161.

Reineck, H.-E., and Singh, I. B., 1980, Tidal flats, Depositional Sedimentary Environments, Springer, p. 430-456

Roest, W. R., and Srivastava, S. P., 1989, Sea-floor spreading in the Labrador Sea: A new reconstruction: Geology, v. 17, no. 11, p. 1000-1003

Salter, J. W., 1857, On Annelide-burrows and Surface-markings from the Cambrian Rocks of the Longmynd. No. 2: Quarterly Journal of the Geological Society, v. 13, no. 1-2, p. 199-206.

Saunderson, H. C., and Lockett, F. P. J., 1983, Flume experiments on bedforms and structures at the dune-plane bed transition: Modern and Ancient Fluvial Systems: International Association of Sedimentologists, Special Publication, v. 6, p. 49-58.

Shanley, K. W., and McCabe, P. J., 1994, Perspectives on the sequence stratigraphy of continental strata: AAPG bulletin, v. 78, no. 4, p. 544-568.

Smith, D. G., 1986, Anastomosing river deposits, sedimentation rates and basin subsidence, Magdalena River, northwestern Colombia, South America: Sedimentary Geology, v. 46, no. 3, p. 177-196

Smith, D. G., and Putnam, P. E., 1980, Anastomosed river deposits: modern and ancient examples in Alberta, Canada: Canadian Journal of Earth Sciences, v. 17, no. 10, p. 1396-1406.

Smith, D. G., and Smith, N. D., 1980, Sedimentation in anastomosed river systems: examples from alluvial valley near Bannf, Alberta: Journal of Sedimentary Research, v. 50, no. 1.

Smith, N. D., Cross, T. A., Dufficy, J. P., and Clough, S. R., 1989, Anatomy of an avulsion: Sedimentology, v. 36, no. 1, p. 1-23

Stanistreet, I. G., Le Blanc, S., Cable, G., and Cable, A. B., 1980, Trace fossils as sedimentological and palaeoenvironmental indices in the Ecca Group (Lower Permian) of the Transvaal: Transactions of the Geological Society of South Africa, no. 83, p. 333-344.

Steel, R., Gjelberg, J., Helland-Hansen, W., Kleinspehn, K., Ná, A., and Rye-Larsen, M., 1985, The Tertiary strike-slip basins and orogenic belt of Spitsbergen.

Steel, R. J., Dalland, A., Kalgraff, K., and Larsen, V., 1981, The Central Tertiary Basin of Spitsbergen: Sedimentary development of a sheared-margin basin, p. 647 - 664.

Stouthamer, E., 2001, Sedimentary products of avulsions in the Holocene Rhine–Meuse Delta, the Netherlands: Sedimentary Geology, v. 145, no. 1, p. 73-92

Tornqvist, T. E., 1993, Holocene alternation of meandering and anastomosing fluvial systems in the Rhine-Meuse delta (central Netherlands) controlled by sea-level rise and subsoil erodibility: Journal of Sedimentary Research, v. 63, no. 4

Uchman, A., 1991, Shallow water" trace fossils in Palaeogene flysch of the southern part of the Magura Nappe, Polish Outer Carpathians, v. 61, p. 61-75.

Uchman, A., 2004, Marine and non-marine trace fossils in Eocene facies of the Central Basin in the northern side of Van Keulenfjorden, Spitsbergen: Wolf Consortium Internal Report 2004, no. 1, p. 45.

Uchman, A., and Krenmayr, H. G., 1995, Trace fossils from lower Miocene (Ottnangian) molasse deposits of Upper Austria: Paläontologische Zeitschrift, v. 69, no. 3-4, p. 503-524

Uroza, C. A., and Steel, R. J., 2008, A highstand shelf-margin delta system from the Eocene of West Spitsbergen, Norway: Sedimentary Geology, v. 203, no. 3, p. 229-245.

Vail, P. R., Mitchum Jr, R. M., and Thompson Iii, S., 1977, Seismic Stratigraphy and Global Changes of Sea Level: Part 4. Global Cycles of Relative Changes of Sea Level.: Section 2. Application of Seismic Reflection Configuration to Stratigraphic Interpretation.

White, C. D., 1929, Flora of the Hermit Shale, Grand Canyon: Arizona. Carnegie Institute of Washington Publication,, p. 405, 221.

Willis, B. J., and Behrensmeyer, A. K., 1994, Architecture of Miocene overbank deposits in northern Pakistan: Journal of Sedimentary Research, v. 64, no. 1

Worsley, D., 2008, The post-Caledonian development of Svalbard and the western Barents Sea: Polar Research, v. 27, no. 3, p. 298-317

Appendix: Lithostratigraphical log, Brogniartfjella West:

Logs are presented in a 1:50 scale. Height is represented in meters above sea-level (m.a.sl.)

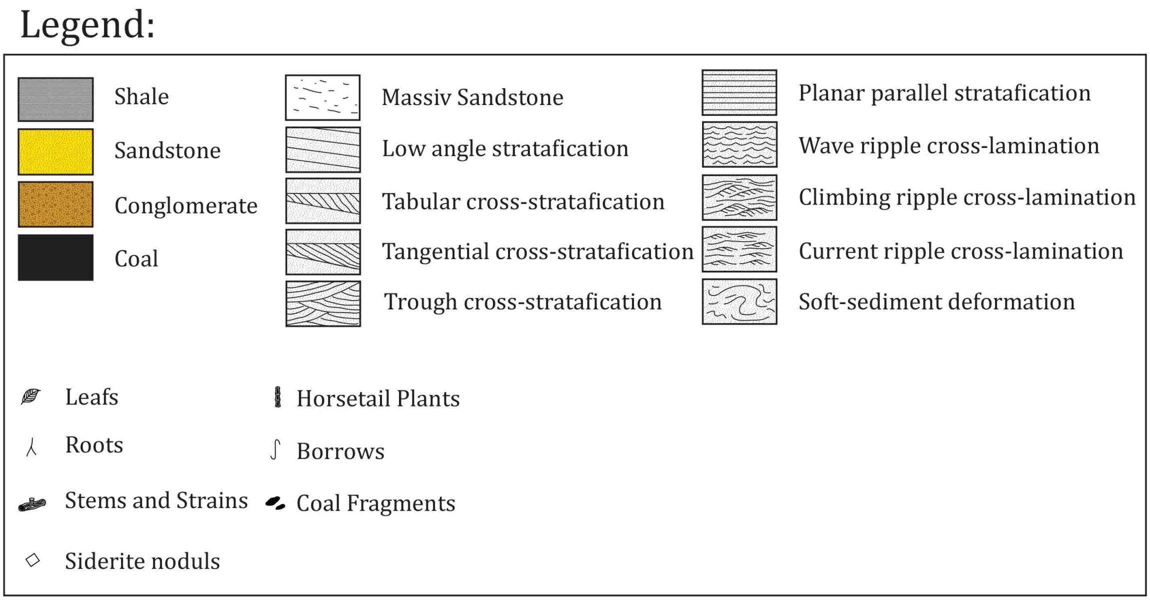

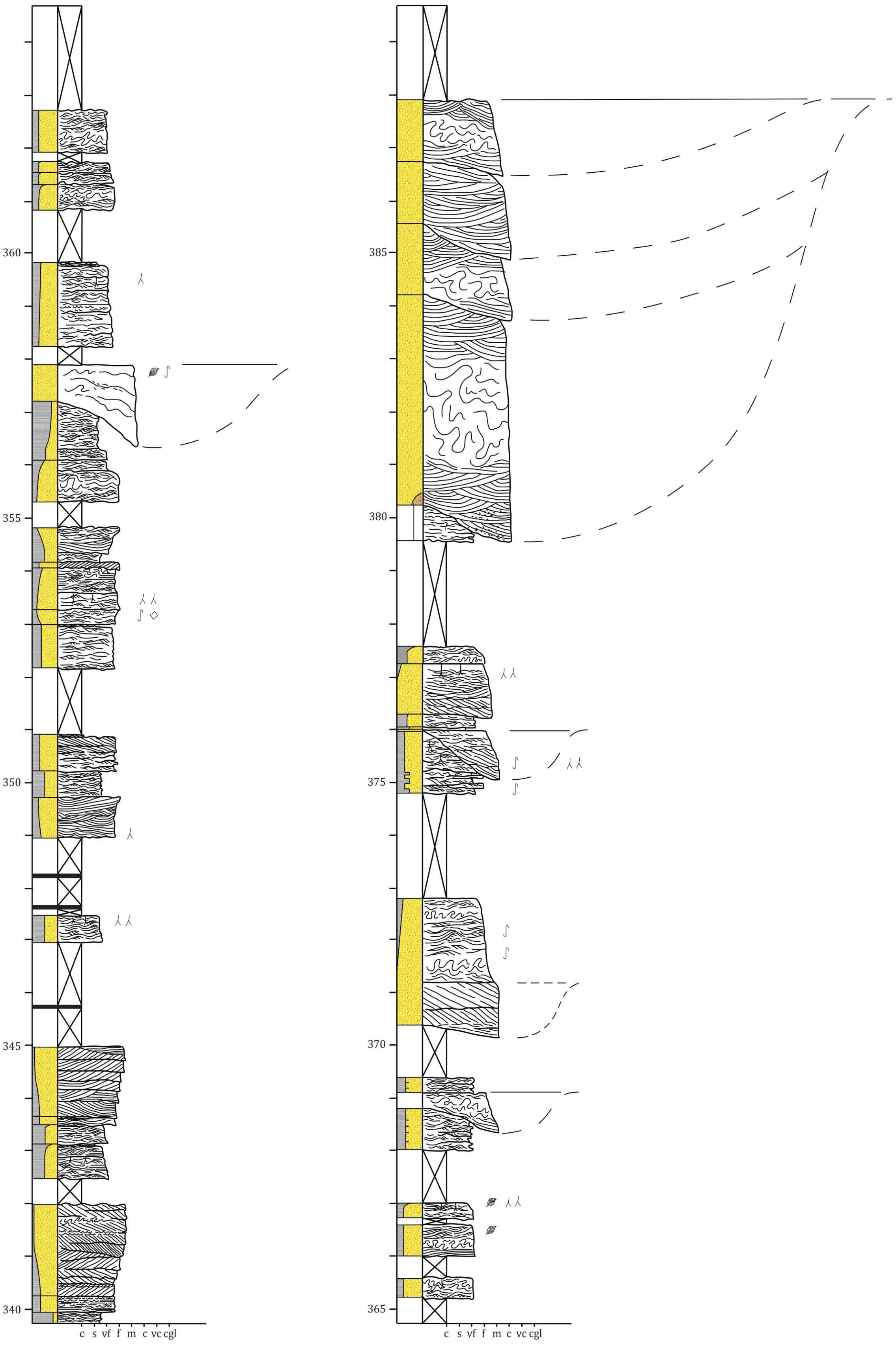
360
355
350
345
340
c s vf f m c vc cgl
385
380
375
370
365
c s vf f m c vc cgl

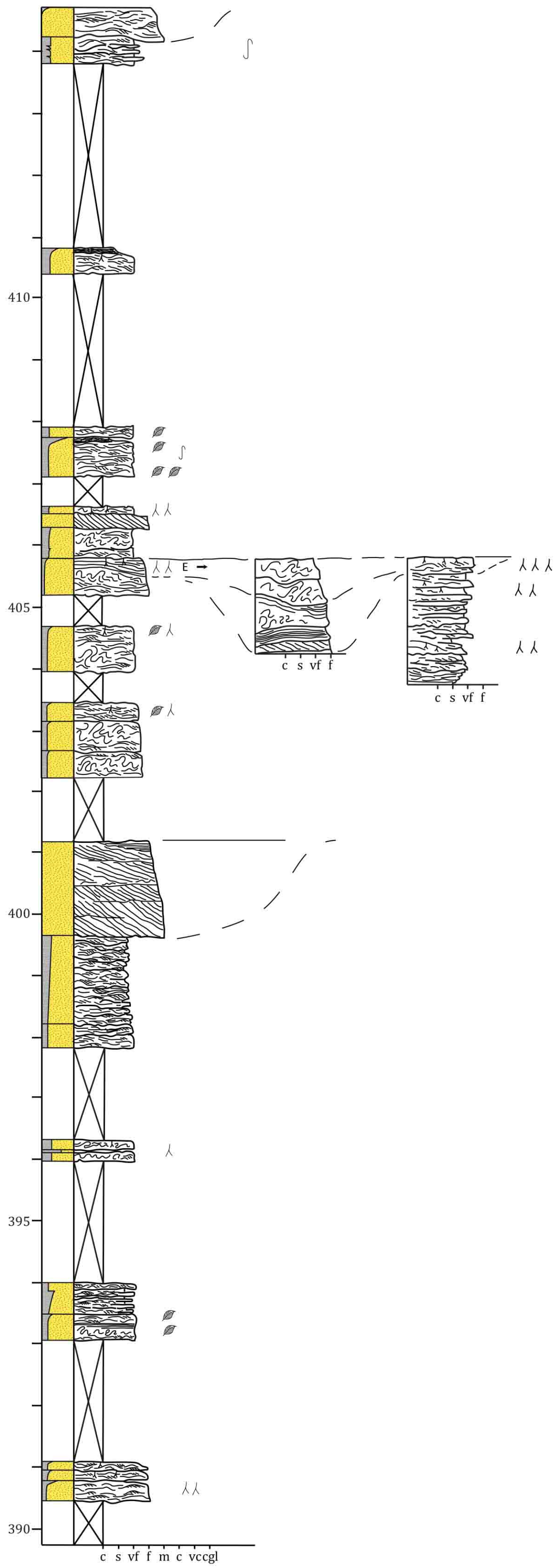
410
405
400
395
390
c s vf f m c vccgl
E
c s vf f
c s vf f
435
430
425
420
415
c s vf f m c vc cgl

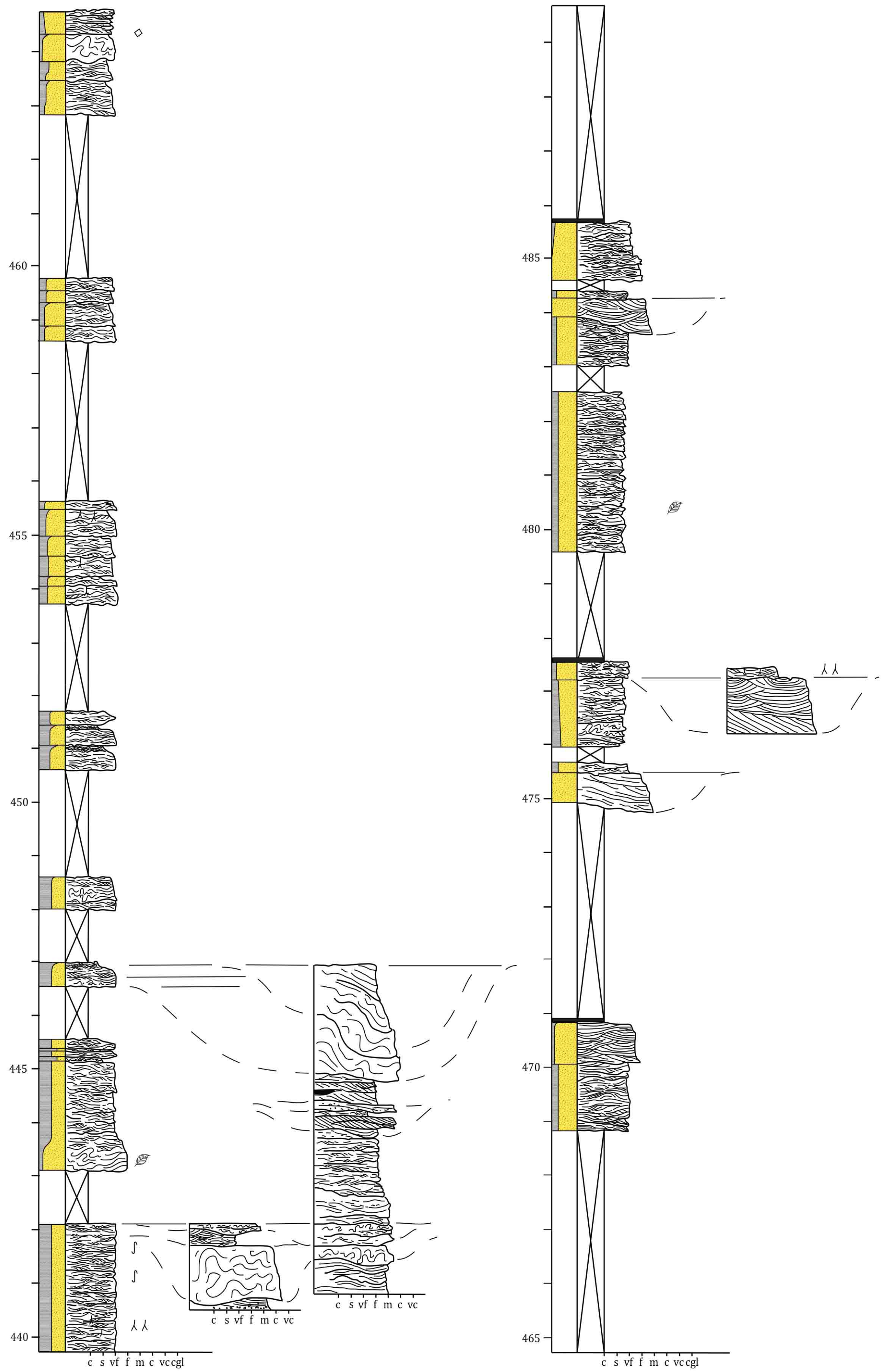
460
455
450
445
440
c s vf f m c vc cgl
c s vf f m c vc
c s vf f m c vc
485
480
475
470
465
c s vf f m c vc cgl

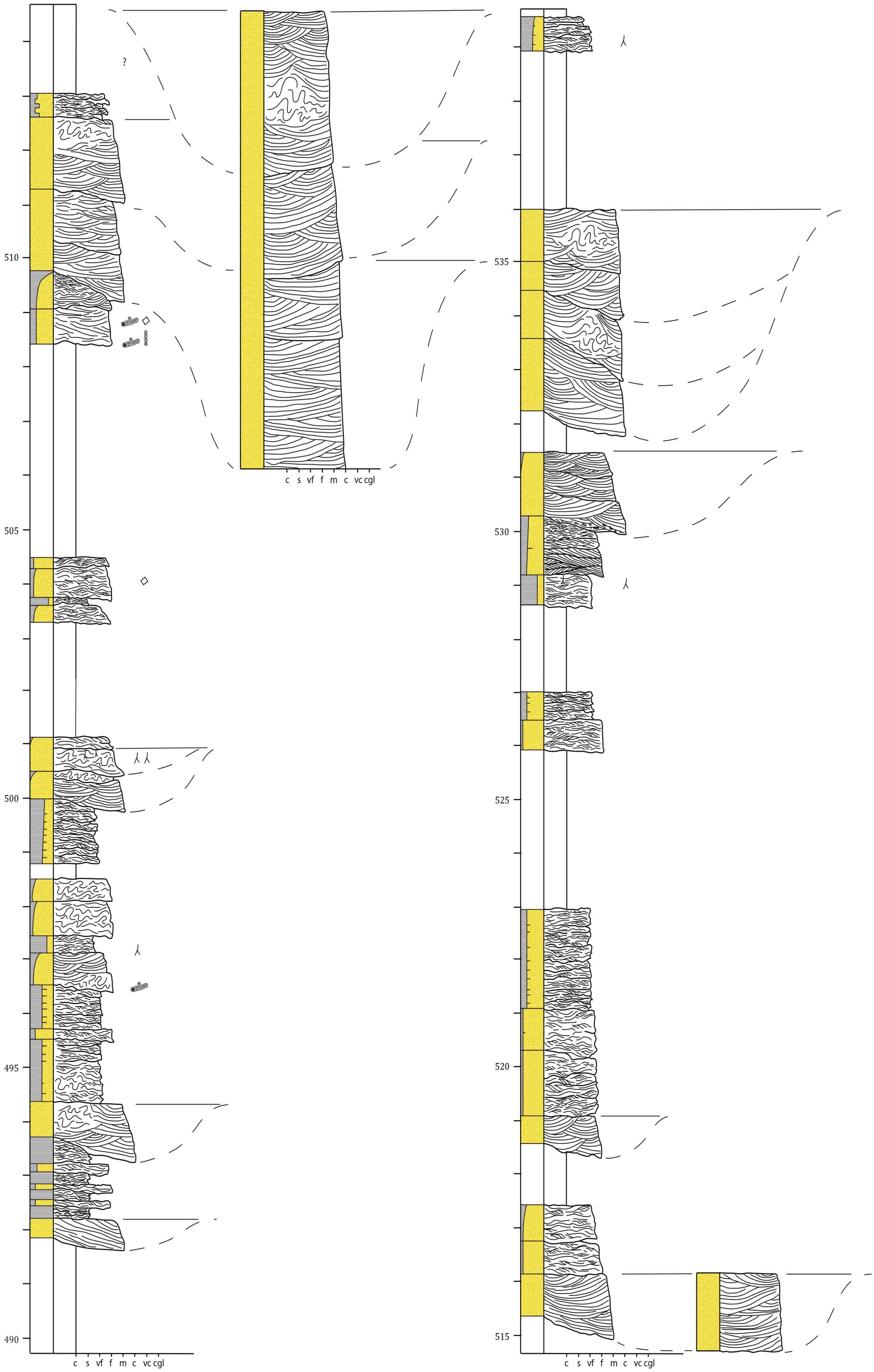
510
505
500
495
490
c s vf f m c vc cgl
c s vf f m c vc cgl
535
530
525
520
515
c s vf f m c vc cgl

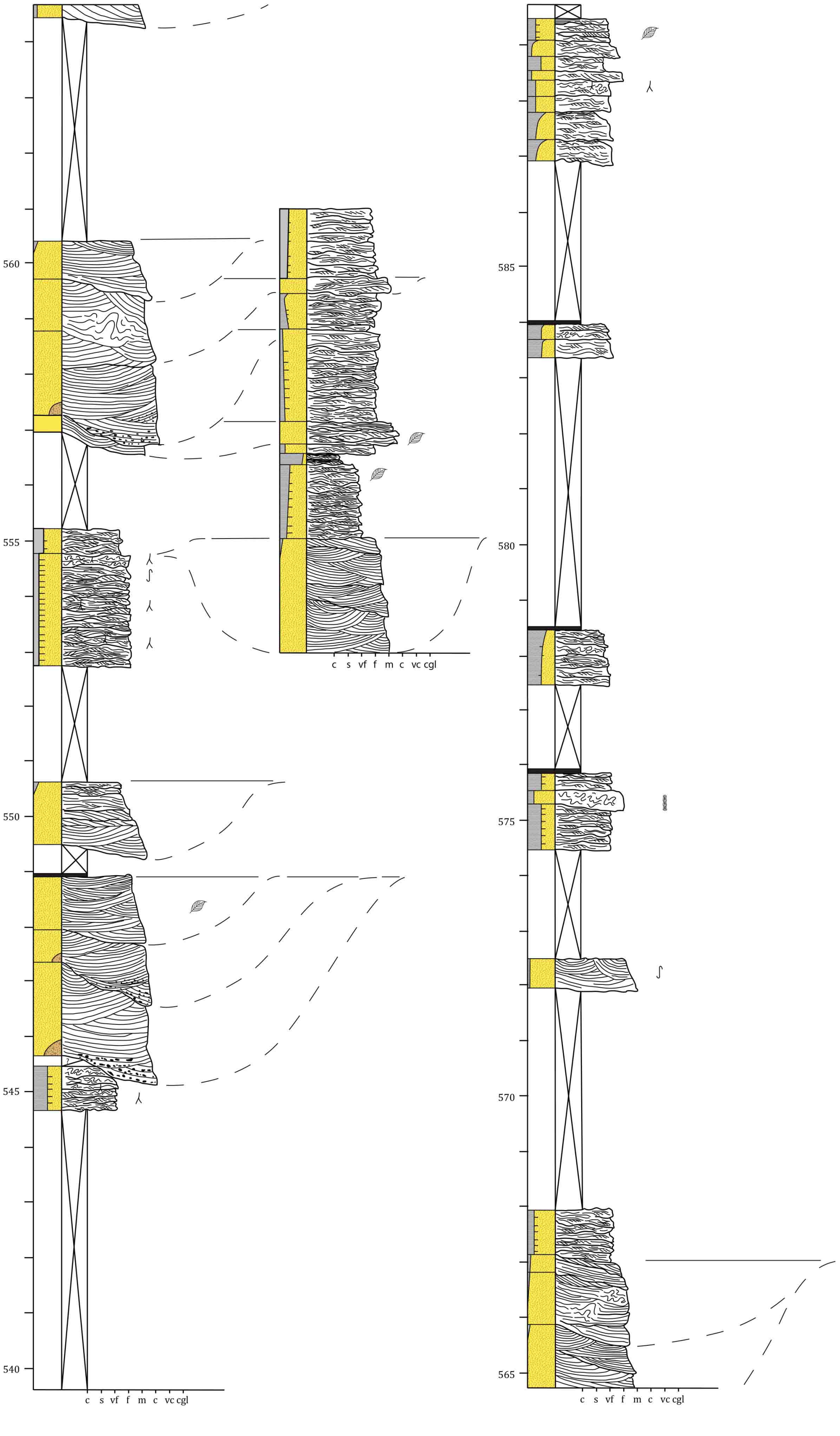

560
555
550
545
540
c s vf f m c vc cgl
c s vf f m c vc cgl
585
580
575
570
565
c s vf f m c vc cgl

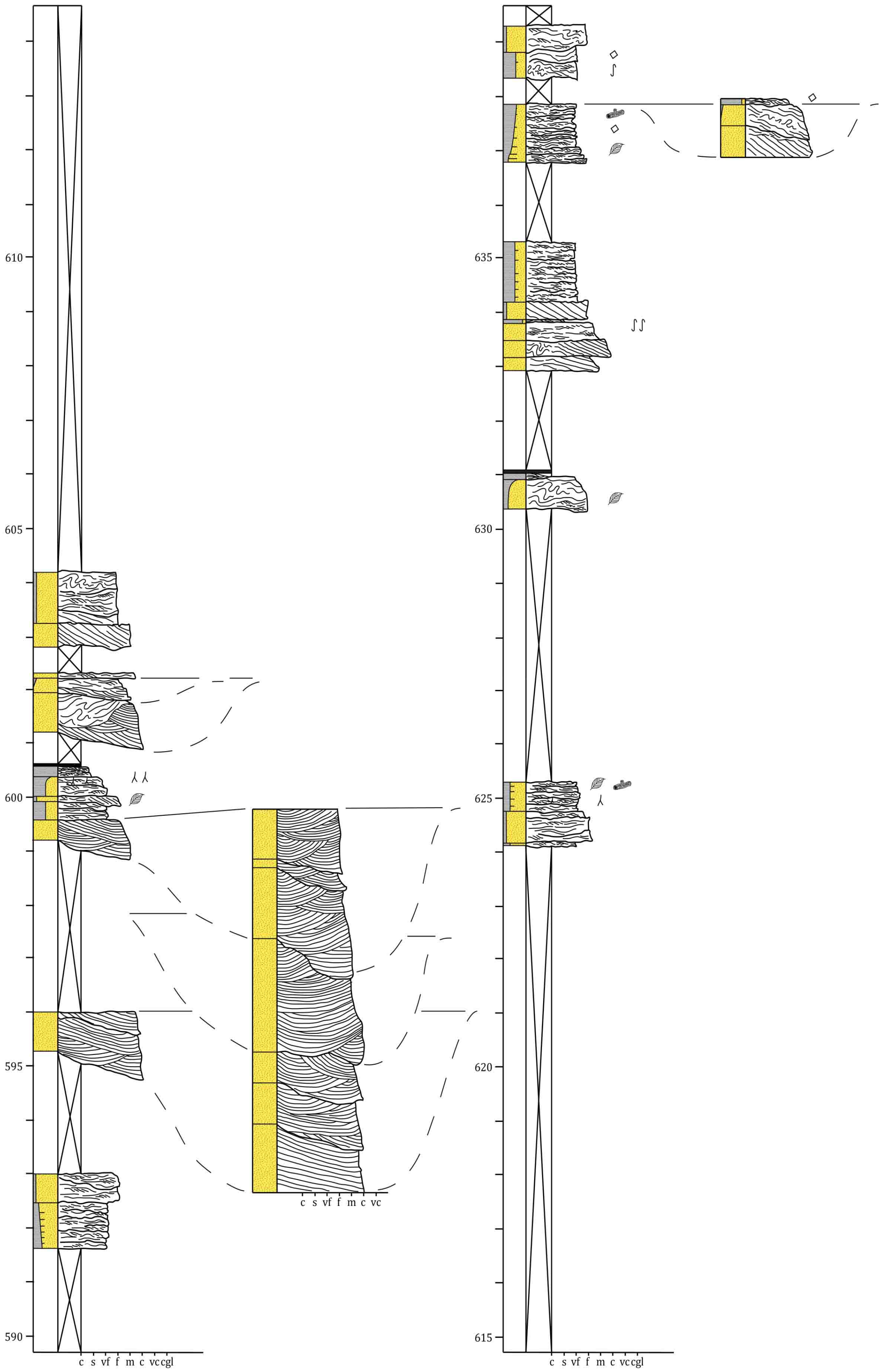
610
605
600
595
590
c s vf f m c vccgl
c s vf f m c vc
635
630
625
620
615
c s vf f m c vccgl

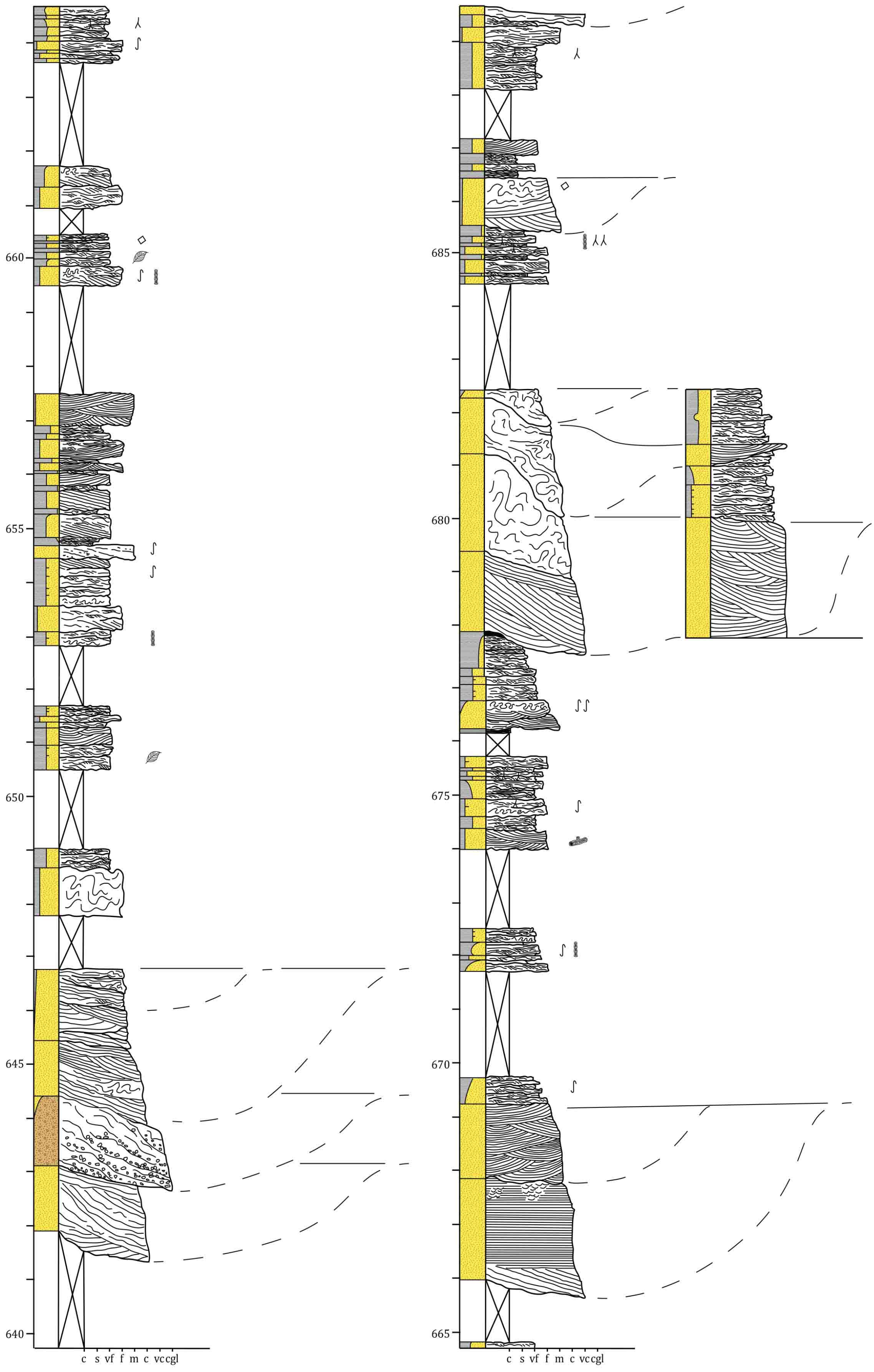

660
655
650
645
640
c s vf f m c vc cgl
685
680
675
670
665
c s vf f m c vc cgl

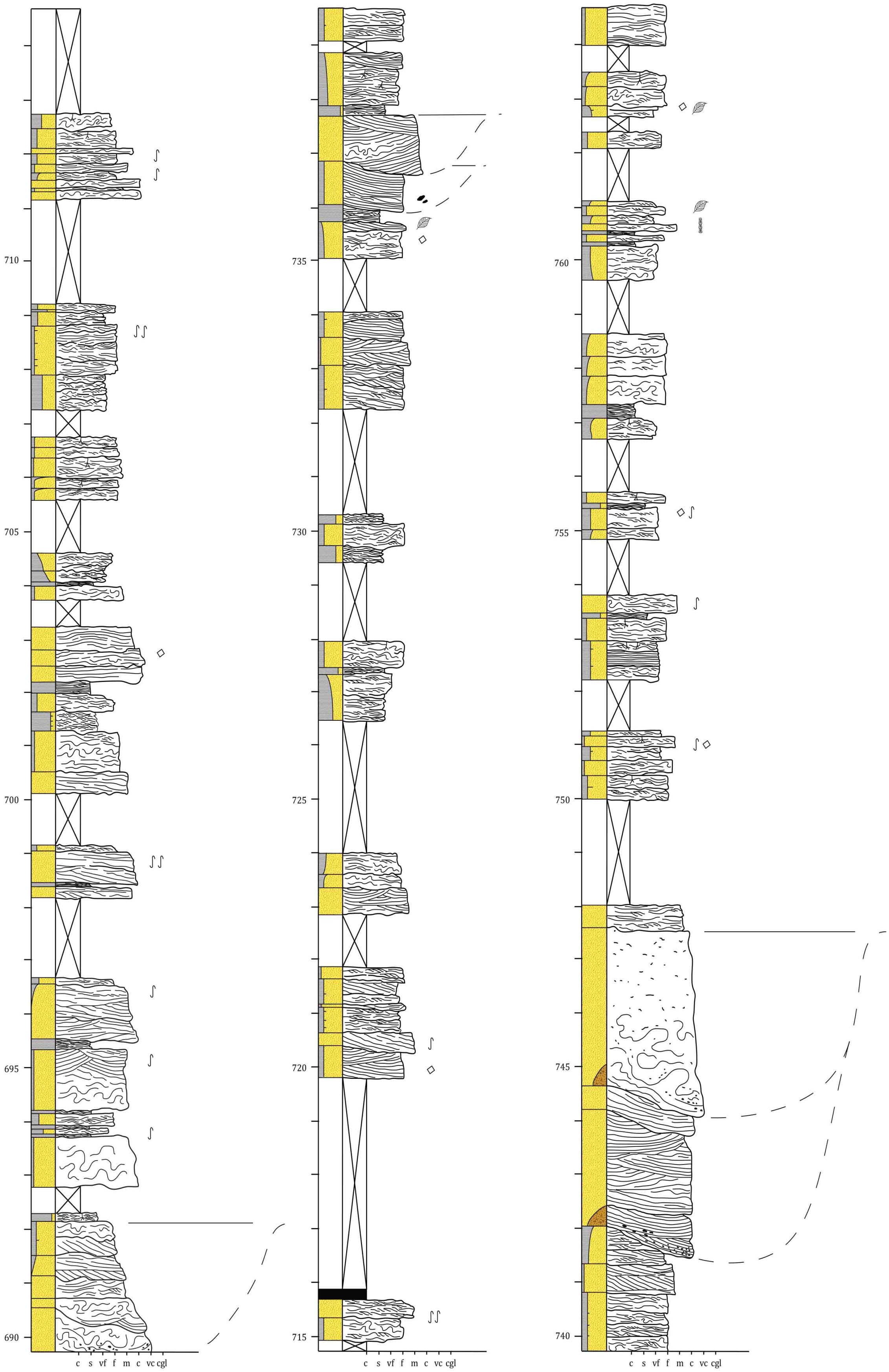
690
695
700
705
710
c s vf f m c vc cgl
715
720
725
730
735
c s vf f m c vc cgl
740
745
750
755
760
c s vf f m c vc cgl

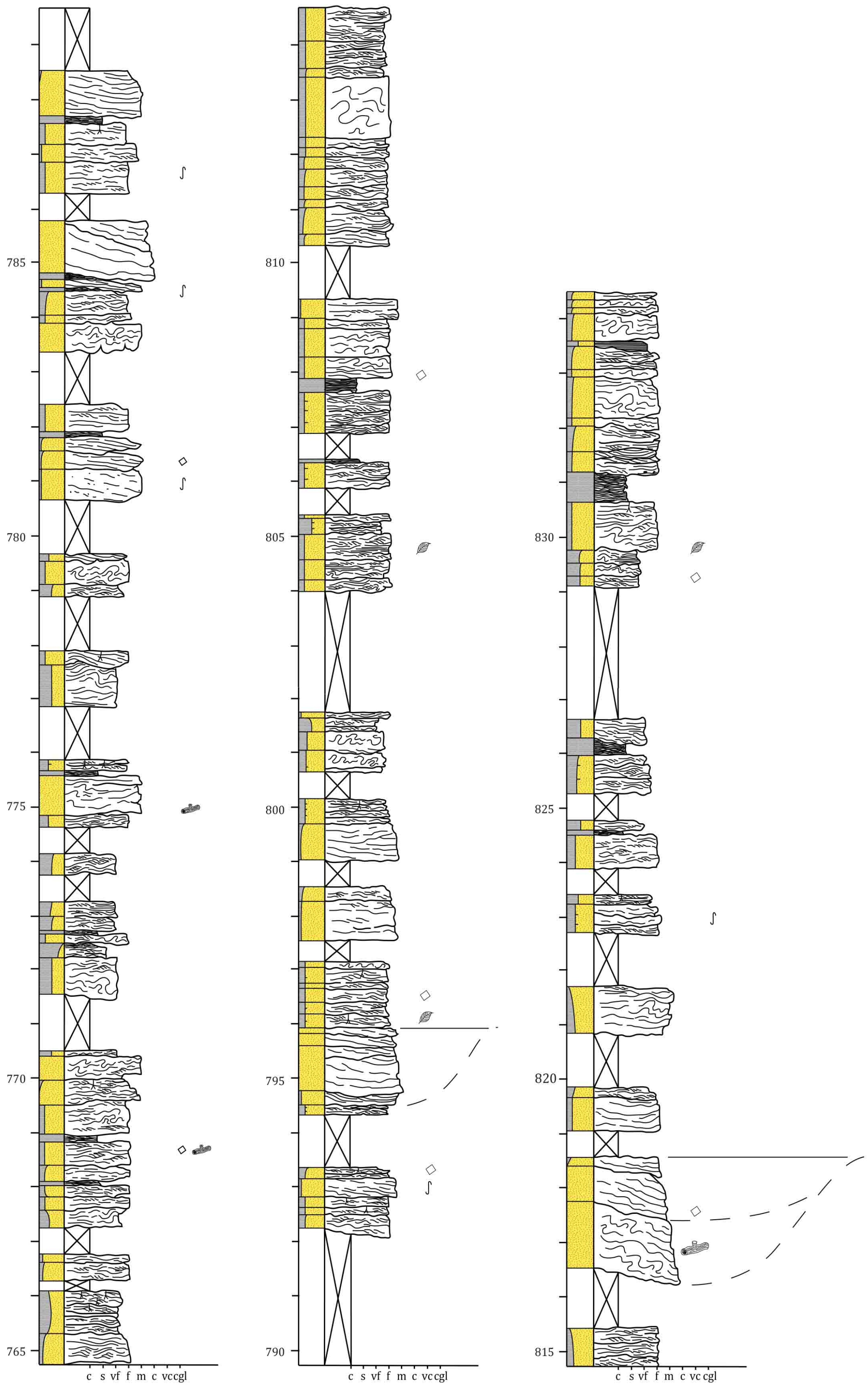
785
780
775
770
765
c s vf f m c vc cgl
810
805
800
795
790
c s vf f m c vc cgl
830
825
820
815
c s vf f m c vc cgl